THE UNIVERSITY OF CHICAGO

DEFINING THE ROLE OF T CELL RECEPTOR - SELF-PEPTIDE/MHC CLASS II INTERACTIONS IN DIRECTING $CD4^+$ T CELL FATE, FUNCTION, AND PATHOGENIC POTENTIAL

A DISSERTATION SUBMITTED TO

THE FACULTY OF THE DIVISION OF THE BIOLOGICAL SCIENCES

AND THE PRITZKER SCHOOL OF MEDICINE

IN CANDIDACY FOR THE DEGREE OF

DOCTOR OF PHILOSOPHY

INTERDISCIPLINARY SCIENTIST TRAINING PROGRAM:

IMMUNOLOGY

BY

DONALD MIGUEL RODRIGUEZ

CHICAGO, ILLINOIS

DECEMBER 2022

To the village that raised me, the family I chose,

the communities of support around me,

and the Creator of it all.

TABLE OF CONTENTS

LIST OF FIGURES

LIST OF TABLES

ACKNOWLEDGEMENTS

The list of those to thank feels endless, as it truly took a village to bring this thesis to fruition. Among the first is Pete Savage, who has served as not only my research mentor, but as a role model for me in many ways. Pete's commitment to graduate student training – in the fullest sense of the term – is unparalleled. For many of his trainees, Pete somehow manages to strike the ideal balance between hands-on involvement, patience with failure, respect for our ideas, and space to grow as scientists. His encouragement and support have been constants during a PhD full of changes and challenges. Moreover, his warmth complements his relentless pursuit of top-notch science, making an environment that has been amazing for me to work in. I hope I can recreate at least a smidge of that environment and persona with my own lab in the future.

I am also incredibly grateful to my past and present labmates, who shared many successes and struggles with me. To Victoria Lee, the trailblazing MD/PhD student (now double doctor) who took me under her wing and got me hooked on T follicular helper cells, thank you for your patience, support, guidance, and friendship. It's been an honor and privilege to team up with you and bring our story to the scientific community. Many thanks to Christine Miller and Jaime Chao, whose commitment to excellent science and even better happy hours inspired me at multiple points throughout this journey. I am eternally grateful to Dave Klawon, not only for his help and advice, but also for his partnership as we navigated graduate school and the transition to senior students together. Your presence alone boosts morale and scientific rigor for the betterment of everyone around you. Lastly, this new crop of Savage Lab trainees is special, and I thank them for fostering a new lab family with me. Matt Walker, Riley Curran, Nicole Ganci, Nikita Maheshwari, and

Joseph Guter, I am thrilled to be staying close by so I may readily witness the great things you do and the even greater people you become as your go through the rest of your training.

Next, my thesis committee deserves profuse thanks for monitoring and fostering my progress over these five years. Fotini Gounari, my committee chair, has always been a source of encouragement and of excellent questions, elevating my work after each presentation. Marcus Clark, the one who helped me decide that 8+ years pursuing an MD and PhD at the University of Chicago would be a good idea, has been a catalyst for my development as a physician-scientist, and I know that will continue through my time in the Medical Scientist Training Program (MSTP). Erin Adams, whose graceful brilliance has marked every single one of our encounters, has continually given me the resources and push I needed to be clearer, more confident, and more thorough with my science. Thank you all for your support and your feedback.

My MSTP, PhD, and original MD cohorts – thank you for providing some of the greatest examples of friendship I have ever known. You have slogged through alongside me, endured my complaining, and bolstered me when I have needed it the most. Reba, Kishan, Emily (Cullum), Maya, Lakshmi, Grace, Meytal, Min, Saara-Anne, Caraline, Allen, you are the core of my Chicago family and my time would have been significantly worse without you all. Same goes for Steven Redford, Emily Fogarty, Divya Gala (as an honorary Committee on Immunology member), Jen Allocco, Sabrina Bennett, Josef Kushner, Anastasia Pozdnyakova, Mika Kachman, and many others in the COI, BSD, MSTP, and Pritzker communities.

I also want to thank the administrators of these programs for cultivating a training environment marked by academic rigor and enrichment. In particular, I thank Kristin McCann, Marisa Davis, Hafsah Mohammed, Alison Anastasio, Sarah Blum, Shanetha Thomas, Lucy Godley, Monica Vela, Keme Carter, Emily Sharp-Kellar, Bethany Shephard, Maria Hernandez,

Juana Villalpando, Sara Roser-Jones, Walter Parrish, and Bana Jabri for believing in me and creating opportunities for me to thrive at UChicago. Additionally, I want to acknowledge our wonderful neighbors on the KCBD 6th floor, including the Kline, Oakes, and Sweis labs. Justin, Xiufen, Sravya, Brendan, Erica, and Diane have always been available for great conversations (and for emergency supplies - a special thanks for those). Speaking of supplies, this work would not have been possible without the support of the Facilities/dock team, the Animal Resources Center (ARC) staff, and the Cytometry & Antibody Technology facility crew, including David, Laura, Bert, Mandel, and Mike. Thank you.

To my chosen family at Yale who helped propel me to Chicago, thank you for your love and enduring support. I would have never considered pursuing an MSTP or graduate work in immunology without the guidance of Amanda Hernandez-Jones, who truly has been a sister in everything but blood relation. I am forever grateful to you for showing me that I could have a place in science, and for seeing brilliance and resilience in me when I often fail to see those in myself. To the people who have kept me sane for years now, Chris, Evelyn, Román, Sebi, Sal, Jenny, Liz, Gracia, Cristina, Ben: thank you for dealing with my shade-is-love mentality and for reciprocating it. A special shout-out goes to Stephen Pitti, Alicia Schmidt-Camacho, and Camille Lizarríbar for showing me what Hispanic excellence in academia and university administration looked like as an impressionable 18-year-old. Your impact on my career trajectory cannot be understated.

To the communities I hail from, whose representation in science and medicine continues to grow, thank you for continuously motivating me to reach the finish line. You are the inspiration fueling my dream of promoting those who have been historically excluded from the ivory tower. Your perspectives and experiences are needed in this space for all of us to thrive. To that end, I owe many thanks to the Latino Medical Student Association (LMSA) and the Student National

Medical Association (SNMA) for giving me avenues to fight the "good fight" and work on behalf of current and future patients and providers across the country. Moreover, the family I gained through LMSA - Jose Grajales, Alex Alejos, Jesús Acevedo Cintrón, Karina Diaz, Luke Torre-Healy, Christian Surí, Camilo Acuña, Valeria Valbuena, Julia Su, Eric Molina, and many more - will remain family for years to come, and I'm looking forward to celebrating this accomplishment with you all. (This includes Gracia, also part of the Yale crew, and JP Sánchez, with all your visionary craziness.)

To my partner, Mary Frith, you are the best part of this chosen family. Thank you for building me up, making me laugh, encouraging me to be silly, and sharing this MD/PhD journey with me. Moreover, thank you for the opportunity to bond with your family as my own, and many thanks to Beth, Jim, Erin, Bobby, Joseph, and many more for welcoming me with open arms.

Finally, I would not be here without my parents and sisters, who have sacrificed more than I know for this moment to arrive. Mom, Dad, Rossy, and Marlyn, words will never not enough to describe how important you are to me and to this thesis. Thank you from the bottom of my heart for making me into the person I am today. Please know that this work is for you and for the Lord. I love you all so much.

ABSTRACT

In both humans and mice, $CD4^+$ T cells reactive to self-derived antigens have been implicated in a range of autoinflammatory processes. To promote disease, such cells must evade tolerogenic mechanisms in the thymus and in secondary lymphoid organs. However, the factors that render self-reactive $CD4^+$ $Foxp3^{neg}$ conventional (Tconv) cells prone to regulation remain incompletely understood. Moreover, it is unclear whether these same factors govern the pathogenic potential of self-reactive $CD4^+$ Tconv cells. Previous work on this topic has focused on the sensitivity with which a $CD4^+$ T cell recognizes and responds to a given peptide-MHC class II (pMHC-II) ligand. Yet, to assess the impact of varying T cell sensitivities, many studies have relied on the analysis of T cells reactive to foreign model antigens; immune responses towards such antigens may not recapitulate those targeting bona fide self-antigens. Using T cell receptor (TCR) profiling paired with in vivo clonal analysis of T cell differentiation, we characterized two panels of naturally occurring $CD4^+$ Tconv cell clones reactive to endogenous self-ligands. The first consisted of self-reactive $CD4^+$ Tconv cell clones that infiltrate the prostate following systemic Treg cell ablation. A subset of these clones were highly proliferative in the lymphoid organs at steady state and exhibited overt reactivity to self-ligands displayed by dendritic cells (DCs), yet were not purged by clonal deletion. These clones spontaneously adopted numerous hallmarks of T follicular helper (Tfh) cells, including expression of Bcl6 and PD-1. yet failed to produce common effector cytokines at baseline. The second panel of naturally occurring $CD4^+$ Tconv cell clones consisted of TCRs reactive to a known tissue-specific antigen (TSA), $Tcaf3_{646\text{-}658}$ (termed "C4" peptide). Analysis of these clones revealed preferential thymic $Foxp3^+$ regulatory T (Treg) cell differentiation among clones exhibiting higher sensitivities to C4/I-A^b. Notably, less sensitive C4-reactive clones retained the ability to infiltrate the prostate in various inflammatory contexts,

including infection, systemic Treg cell ablation, and oncogene-driven prostate tumors. Collectively, our work identifies two distinct self-reactive $CD4^+$ Tconv cell populations kept in check by Treg cells at steady state: one that interacts with both DCs and B cells by adopting a Tfh-like phenotype, and one that senses TSAs but remains phenotypically naïve until released from mechanisms of peripheral T cell tolerance. Future work will elucidate how the interplay between these populations shapes autoimmune and antitumor responses.

ABBREVIATIONS

(n)Tfh	(naturally occurring) T follicular helper cell
(p/t)Treg cell	(peripherally induced or thymically derived) $Foxp3^{+}$ $CD4^{+}$ regulatory T cell
(s)pMHC-I/II	(Self-) peptide complexed to major histocompatibility complex class I / II
2D-MP	Two-dimensional micropipette-based assay for affinity measurement
AF	Antigen-free
APC	Antigen-presenting cell
APL	Altered peptide ligand
ASC	Antibody-secreting cell
BCR	B cell receptor
CD4+ Tconv cell	$Foxp3^{neg}$ $CD4^{+}$ conventional T cell
CD4SP/CD8SP	$CD4^{+}$ or $CD8^{+}$ single-positive thymocyte
CDR	Complementarity-determining region
CNS	Central nervous system
(c/m)TEC	Cortical or medullary thymic epithelial cell
CTL	$CD8^{+}$ cytotoxic T lymphocyte
Cy	Cyclophosphamide
DAG	Diacylglycerol
DC	Dendritic cell
DEG	Differentially expressed gene
DN	$CD4^{neg}$ $CD8^{neg}$ double-negative thymocyte

DP	$CD4^+$ $CD8^+$ double-positive thymocyte
DT(R)	Diphtheria toxin receptor
DZ	Dark zone of germinal center
EAE	Experimental autoimmune encephalomyelitis
ERV	Endogenous retrovirus
FACS	Fluorescence-activated cell sorting
FBS	Fetal bovine serum
Flu	Fludarabine
GC	Germinal center
GF	Germ-free
HA	Influenza hemagglutinin
HP	Homeostatic proliferation
ICB	Immune checkpoint blockade therapy
IL / IFN	Interleukin / interferon
IPEX	Immunodysregulation, polyendocrinopathy, enteropathy, X-linked
IS	Immunological synapse
ITAM	immunoreceptor tyrosine–based activation motif
LCMV	Lymphocytic choriomeningitis virus
Lm	*Listeria monocytogenes*
LZ	Light zone of germinal center
MCC/PCC	Moth cytochrome c / pigeon cytochrome c
MOG	Myelin oligodendrocyte glycoprotein
MS	Multiple sclerosis

Mtb	*Mycobacterium tuberculosis*
NeoAg	Cancer neoantigen
NOD	Non-obese diabetic mouse model of type 1 diabetes
OVA	Chicken ovalbumin
PAMP	Pathogen-associated molecular pattern
PE	Phycoerythrin
pLN	Peri-aortic (or prostate-associated) lymph node
PRR	Pattern-recognition receptor
SLE	Systemic lupus erythematosus
SPF	Standard pathogen-free
SPR	Surface plasmon resonance
TAA	Tumor-associated antigen
TCR	T cell receptor
TCRrg / TCRtg	T cell receptor retrogenic or transgenic mice
TF	Transcription factor
Th(1)	T helper type (1) cells
TIL	Tumor-infiltrating lymphocytes
TRAMP	Transgenic adenocarcinoma of mouse prostate
TSA	Tissue-specific antigen

CHAPTER I: INTRODUCTION

Self/non-self discrimination by the mammalian immune system

The mammalian immune system consists of multiple effectors acting in concert to defend the host against pathogenic challenges. These effectors include cellular and humoral components of innate immunity, such as granulocytes, monocytes, dendritic cells (DCs) and complement, as well as components of the adaptive immune system - namely, B and T lymphocytes[1]. These effectors differ in their ability to recognize, respond to, and "remember" foreign antigens[2–4]. In contributing to antimicrobial responses, these effectors promote the generation and function of cytokines, cytotoxic molecules, and other mediators of inflammation. However, such agents may have the unintended consequence of inflicting collateral damage upon host tissues, which the immune system must limit to ensure host survival and function. Thus, in disease settings, defending the host involves balancing resistance to pathogens with protection against self-inflicted injury[5]. To prevent unwanted immune responses against self-derived antigens, the immune system has developed multiple mechanisms to maintain a state of tolerance towards self while enabling effective responses against foreign entities. Many of these mechanisms rely on the ability of immune cells to successfully discriminate between self and non-self[6].

Self/non-self discrimination refers to the immune system's ability to identify molecules derived from exogenous sources based on the differences those molecules possess in comparison to endogenous molecules derived from host tissues[7]. One hallmark of the innate immune system includes recognition of evolutionarily conserved features of pathogens, referred to as pathogen-associated molecular patterns (PAMPs), by germline-encoded pattern recognition receptors (PRRs)[8]. Upon PRR binding of a known exogenous ligand, such as lipopolysaccharide (LPS) or

double-stranded RNA, innate immune cells rapidly upregulate cytokines and antimicrobial peptides to limit pathogen replication, prevent further infection, and eliminate infected host cells[9]. In addition, DCs integrate PRR and/or other danger signals with the uptake of pathogen-derived antigens, which are subsequently processed into peptides and loaded onto major histocompatibility complex (MHC) molecules[10]. This integration leads to DC maturation; upregulation of the B7 co-stimulatory ligands, CD80 and CD86; and presentation of foreign peptide-MHC class I (pMHC-I) and class II (pMHC-II) complexes to $CD8^+$ and $CD4^+$ T cells, respectively[11]. Thus, the innate immune system relies on detection of typical features of microbes which mammalian cells lack to both provide a first line of defense and activate adaptive immunity.

Nevertheless, to successfully discriminate between self and non-self, the immune system must grapple with at least two major challenges. First, the higher proliferative and mutational rates of pathogenic microorganisms allow them to evolve much faster than mammalian cells, enabling the former to more rapidly develop immune evasion mechanisms[12]. How does the immune system respond to foreign pathogens capable of constant change? In this domain, the innate immune system is helped in part by targeting PAMPs – which often cannot be altered by the microbe without reducing its fitness – as well as by recognizing instances of "missing,"[13] "altered,"[14] or "damaged"[15,16] self. For more complete protection against pathogens, however, the immune system must also rely on B and T cells harboring somatically rearranged antigen receptors. Deficits in either lymphocyte compartment - or in the ability to rearrange antigen receptors, as in the case of Rag1 and Rag2 mutations[17,18] - leave the host susceptible to recurrent, life-threatening infections.

In generating a diverse repertoire of B and T cell receptors, the immune system develops the ability to respond to a broad range of antigens – including those from self[19,20]. Herein lies the

second challenge: how does the immune system train B and T cells on self, in order to avoid autoimmunity? Through mechanisms of central tolerance, developing B and T cells are exposed to self-derived antigens in the bone marrow and thymus, respectively; this enables deletion, diversion, or restraint of overtly self-reactive lymphocytes prior to such cells' migration into secondary lymphoid organs (SLOs), including spleen and lymph nodes[21,22]. In the periphery, mechanisms of peripheral tolerance work to prevent self-reactive lymphocytes from encountering their cognate antigens and curtail inappropriate activation of these cells upon antigen encounter[21,23]. For T cells, additional layers of regulation exist; in contrast to B cell receptors (BCRs), which may directly bind peptide and non-peptide antigens in their native form, T cell receptors (TCRs) may only recognize peptide antigens bound to MHC molecules[24]. Moreover, $CD4^+$ T cells bind antigens presented on MHC class II molecules, the expression of which is largely limited to professional antigen-presenting cells (APCs)[25]. As conventional $CD4^+$ T (Tconv) cells can potentiate B, $CD8^+$ T, and myeloid cell responses[26], immune tolerance depends on restricting the possibility and productivity of interactions between self-reactive $CD4^+$ Tconv cells and self-peptide-MHC class II complexes (spMHC-II).

This dissertation will discuss past, present, and future work aimed at understanding the role of TCR:spMHC-II interactions in establishing and enforcing immune tolerance. Through robust clonal analyses, our most recent work demonstrates that the endogenous $CD4^+$ T cell repertoire contains cells that actively sense *bona fide* self-antigens at steady state and infiltrate non-lymphoid organs in settings of immune perturbation. This work also raises key questions regarding the ways in which TCR:spMHC-II interactions shape a $CD4^+$ Tconv cell's propensity to mount autoimmune and anti-tumor responses.

T cell receptor structure and the immunological synapse

A T cell surveys the body's tissues for immunogenic peptides using its T cell receptor: a heterodimeric transmembrane receptor capable of binding short peptide fragments bound to MHC class II molecules on the surface of APCs. Studies of T cell development since the early 1990s have revealed the existence of multiple T cell lineages, differentiated by their TCRs and antigen-binding properties (summarized in refs[27,28]). Conventional αβ T cells comprise the most prevalent T cell subset in mice and humans and are distinguished by the expression of the αβTCR: a heterodimeric antigen receptor consisting of one TCRα and one TCRβ chain covalently linked by a disulfide bond. Each TCR chain possesses a constant region and a variable region. The constant region includes a short cytoplasmic tail devoid of signaling capabilities, a transmembrane domain, and a membrane-proximal connecting peptide important for association of the TCR with the CD3 signaling complex. The variable region contains three complementarity-determining regions (CDRs) which make contacts with the sides (CDR1 and CDR2) and peptide-binding pocket (CDR3) of MHC molecules[29]. These loops determine the ability of a TCR to bind pMHC ligands, the strength (or affinity) of the TCR:pMHC interaction, and the orientation in which TCR binding to pMHC occurs[30–32].

While the αβTCR itself is sufficient for initial binding to pMHC, productive T cell signaling occurs through the formation of the immunological synapse (IS), a specialized membrane structure at the interface between a T cell and an APC.[33,34] The IS consists of the TCR/CD3 complex, whose engagement triggers downstream signaling events; the coreceptor CD4 or CD8, which stabilize TCR-ligand interactions by binding to the sides of MHC class I and II molecules, respectively; cell adhesion molecules, which support proximity between T cells and APCs; and co-stimulatory and co-inhibitory molecules, which modulate T cell signaling, function, and

survival. For a naïve $CD4^+$ T cell, binding of pMHC-II ligands leads to TCR crosslinking and Lck kinase recruitment to the IS, where it can phosphorylate immunoreceptor tyrosine–based activation motifs (ITAMs) present within the cytoplasmic tails of CD3 subunits[35]. These phosphorylated ITAMs are bound by the Zap70 kinase, leading to the latter's release from autoinhibition and further activation via Lck phosphorylation[36]. Active Zap70 then promotes subsequent TCR signaling events, such as the recruitment of LAT and Slp76, as well as the activation of Ras/MAPK, PI3K, and calcium/NFAT pathways important for $CD4^+$ T cell proliferation and differentiation[37,38]. This process is cumulatively referred to as "Signal 1;" naïve T cells require this along with signals derived from ligation of the CD28 co-stimulatory receptor – "Signal 2" – for complete activation to occur[39].

Consequences of TCR signaling

Complete activation of peripheral $CD4^+$ Tconv cells results in two key outcomes: clonal expansion and acquisition of effector function. TCR engagement and co-stimulation trigger proliferation of the $CD4^+$ Tconv cell clone that has successfully recognized antigen, thereby generating multiple daughter cells bearing the same TCR and capable of responding to the antigen of interest. As the estimated clonal frequencies of naïve T cells of a given pMHC specificity often fall below 100 cells per million, clonal expansion is crucial for facilitating efficient antigen detection and clearance[40]. With regards to effector function, $CD4^+$ Tconv cells may adopt one of several possible T helper (Th) cell lineages following activation[41]. Each lineage expresses a master transcription factor (TF), upregulates signature cytokines and hallmark phenotypic markers, and exerts functions that are tailored for responding to a particular immune challenge (summarized in refs[10,42]). Briefly, Th1 cells express the lineage-defining TF T-bet (encoded by *Tbx21*) and mediate

the elimination of intracellular pathogens by secreting IFN-γ to activate the phagocytotic and microbicidal functions of macrophages and DCs. Th2 cells rely on expression of Gata-3 to orchestrate protective functions against helminths, roping in eosinophils, basophils, and other cells to do so. Rorγt^{+} Th17 cells use IL-17 and other cytokines to recruit and activate neutrophils and help defend the host against extracellular pathogens. T follicular helper (Tfh) cells provide B cells with key cytokines and co-stimulatory cues to develop potent antibody-mediated immune responses against viruses and bacteria. (The function of regulatory T, or Treg, cells, and its dependence on TCR-derived signals, is discussed later in this Introduction.) As illustrated thus far, Th cells work in concert with other immune cell types to eliminate the relevant antigenic insult.

Once the offending antigen is removed, contraction occurs. During this process, the majority of antigen-specific CD4^{+} Tconv cells undergo apoptosis, with a minor subset persisting as memory CD4^{+} T cells[43]. Should the host experience the same antigen again, memory CD4^{+} T cells are epigenetically and transcriptionally poised to respond more quickly upon secondary challenge, leading to improved antigen clearance and protection for the host.

T cell development & antigen receptor rearrangement

Because T cell function depends on successful signaling through TCR/CD3, the process of thymopoiesis must result in the generation of cells bearing TCRs capable of binding ligand and promoting signal transduction[44]. T cell precursors are thus subjected to multiple developmental checkpoints that ensure successful expression of a functional TCR. The probing of TCR function occurs in the thymus, which is seeded by lymphoid progenitors derived from hematopoietic stem cells in the bone marrow[45]. At the earliest stage of thymic development, these precursors lack expression of the coreceptors CD4 and CD8, and are referred to as double-negative (DN)

thymocytes. During this stage, thymocytes begin to form their antigen receptors through the process of V(D)J recombination, which involves the splicing of individual germline-encoded variable (V), diversity (D; TCRβ only), and joining (J) immunoglobulin gene segments together in order to yield exons encoding for TCR chains[46].

For αβ T cells, recombination of the *Tcrb* locus occurs first, with assembly of one Dβ (*TRBD)* and one Jβ (*TRBJ*) segment followed by joining of one Vβ (*TRBV*) segment to the rearranged DJ segment. Each instance of somatic rearrangement is mediated by the recombination activating genes 1 (Rag1) and 2 (Rag2), which form a heterotetramer that binds recombination signal sequences (RSSs) proximal to V, D, and J segments[47]. The Rag complex facilitates double-stranded DNA breaks near two gene segments, leading to excision of intervening sequences and formation of a DNA hairpin resolved via the classical non-homologous end joining pathway. Once a VDJ segment is formed, it is transcribed with the TCRβ constant region and translated if in frame. The resulting TCRβ chain is then paired with a germline-encoded pre-TCRα chain to form the pre-TCR; this triggers the first developmental checkpoint, known as β-selection. To survive, a thymocyte must be able to experience signaling through the pre-TCR following ligation of pMHC molecules expressed by cells within the thymic cortex[48]. If a thymocyte produces a TCRβ chain with no reactivity to pMHC molecules, or if it fails to produce an in-frame TCRβ exon, the absence of TCR signaling at this stage leads to death by neglect, through which non-signaled thymocytes undergo apoptosis[49]. In contrast, thymocytes exhibiting at least weak TCR-mediated signals are rescued from cell death and encouraged to continue their developmental trajectory.

TCR-mediated signals also trigger migration to the thymic medulla, maturation to the $CD4^+$ $CD8^+$ double-positive (DP) stage, and recombination of the *Tcra* locus[48]. As above, the Rag complex mediates splicing of one Vα (*TRAV*) to one Jα (*TRAJ*) segment to yield a TCRα exon.

Following TCRα rearrangement, a thymocyte must express the newly rearranged TCRα chain, pair it with the recently assembled TCRβ chain, and undergo another developmental checkpoint, involving interactions with pMHC molecules displayed on medullary APCs. Prevailing models of thymocyte development posit that DP thymocytes transiently downregulate surface expression of CD8[50]. In doing so, thymocytes bearing MHC class II-restricted TCRs retain the ability to bind pMHC-II molecules and maintain TCR signaling, whereas thymocytes with MHC class I-restricted TCRs exhibit reduced pMHC-I contact and signaling due to diminished co-receptor expression. This temporal regulation of TCR signaling governs the expression of transcription factors critical for differentiation of CD4 single-positive (CD4SP) versus CD8 single-positive (CD8SP) cells. However, this canonical developmental trajectory may be altered following agonist TCR:pMHC interactions either before or after the DN-to-DP transition; such interactions can divert thymocytes away from the conventional αβ T cell lineage in favor of alternative T cell fates (reviewed in refs[27,28]). In the absence of agonist signaling, thymocytes emigrate to the periphery as mature naïve $CD4^+$ or $CD8^+$ αβ T cells, ready to expand upon antigen encounter.

As the genomes of mice and humans harbor multiple V, D, and J segments, V(D)J recombination affords a thymocyte millions of potential gene segment combinations for generating a TCR, enabling combinatorial diversity of TCRs among the total T cell pool[51]. Because the non-germline VJ and VDJ regions comprise the TCR CDR3α and CDR3β loops, respectively, each combination of gene segments can yield a TCR with distinct antigen binding properties. Thus, somatic rearrangement of TCR gene segments creates combinatorial diversity within the T cell repertoire, allowing the mammalian immune system to recognize a greater breadth of antigens than would be possible through germline-encoded receptors. Moreover, the process of resolving DNA hairpins at the junction sites between gene segments often leads to the addition and/or deletion of

nucleotides. Such changes can modify the amino acid sequence and/or the reading frame of the TCR exon. As a result, V(D)J recombination introduces junctional diversity, which, when combined with combinatorial diversity, further increases the number of possible TCRs.

Generation of self-reactive TCRs and the need for T cell tolerance

While the stochastic nature of V(D)J recombination allows the immune system to generate a diverse TCR repertoire, it also produces TCR exons that fail to encode a TCR chain, give rise to TCR chains that cannot successfully pair with one another, or yield TCRs incapable of binding MHC molecules[49]. Thymocytes experiencing any of these failures do not receive TCR-mediated survival signals during development and, as a result, do not reach the periphery. Of the TCR exons that give rise to functional receptors, a subset produces TCRs that bind strongly to pMHC molecules bearing self-derived peptide ligands. If left unchecked, T cells bearing self-reactive TCRs may undergo activation and mount pro-inflammatory responses against a self-antigen, thereby promoting autoimmunity.

Mechanisms of central tolerance for $CD4^+$ T cells

To prevent unwanted self-directed immune responses, the mammalian immune system employs several mechanisms aimed at culling or curbing self-reactive $CD4^+$ T cells. In the thymus, mechanisms of central tolerance rely on the display of self-antigens to developing T cells to prevent their egress as $CD4^+$ Tconv cells. During the DN stage of thymic development, thymocytes encounter self-antigens primarily through interactions with cortical thymic epithelial cells (cTECs). cTECs highly express cathepsin L and thymus specific serine protease, specialized enzymes that cleave endosomal polypeptides to be loaded on MHC class II. Both enzymes are

required for $CD4^+$ T cell development, as genetic ablation of either enzyme or both impairs positive selection of MHC-II-reactive T cell clones.[52,53] Interactions with spMHC-II on cTECs can result in death by neglect, positive selection, or negative selection, by which thymocytes receiving strong TCR signaling upregulate BH3 effectors of apoptosis, such as Bim, and undergo cell death[54,55]. As negative selection acts to remove specific clones that exhibit high extents of self-reactivity, this process is also referred to as clonal deletion.

Another possible fate for MHC-II-reactive thymocytes includes differentiation into the $Foxp3^+$ $CD4^+$ regulatory T (Treg) cell lineage. Treg cells are required throughout life and act to limit inflammation, maintain host tissue homeostasis, and promote tissue repair[56,57]. In combination with co-stimulation through CD28, moderate TCR signaling is thought to induce upregulation of the Treg cell lineage-defining transcription factor, Foxp3, and the high-affinity interleukin-2 (IL-2) receptor, CD25 (IL2Rα)[58]. Foxp3 enables at least a fraction of a Treg cell's suppressive program, while repressing expression of transcription factors and cytokines associated with pro-inflammatory $CD4^+$ Tconv cell subsets. CD25 sensitizes Treg precursors to the survival and proliferative cues imparted by IL-2 signaling. While the majority of Treg cells in mice originate from the thymus (tTregs), the relative contributions of the thymic cortex versus the medulla on tTreg differentiation remain unclear. Using mixed bone marrow chimeras with wild-type (WT) and CCR7-deficient marrow, the Rudensky group observed Foxp3 expression among *Ccr7*$^{-/-}$ DP and CD4SP thymocytes, which have undergone positive selection but fail to migrate to the thymic medulla[59]. Similar results were observed using *Ab1*^{null} K14-$A\beta^b$ mce, in which MHC class II expression is restricted to keratin 14-expressing cTECs. However, Liston *et al.* focused primarily on Foxp3 positivity; more recent studies have highlighted the existence of two distinct Treg precursor populations: $Foxp3^{lo}$ $CD25^{neg}$ and $Foxp3^{neg}$ $CD25^+$ cells[60]. While the former

population was observed in both the thymic cortex and medulla, the latter was found exclusively in the medulla. Moreover, mature Treg cells derived from Foxp3^{lo} CD25^{neg} precursors failed to control experimental autoimmune encephalomyelitis (EAE) severity to the same extent as did mature Treg cells derived from Foxp3^{neg} CD25^{+} precursors, suggesting that the thymic cortex may give rise to Treg cells whose quality and/or specificities vary from those of medullary-derived Treg cells. Collectively, while these findings point to uncertainty regarding the developmental origins of Treg cell heterogeneity, prevailing models of thymopoiesis regard the thymic cortex mainly as the location in which positive selection and MHC restriction occur.

In contrast, the thymic medulla is viewed as the key site in which central T cell tolerance is imposed. Following positive selection, DN thymocytes upregulate CD4, CD8, and CCR7, which enables CCL19/21-dependent migration to the medulla[45]. There, DP thymocytes engage spMHC-II on medullary thymic epithelial cells (mTECs) and other thymic APC populations, including B cells, conventional DC subsets (cDC1s and cDC2s), and plasmacytoid DCs. In particular, medullary TECs (mTECs) express the transcriptional regulator Aire, which enables ectopic expression of tissue-specific antigens (TSAs) in these cells[61]. In doing so, Aire allows thymocytes to be "trained" on a wider range of self-peptides that would otherwise be absent in the thymus but may be encountered in the periphery. If thymocytes during the neonatal period cannot undergo Aire-dependent training on TSAs, such as in the case of Aire deficiency, mice and humans develop multiorgan autoimmunity[62]. Lymphocytic infiltration of specific tissues in *Aire*$^{-/-}$ individuals is associated with defective negative selection of CD4^{+} and CD8^{+} T cells exhibiting high extents of reactivity to TSAs, as well as poor TSA-specific tTreg cell differentiation[63–65]. As certain organs are spared from autoimmunity in *Aire*$^{-/-}$ individuals, Aire may not facilitate thymic expression of all TSAs. Moreover, the extent to which a self-reactive thymocyte undergoes deletion versus tTreg

cell induction may depend on which APC presents spMHC-II[66]. Aire-regulated self-antigens may be presented by mTECs themselves or may be transferred from mTECs to thymic DCs; antigen transfer from mTECs to DCs is unidirectional, constitutive, and required for the development of a subset of organ-specific Treg cell clones[67,68]. Independently of Aire, thymic DCs and B cells may also present their own set of endogenous self-antigens and are thought to play non-redundant roles in negative selection and thymic Treg cell induction[69,70]. Thus, to impose central T cell tolerance, a collection of medullary APCs limits thymic egress of self-reactive $CD4^+$ T cell clones through negative selection or skewing towards the tTreg cell fate.

Mechanisms of peripheral tolerance for $CD4^+$ T cells

As discussed above, tolerogenic mechanisms in the thymus are critical for immune homeostasis, as failure to eliminate highly self-reactive thymocytes (as in the case of Bim deficiency[54]) or display tissue-restricted self-antigens (as in the case of Aire deficiency[71]) leads to multiorgan autoimmunity. However, numerous studies have demonstrated the existence of self-reactive $CD4^+$ Tconv and $CD8^+$ T cells in the periphery of healthy mice[64,72,73] and humans[74–76], indicating that negative selection and thymic Treg cell differentiation minimize, but do not completely prevent, the development of self-reactive clones. As such clones may pose risk for autoimmunity, tolerogenic mechanisms in the periphery must compensate for imperfect processes of central T cell tolerance in order to avert disease.

The "toolbox" of peripheral T cell tolerance contains several mechanisms for limiting self-reactive $CD4^+$ Tconv cell activation; these include ignorance to antigen, peripheral deletion, induction of anergy, pTreg induction, and Treg-mediated suppression[77]. As part of ignorance, self-reactive $CD4^+$ Tconv cells may be prevented from encountering their cognate antigens by physical

barriers (e.g., the blood-brain barrier) and/or by inefficient antigen processing or presentation. This separation of autoreactive T cells from spMHC-II averts unwanted activation of the former. While "ignorant" self-reactive $CD4^+$ Tconv cells are antigen-inexperienced, they are not functionally impaired and may undergo activation in the case of sufficient pMHC-II availability.

Should antigen encounter take place, the lack of co-stimulatory ligands on DCs at steady state facilitates peripheral deletion among self-reactive $CD4^+$ Tconv cells. Co-stimulation through CD28 is typically provided to naïve T cells by mature DCs, which have taken up exogenous antigen and received additional pro-inflammatory signals, such as PRR sensing of PAMPs or recognition of other danger signals[11]. In the absence of infection or inflammation, DCs are predominantly immature[78]; while these APCs may still express endogenous self-antigens loaded onto MHC class II molecules, they generally do not upregulate CD80 (B7-1) or CD86 (B7-2). CD28/B7 interactions enhance T cell survival by promoting expression of anti-apoptotic Bcl2 family proteins, such as BclXL[79]. Without CD28 signaling, T cells fail to counter pro-apoptotic factors upregulated downstream of TCR signaling. Thus, at steady state, a self-reactive $CD4^+$ Tconv cell clone can bind to spMHC-II ligands on immature DCs and receive Signal 1; doing so, however, would increase that clone's propensity for apoptosis as a result of missing Signal 2.

Yet, even without co-stimulation, self-reactive $CD4^+$ Tconv cells that experience TCR stimulation are not entirely eliminated from the peripheral repertoire. A fraction of such cells survives and may be restrained via T cell anergy, defined as a state of functional hyporesponsiveness to further TCR stimulation[80]. Early evidence for T cell anergy stems from allograft transplantation studies by Bluestone and colleagues, in which investigators used *in vitro* and *in vivo* anti-CD3 antibody administration to mimic the phenomenon of providing Signal 1 but not Signal 2 to T cells[81,82]. In these studies, while the majority of recipient $CD4^+$ T cells are

depleted following antibody administration, the $CD4^+$ T cells that remain exhibit decreased proliferation and cytokine production when re-stimulated *ex vivo* with anti-CD3[79]. This observation was further supported by work from the Schwartz group, which assessed the function of TCR-transgenic (TCRtg) $CD4^+$ T cells reactive to defined foreign antigens after intravenous transfer of the T cells' cognate antigen. Following contraction of the antigen-specific $CD4^+$ T cell population, surviving antigen-experienced $CD4^+$ T cells displayed impaired upregulation of activation markers, reduced secretion of IL-2, and minimal expansion compared to naïve cells bearing the same TCR[80,83]. While aspects of *in vitro* versus *in vivo* T cell anergy differ, functional defects of anergic $CD4^+$ Tconv cells are generally attributable to impairments in signaling at the level of Ras, MAPK and AP-1 following TCR-dependent upregulation of molecular mediators of T cell dysfunction[84]. These mediators include transcription factors Egr2 and Egr3, E3 ubiquitin ligases Cbl and GRAIL, and diacylglycerol (DAG) kinases responsible for breaking down the secondary messenger DAG. Of note, many of the molecular and functional features of T cell anergy may be reversed upon removal of antigen, co-stimulation through CD28 and/or OX-40, or provision of IL-2. This raises the possibility of inadvertently activating self-reactive $CD4^+$ Tconv cells, should an ongoing immune response provide the co-stimulatory ligands and cytokines needed for release from anergy.

As a failsafe, Treg cells exist to limit instances in which a self-reactive $CD4^+$ Tconv cell receives TCR stimulation and co-stimulation. As discussed above, the majority of Treg cells originate in the thymus following interactions with spMHC-II ligands presented by thymic APCs. In addition, a subset of the overall Treg cell pool consists of peripherally induced Treg (pTreg) cells, which arise from mature $CD4^+$ Tconv cells that upregulate Foxp3 and CD25 following antigen encounter in the periphery. pTreg induction is facilitated by sensing of transforming

growth factor beta (TGFβ), released by a subset of tolerogenic immature DCs and by Treg cells themselves[85,86]. The nature of antigens recognized by pTreg cells and the requirement of co-stimulation for pTreg cell induction remain incompletely understood. However, multiple groups have found limited overlap between the pTreg and tTreg TCR repertoires, indicative of recognition to distinct sets of antigens[86,87]. Moreover, recent work by Surh and colleagues showed that the majority of pTreg cells were induced following the introduction of commensal microbes or dietary antigens, suggesting that these cells prevent pro-inflammatory responses against nonharmful peptides[88]. Thus, foreign-reactive CD4+ Tconv cell clones that are not curbed by central tolerance may be leveraged by the host to avoid unwanted immune-mediated damage. Of note, pTreg cell differentiation was still observed among naïve $CD4^+$ Tconv cells adoptively transferred into *Rag1*$^{-/-}$ germ-free (GF) mice fed an elemental antigen-free (AF) diet[89]. Moreover, deficiency or depletion of pTreg cells leads to colitis and impaired maternal-fetal tolerance[90,91]. These findings demonstrate that the immune system can restrain the pathogenic potential of CD4+ Tconv cell clones that bypass central tolerance by converting them into pTreg cells.

These tolerance mechanisms notwithstanding, suppression in *trans* by tTreg cells represent a linchpin of peripheral tolerance, as indicated by the fatal lymphoproliferative and multiorgan autoimmune disease observed in mice (scurfy) and humans (IPEX) due to genetic inactivation of Foxp3[92]. Similar disease occurs if Treg cells are selectively ablated, as in *Foxp3*^{DTR} mice, which express the human diphtheria toxin (DT) receptor in Foxp3-expressing cells and experience Treg cell loss upon DT administration[93]. Autoimmunity also ensues in mice whose Treg cells have been functionally impaired; examples include *Foxp3*^{Cre} *Cd25*$^{fl/fl}$, *Foxp3*^{Cre} *Ctla4*$^{fl/fl}$, and *Foxp3*^{Cre} *Il10ra*$^{fl/fl}$ mice, which exhibit Treg-specific deletion of the high-affinity IL-2 receptor[94], the co-inhibitory receptor CTLA-4[95], and the IL-10 receptor[96], respectively. Each of these mouse models

displays robust lymphocytic infiltration of skin, gastrointestinal tract, and/or other non-lymphoid tissues, accompanied by increased mortality. In this vein, Treg-specific ablation studies have elucidated several suppressive modalities of Treg cells, which include depletion of local IL-2 levels via CD25, depriving nearby effector T cells of IL-2; use of CTLA-4 to disrupt CD28-B7 interactions between T cells and APCs; and production of soluble anti-inflammatory mediators and cytokines, such as IL-10. By leveraging these and other suppressive functions, Treg cells can antagonize co-stimulation, expansion, and function of self-reactive $CD4^+$ Tconv cells and drive them towards anergy, deletion, or pTreg differentiation[56,97,98].

The role of TCR:spMHC-II interactions in promoting Treg cell function

Still, open questions remain regarding the ability of Treg cells to prevent antigen recognition by self-reactive $CD4^+$ Tconv cells. While it is well appreciated that Treg cells require TCR signaling to exert their suppressive function, ongoing work continues to elucidate the ways in which TCR:spMHC-II interactions govern Treg cell function[99–101]. Three such ways are reviewed herein. First, TCR signaling in Treg cells triggers differentiation into an effector Treg (eTreg) state, marked by enhanced suppressive capacity[102]. By studying *Foxp3*$^{Cre\text{-}ERT2}$ *Tcra*$^{fl/fl}$ mice, which exhibit tamoxifen-inducible Treg-specific loss of the TCRα chain, Levine *et al.* link autoimmunity in these mice to a loss of $CD44^{hi}$ $CD62L^{lo}$ effector Treg cells, suggesting that Treg cells must undergo activation and differentiation into the eTreg state in order to achieve full suppressive capacity[99]. Similarly, Vahl *et al.* note that TCR ablation on Treg cells leads to diminished expression of IL-10[100]; this latter finding was corroborated by observations of reduced IL-10 positivity when Treg cells were treated with the TCR signaling inhibitor tacrolimus[103]. However, these studies both reported similar, if not heightened, extents of IL-2 receptor expression

and signaling in the absence of TCR signaling, indicating that only part of the Treg suppressive program is TCR-dependent. Moreover, analyses of Treg cells in Nur77^{GFP} mice – whose expression of a fluorescent reporter positively correlates with the intensity of TCR signaling[104] – found similar CD62L expression among GFP^{hi} and GFP^{lo} cells[105]. This raises three interesting possibilities: (1) Nur77^{GFP} expression by Treg cell subsets reflects signaling derived from both cognate and non-cognate interactions with spMHC-II, obscuring the relative contributions of agonist versus tonic signaling on eTreg cell differentiation; (2) TCR signals are necessary but not sufficient to induce differentiation from the CD62L^{hi} central Treg (cTreg) to the CD62L^{lo} eTreg state; and/or (3) TCR signaling can be antagonized or counterbalanced by other signaling pathways to prevent cTreg-to-eTreg cell conversion.

Second, TCR:pMHC-II binding allows for apposition of Treg cells with APCs, along with upregulation and activation of cell adhesion molecules. Together, these events allow Treg cells to engage in prolonged contacts with APCs, leading to the latter's downregulation of CD80 and CD86. The Sakaguchi group first demonstrated this by studying DO11.10 TCRtg Treg cells, which react to a chicken ovalbumin (OVA) peptide presented on MHC class II molecule I-A^{d}. *In vitro* co-culture assays revealed that DO11.10 TCRtg Treg cells aggregated around DCs and B cells only in the presence of antigen and only when the TCR-induced integrin LFA-1 was allowed to bind to its targets[106]. Down-regulation of CD80 and CD86 occurred in a CTLA-4-dependent manner, an observation corroborated by later work implicating CTLA-4 in Treg cell-mediated removal of CD80/86 from DCs via trogocytosis[107]. In the examples presented thus far, TCR-mediated antigen recognition by Treg cells promotes several antigen-nonspecific suppressive mechanisms. By imposing a TCR requirement for Treg function, the immune system may limit

potent anti-inflammatory actions to discrete microenvironments, rather than allowing Treg cells to have systemic effects[108].

Third, a Treg cell may use its TCR to restrict the number of spMHC-II complexes available for $CD4^+$ Tconv cells with matched specificity. This constitutes antigen-specific suppression, which can occur through ligand occupancy and/or ligand stripping. Treg cells may use their TCR to outcompete their $CD4^+$ Tconv cell counterparts for binding to spMHC-II ligands[109]. By occupying sites of spMHC-II, Treg cells would block naïve $CD4^+$ Tconv cells from accessing self-ligands, thereby preventing priming of the latter against self. In the same vein, Treg cells may disrupt ongoing interactions between $CD4^+$ Tconv cells and APCs, leading to limited $CD4^+$ Tconv cell activation. Apart from this "goalkeeping," Treg cells may remove the goal entirely; recent work by Shevach and colleagues showed that Treg cells have the capacity to remove pMHC-II molecules from DCs via trogocytosis and do so in an antigen-specific manner[110]. These demonstrations of antigen-specific suppression by Treg cells help address a longstanding conundrum regarding Treg cell function: in situations where an APC presents self- and foreign-derived antigens simultaneously, Treg cells employing only antigen-nonspecific suppressive mechanisms would preserve tolerance towards self-antigens at the expense of host defense against foreign invaders. Instead, a combination of antigen-specific and -nonspecific mechanisms enables Treg cells to prevent unwanted autoimmune responses while permitting the immune system's resistance to non-self.

Dissecting TCR:pMHC affinity, T cell avidity, sensitivity, and potency

For Treg cells to successfully outcompete $CD4^+$ Tconv cells for binding to spMHC-II molecules, something must impart upon Treg cells a competitive advantage for ligand binding

and/or association with APCs. Such an advantage can be described in terms of a $CD4^+$ T cell's overall avidity for a given pMHC-II ligand. T cell avidity is defined as the strength with which a T cell engages an antigen source, and is primarily dependent on the number and quality of TCR:pMHC interactions[111]. Experimentally, T cell avidity can be approximated via staining of $CD4^+$ T cells with pMHC-II multimers. The original pMHC multimers described by the Davis group consisted of four biotinylated pMHC-I monomers complexed to streptavidin; conjugation of the streptavidin backbone to a fluorophore enabled detection of pMHC-I tetramer-binding $CD8^+$ T cells by flow cytometry[112]. This technology was later adapted to facilitate labeling of antigen-specific $CD4^+$ T cells using pMHC-II tetramers. For both $CD4^+$ and $CD8^+$ T cells, cells exhibiting more intense and/or persistent staining with pMHC tetramers are thought to exhibit greater T cell avidity for that particular pMHC ligand.

Of note, TCR:pMHC interactions can be stabilized by co-receptor binding to invariant regions of MHC. While CD4 and CD8 are known to bind MHC class II and MHC class I molecules, respectively, several groups have shown that the CD4 interaction with MHC-II is weaker than the interaction between CD8 and MHC-I. Moreover, CD4 may preferentially bind already pre-formed TCR:pMHC pairs, suggesting that the degree to which CD4 promotes initial bond formation between TCR and pMHC is minimal[34,113,114]. Thus, contributions of the CD4 co-receptor to avidity for antigen will not be discussed further.

Whereas T cell avidity reflects the contributions of multiple TCR:pMHC bonds, TCR:pMHC affinity refers to the strength of the binding interaction between a single TCR and its pMHC ligand[111]. Key biochemical parameters of the TCR:pMHC interaction include the rate at which the TCR associates with pMHC (on-rate, or k_{on}); the rate at which the TCR:pMHC complex dissociates into its constituent parts (off-rate, or k_{off}); and the half-life of the TCR:pMHC

interaction ($t_{1/2}$; also referred to as dwell time). Additionally, the ratio of off- and on-rates gives rise to the dissociation equilibrium constant (K_D). TCR:pMHC affinity is often conceptualized as the inverse of K_D, such that lower K_D values indicate higher TCR affinities for a particular pMHC ligand. Historically, TCR:pMHC affinities have been measured via surface plasmon resonance (SPR), a three-dimensional binding assay in which individual TCRs are immobilized onto a sensor surface and subjected to flow of soluble pMHC ligands[115]. More recently, a micropipette-based assay has been developed to quantify TCR:pMHC binding parameters in two-dimensional space (2D-MP)[116]; this assay defines effective 2D affinity as a metric that increases in value with stronger TCR:pMHC binding. Whether 2D or 3D affinity measurements are employed, increased TCR:pMHC affinity has been associated with greater T cell avidity, as shown by more robust pMHC tetramer labeling of T cells bearing higher-affinity TCRs[117–119]. In fact, it is generally appreciated that pMHC tetramer reagents exhibit a bias towards identifying T cells with greater avidities and higher TCR:pMHC affinities. pMHC multimers often fail to detect low-avidity antigen-specific T cells, despite mounting evidence that such cells contribute to ongoing immune responses[120,121].

The involvement of pMHC tetramer-negative T cells in immune responses raises a key question: in which ways does TCR:pMHC affinity or T cell avidity affect T cell function? What dictates a T cell's sensitivity to antigen versus a T cell's potency? Importantly, these terms all differ from one another, despite the misleading tendency to treat them as interchangeable. Affinity and avidity are defined above. Sensitivity – also referred to as "functional avidity" – describes a T cell's propensity to translate external cues into cell-intrinsic functional responses. These include phosphorylation of proximal (e.g., ZAP70) and distal (e.g., Erk) components of the TCR/CD3 signaling cascade, induction of TCR-dependent negative regulators (e.g., Nur77, Egr2), and T cell

proliferation or cytokine production. Potency specifically relates to whether a T cell's function culminates in a larger, cell-extrinsic immune response, such as pathogen clearance, tumor rejection, or disease incidence. However, for each of these terms, readouts are often reported across a range of antigen concentrations, enabling comparison of distinct T cell clones and their relative characteristics at a given antigen dose.

Like T cell avidity, T cell sensitivity integrates signals derived from multiple TCR:pMHC interactions, which can be affected by the affinity of each TCR:pMHC bond and modulated by co-stimulatory and cytokine-derived signals. However, T cell sensitivity to antigen is also modulated by the effects of co-stimulatory, co-inhibitory, and cell adhesion molecules. (The related terms, TCR signal strength and signal quality, ignore these influences but often use many of the same readouts.[122]) Multiple studies have found that Treg cells form tighter and more long-lasting clusters with DCs compared to $CD4^+$ Tconv cells, even when the Treg and $CD4^+$ Tconv cells bear the same TCR[106,110,123]. These observations likely arise due to differential expression[123], regulation[124], and/or function[125] of integrins on Treg versus $CD4^+$ Tconv cells. However, CTLA-4/B7 interactions as well as DC expression of chemokines that preferentially recruit Treg cells may also play a role[107,126]. While these findings implicate TCR-independent mechanisms in increasing Treg cell access to spMHC-II molecules, more work is required to assess how non-TCR-related aspects of the Treg cell program shape Treg cell interactions with APCs.

Moreover, T cell sensitivity relies on whether a T cell has previously been exposed to cognate antigens and whether a T cell experiences strong tonic signaling at baseline. The effects of past antigen encounter on T cell sensitivity are readily observed among memory or anergic T cells, which - when compared to naïve T cells bearing the same antigen specificity - respond to antigen more or less rapidly, respectively[127,128]. Regarding the role of tonic signaling, T cells

reactive to foreign antigens transiently engage in non-cognate interactions with spMHC molecules expressed by DCs at steady state. Ablation of DCs or transfer of $CD4^+$ T cells into either MHC-II-deficient or -mismatched recipients led to poorer T cell signal transduction and proliferation following exposure to cognate pMHC-II ligands *in vitro*[129,130]. Moreover, a recent characterization of two $CD4^+$ T cell clones reactive to *Listeria monocytogenes* (*Lm*) demonstrated that tonic signaling in response to spMHC-II led to increased levels of baseline CD3ζ phosphorylation, along with greater Erk phosphorylation and production of IL-2 upon cognate TCR:pMHC interactions[131]. These confounding variables notwithstanding, studies that dissect the TCR- and non-TCR-based components on T cell sensitivity to spMHC-II can be powerful for understanding how Treg and self-reactive $CD4^+$ Tconv cells compete with each other for access to antigens.

Basis of increased Treg cell sensitivity for spMHC-II ligands conferred by Treg TCRs

Several lines of evidence support the notion that, compared to $CD4^+$ Tconv cells, Treg cells exhibit higher sensitivities for spMHC-II due to their TCRs. First, studies comparing the TCR repertoires of Treg and $CD4^+$ Tconv cells note that Treg and $CD4^+$ Tconv TCRs are largely distinct, implying that these two populations differ in their ability to bind and/or respond to pMHC-II ligands[132,133]. In line with this, $CD4^+$ Tconv cells transduced with Treg-derived TCRs proliferated extensively and induced wasting disease following transfer into lymphopenic mice, indicating that the Treg cell repertoire is enriched for clones with increased reactivity to spMHC-II. Similar findings were reported by the Fillatreau group, which studied Treg and $CD4^+$ Tconv cells reactive to the myelin oligodendrocyte glycoprotein (MOG) self-antigen[72]. Kieback *et al.* transduced a TCR-deficient cell line with MOG-reactive Treg or $CD4^+$ Tconv cell TCRs, stimulated the resulting cells with a range of MOG peptide doses, and observed that Treg TCRs induced more

IL-2 production than $CD4^+$ Tconv TCRs at each peptide concentration tested. Furthermore, comparisons of Treg versus $CD4^+$ Tconv cells in the SLOs of $Nur77^{GFP}$ reporter mice revealed greater GFP expression among Treg cells at steady state, demonstrating that polyclonal Treg cells experience more frequent and/or more intense TCR signals in response to endogenous pMHC-II ligands[104].

In several studies of thymic development, greater T cell sensitivity to spMHC-II has been associated with tTreg cell differentiation. Early work by Caton and colleagues demonstrated that $CD4^+$ T cells reactive to a I-E^d-restricted peptide derived from influenza hemagglutinin (HA) developed into Treg cells only when the HA peptide was transgenically expressed in host cells[134]. When the HA-specific TCR was mutated to reduce its TCR affinity for HA/I-E^d, tTreg cell development was abrogated, demonstrating the role of high-affinity TCR:pMHC-II interactions in promoting the tTreg cell fate[135]. Later work by the Hsieh group expanded on this finding using transgenic mice expressing membrane-bound OVA under the control of the rat insulin promoter (RIP)[136]. In RIP-mOVA mice, OVA serves as a model "self" antigen; introduction of BALB/c thymocytes bearing TCRs with varying affinities for $OVA_{323-339}$/I-A^d revealed that the efficiency of Treg cell development increased with increasing TCR:pMHC-II affinity. More recently, Stadinski *et al.* used pMHC tetramers to identify naturally occurring $CD4^+$ T cell clones reactive to an endogenous self-antigen, Padi4[137]. In measuring the pMHC-II binding kinetics of Padi4-reactive TCRs, the authors found that TCRs exhibiting intermediate dwell times with Padi4/I-A^b enabled tTreg cell induction, whereas shorter dwell times led to development as $CD4^+$ Tconv cells. Collectively, these and other findings demonstrate that Treg cells are selected based on more potent and/or prolonged interactions with spMHC-II ligands in the thymus. tTreg cell differentiation also depends on the spatiotemporal availability of spMHC-II ligands, cytokines, and other factors.

Nevertheless, prevailing models of $CD4^+$ T cell development postulate that agonist TCR:spMHC-II interactions drive the development of Treg cells, which generally exhibit greater sensitivity to spMHC-II compared to their $CD4^+$ Tconv cell counterparts[66]. While a minor fraction of $CD4^+$ T cell clones are shared between the Treg and $CD4^+$ Tconv cell repertoires, population-level differences in T cell sensitivity to self – as imposed by mechanisms of central tolerance – likely contribute to Treg-mediated control of $CD4^+$ Tconv cells.

Role of T cell sensitivity in tTreg cell differentiation versus negative selection

Prior to examining the impact of T cell sensitivity on the function of self-reactive $CD4^+$ Tconv cells, it is important to note that evidence supporting T cell sensitivity to self-antigens as a primary determinant of the developmental fates of MHC-II-restricted thymocytes stems largely from the study of foreign-reactive TCRs responding to transgenically expressed model antigens. The affinity model of thymic development posits that that intermediate TCR-pMHCII affinities – at the threshold between positive and negative selection – promote optimal tTreg cell development, allowing Treg cell clones to differentiate while also evading clonal deletion. However, in studies using engineered TCR-ligand systems, increasing TCR:pMHC-II affinities have been associated with increased and concomitant occurrence of both tTreg cell differentiation and clonal deletion. For example, the aforementioned work by Jordan *et al.* showed that, in HA-transgenic, their high-affinity HA-reactive $CD4^+$ T cell clone underwent clonal deletion, with approximately half of the remaining cells expressing Foxp3[135]. In contrast, their low-affinity HA-specific clone experienced neither deletion nor diversion into the Treg cell lineage. Similarly, Lee and colleagues demonstrated that both intermediate- and high-affinity OVA-specific TCRs facilitated tTreg cell development, with the latter also triggering clonal deletion. Moreover, the idea that TCR-pMHCII

affinity exclusively determines whether a self-reactive thymocyte undergoes clonal deletion or Treg cell development is inconsistent with data from studies examining polyclonal Treg cells reactive to natural endogenous ligands. Specifically, Stritesky *et al*. noted that Treg cell expression of $Nur77^{GFP}$ is similar to that of Tconv cells rescued from negative selection in mice lacking the pro-apoptotic Bcl-2 family member Bim[138]. This finding suggests that the strength of TCR signals encountered by polyclonal Treg cells is comparable to that of thymocytes destined to undergo deletion. At the clonal level, Hsieh and colleagues demonstrated that the G113 TCR, a naturally occurring Treg-derived TCR, facilitates Treg cell development with no evidence of coincident clonal deletion[139]. Consistent with this, our own studies of the naturally occurring C4-reactive MJ23 Treg cell clone demonstrate that the thymic presentation of C4 peptide does not impact the frequency of MJ23-expressing thymocytes at different stages of development, suggestive of minimal clonal deletion[65,140,141]. Collectively, these and other studies suggest that increasing TCR affinity for a given spMHC-II ligand can promote both clonal deletion and tTreg cell development, leaving the factors that drive one of these outcomes over the other unclear. The timing of self-antigen exposure, the density and expression patterns of self-antigens, the nature of the APC presenting self-antigens, and the availability of pro-survival cytokines all contribute to the fate determination process of self-reactive MHC-II-restricted thymocytes.

Relationship between $CD4^+$ Tconv cell potency and sensitivity to pMHC-II

In many settings of autoimmunity, self-reactive $CD4^+$ Tconv cells clearly egress from the thymus, escape Treg control, and actively contribute to disease. To what extent does T cell sensitivity to spMHC-II affect the potency of self-reactive $CD4^+$ Tconv cells? Using a variety of TCR-antigen systems and inflammatory settings, numerous groups have sought to define the

impact of T cell sensitivity to pMHC-II on each facet of $CD4^+$ Tconv cell function; many such studies unfortunately paint a conflicting picture of this relationship.

To vary the TCR:pMHC component of T cell sensitivity, one can either study distinct TCRs recognizing the same pMHC ligand or use varying pMHC ligands capable of binding the same TCR. The latter is often accomplished by using altered peptide ligands (APLs); in an APL system, a TCR's cognate antigen is mutated to create similar peptides harboring single amino acid substitutions[142]. These subtle changes in peptide sequence can allow an APL to trigger stronger or weaker stimulation of the TCR under study, often as a result of differing TCR-APL binding kinetics relative to those of the cognate TCR:pMHC interaction. Several studies have employed APLs to characterize responses of $CD4^+$ Tconv cells reactive to moth cytochrome c (MCC)-derived peptides. In doing so, they have demonstrated that MCC-reactive $CD4^+$ Tconv cells engaging in lower-avidity interactions with "weak" APLs do not proliferate as quickly or as extensively as MCC-reactive $CD4^+$ Tconv cells that undergo higher-avidity interactions with MCC[127,143,144]. Similar findings were observed for $CD4^+$ T cells reactive to influenza-derived nucleoprotein[145], as well as for the OVA-reactive $CD8^+$ T cell clone OT-I[146]. However, in APL studies, it remains unclear whether a history of strong encounter with pMHC translates to potent T cell responses. Johanns *et al.* found that *Salmonella typhimurium (St)* -specific $CD4^+$ T cells exhibit similar extents of pathogen control whether they are first primed with a "strong" *St* APL or are left unprimed[147]. In contrast, following adoptive transfer, influenza-specific memory $CD4^+$ T cells promoted improved survival of mice upon influenza infection when initial priming of those cells involved higher-avidity interactions with influenza APLs[145]. Further complicating the issue, a recent study found that OT-I cells failed to reject subcutaneous MCA205 tumors regardless of

the OVA APL expressed by the tumor[148]. Collectively, these studies illustrate how use of APL systems has led to inconclusive evidence linking T cell sensitivity to potent T cell responses.

In experiments that vary the TCR and keep the antigen consistent, a slightly clearer picture emerges. Gallegos *et al.* profiled two $CD4^+$ T cell clones reactive to *Mycobacterium tuberculosis* (*Mtb*), termed C7 and C24[149]. Compared to C7, the C24 clone more readily bound *Mtb*-specific pMHC-II tetramer and proliferated more robustly at low *Mtb* ESAT6 peptide concentrations, indicating the C24 is more sensitive to ESAT6 than C7 is. However, in adoptive transfer experiments, when mice receiving C24 were exposed to *Mtb* infection, these mice exhibited worse pathogen burden compared to mice that received C7, pointing to a disconnect between T cell sensitivity and T cell potency. The authors attribute this disconnect to TCR downregulation by the C24 clone, although decreased survival of high-avidity $CD4^+$ T cells and/or reduced cytokine production by these cells may also contribute to poorer T cell potency[150]. Similar findings were reported in the context of autoimmunity, when the Vignali group characterized eight TCRs recovered from $CD4^+$ T cells that had infiltrated the islets of non-obese diabetic (NOD) mice[151]. The TCRs studied by Bettini *et al.* spanned a tenfold range of effective 2D TCR affinities for the same insulin-derived spMHC-II ligand. Notably, insulin beta-reactive $CD4^+$ Tconv cells bearing higher- or lower-affinity TCRs induced similar extents of insulitis when transferred into lymphopenic NOD.*scid* recipients. The clone with the highest TCR:InsB/I-A^{g7} affinity failed to promote diabetes, likely through TCR downregulation, induction of anergy, and/or activation-induced cell death. Together, these findings suggest that the potency of $CD4^+$ Tconv cells exhibiting high sensitivity to pMHC-II ligands is curbed by cell-intrinsic mechanisms of peripheral T cell tolerance. Whether this leads to preferential expansion or function of lower-sensitivity $CD4^+$ Tconv cells as an immune response progresses remains fiercely debated[119,121,144,152–155] (see

Discussion). Regardless, $CD4^+$ Tconv cells with lower sensitivities to pMHC-II demonstrate the ability to expand and exert effector functions following antigen encounter. Thus, self-reactive $CD4^+$ Tconv cells, which appear more likely to avoid clonal deletion or Treg cell induction in the thymus, still exhibit sensitivities to spMHC-II ligands that are permissive for pathogenesis. Release from cell-extrinsic peripheral tolerance mechanisms, such as Treg-mediated suppression, may enable these cells to drive autoimmune responses.

Th cell differentiation & function as a product of sensitivity to pMHC-II

Although T cell sensitivity for spMHC-II may not perfectly correlate with autoimmune disease incidence or severity, it may still affect the skewing of self-reactive $CD4^+$ Tconv cells towards different Th cell fates. This holds implications for autoimmune diseases in which multiple immune cell types are involved, as each Th subset is specialized to interface with different subsets of immune cells[10,42]. Multiple studies of foreign-reactive $CD4^+$ T cell clones have varied either the antigen dose used for stimulation or the relative TCR:pMHC-II affinity, observing increased Th1 and decreased Th2 cell differentiation with increasing TCR stimulation[156–160]. Moreover, in work by Germain and colleagues, elevated pMHC-II concentrations favored Th1 cell induction even in the presence of a Th2-promoting adjuvant, indicating that T cell sensitivity for pMHC-II could outweigh the impact of co-stimulation and cytokines on Th fate determination. However, the impact of T cell sensitivity for pMHC-II on Th17 cell differentiation is less clear, with groups reporting improved Th17 cell induction under conditions of stronger[161] or weaker[162] TCR stimulation. Regarding Tfh cell differentiation, a recent study profiling polyclonal $CD4^+$ Tconv cells reactive to lymphocytic choriomeningitis virus (LCMV) found that LCMV-specific Tfh cells exhibited increased 2D TCR:pMHC-II affinities, TCR expression levels, and IL-2 production

compared to non-Tfh cells of matched antigen specificity[163]. This finding fits with earlier results from the McHeyzer-Williams group, which observed greater Tfh cell differentiation among TCRtg $CD4^+$ Tconv cells with higher TCR affinities for PCC/I-E^k [164]. While these studies point to a positive correlation between T cell sensitivity to pMHC-II and Tfh cell differentiation, Kotov *et al.* note that high-affinity TCR:pMHC-II interactions also leads to the upregulation of CD25[165]; signaling through the IL-2 receptor-STAT5 axis induces the Bcl6 antagonist, Blimp-1, and inhibits Tfh cell differentiation[166,167]. Collectively, these findings suggest that heightened T cell sensitivity to pMHC-II promotes the generation of both Tfh and Th1 cells, and that the Tfh-versus-Th1 cell fate decision is primarily driven by co-stimulatory and/or cytokine-derived signals[168,169].

Once a $CD4^+$ Tconv cell adopts a given Th cell fate, its sensitivity to pMHC-II may continue to shape its Th-specific functions. To date, few studies have rigorously assessed a direct link between T cell sensitivity to pMHC-II and interferon-gamma (IFN-γ) production in already differentiated Th1 cells. However, higher-affinity TCR:pMHC-II interactions may indirectly support Th1 cell function by inducing greater upregulation of CD40 ligand (CD40L) and IL12Rβ2. CD40L provides co-stimulation to CD40-expressing DCs and is necessary but not sufficient to trigger DC expression of IL-12. Still, greater magnitudes of CD40-mediated signaling can enhance the amount of IL-12 secreted by DCs[170]. This increased IL-12 – sensed through IL12Rβ2 – likely drives increased IFN-γ release from existing Th1 cells. A clearer link may be drawn between T cell sensitivity to pMHC-II and Tfh cell function. Tfh cells license B cells to undergo immunoglobulin (Ig) class switch recombination at the T-B border[171] and somatic hypermutation within germinal centers (GCs)[172]. Tfh cells provide this B cell help in the form of IL-21 and CD40L[169]; expression of each is positively correlated with T cell sensitivity to pMHC-II[173–175]. Moreover, in the GC, B cells that have undergone activation following ligation of antigen alternate

between periods of proliferation in the dark zone (DZ) and selection in the light zone (LZ)[176]. In the LZ, GC B cells capable of internalizing, processing, and presenting antigen to GC Tfh cells receive cues that promote GC B cell survival, migration to the DZ, proliferation, and exit as antibody-secreting cells (ASCs). GC B cells with higher BCR avidities for antigen are thought to more readily capture and present antigen to GC Tfh cells, leading to preferential selection and expansion of high-avidity GC B cells[177,178]. Notably, higher-affinity TCR:pMHC-II interactions were found to increase Tfh proliferation within the GC, as well as the magnitude of signals associated with positive selection within GC B cells[179]. While further work is required to carefully assess how Tfh cell sensitivity to pMHC-II affects the affinities of antibodies generated by ASCs[180], the studies summarized here indicate that elevated T cell sensitivity to pMHC-II leads to increased GC Tfh cell numbers, improved delivery of B cell help, and modulation of the B cell clones that participate in GC reactions.

Th1 and Tfh cells in autoimmunity and antitumor immunity

Prior to the identification of other Th subsets, Th1 cells were considered the key drivers of disease in organ-specific T cell-mediated autoimmunity. In contrast, skewing of the immune system towards a Th2 response predispose mice and humans to allergy and atopy. The discovery of Th17 cells prompted a reevaluation of Th1 cells' central role in autoimmunity, leading to revised paradigms of pathogenesis for multiple sclerosis (MS), inflammatory bowel disease (IBD), and rheumatoid arthritis (RA), among other disorders. In particular, Th1 and Th17 cells are thought to jointly promote demyelination and immune cell recruitment in MS and its murine model, EAE. In EAE, adoptive transfers of myelin-specific $CD4^+$ Tconv cells after *in vitro* polarization to either the Th1 or Th17 cell program led to similar extents of disease severity. However, Th1 cell transfers

preferentially induced infiltration of monocytes and macrophages into the central nervous system (CNS), whereas Th17 cell transfers enabled the recruitment of neutrophils. This finding highlights how the respective contributions of different Th cell subsets can shape both the complexity and course of autoimmune responses.

With the identification of Tfh cells came a similar appreciation of collaboration between Tfh and Th1 cells in autoimmunity. For example, Tfh cells had been implicated separately in the pathogenesis of systemic lupus erythematosus (SLE), a systemic autoimmune disorder characterized by autoantibody production against nuclear antigens. In SLE, formation and deposition of antigen-antibody complexes in skin, kidney, blood vessel walls, and other sites triggers complement activation and inflammation, leading to progressive damage of host tissues[181]. SLE-prone *Roquin*$^{san/san}$ mice, which exhibit deficits in the mRNA-repressing ubiquitin ligase, Roquin1, were shown to harbor increased frequencies of Tfh cells, which were capable of inducing SLE upon adoptive transfer into WT recipients[182]. Interestingly, in a subsequent study of both the *Roquin*$^{san/san}$ and *Fas*$^{-/-}$ models of SLE, increased IFN-γ expression by CD4^{+} Tconv cells was shown to promote elevated Tfh cell numbers and autoantibody production, suggesting that Th1 cells may support Tfh cell recruitment and/or expansion within sites of inflammation[183]. Moreover, in patients with advanced lupus nephritis, a more serious complication of SLE, the glomeruli of the kidney exhibit increased expression of the Th1-inducing cytokines IL-12 and IL-18, as well as increased infiltration of T-bet^{+} and IFN-γ-producing CD4^{+} Tconv cells[184,185]. SLE-prone mice deficient in either IFN-γ or its receptor do not develop glomerulonephritis, further emphasizing the importance of Tfh-Th1 cell crosstalk in the progression of autoimmunity. Lastly, as primary producers of IFN-γ, Th1 cells facilitate the secretion of the IgG2a antibody subtype, whose more potent binding to Fc gamma receptors has been associated with higher pathogenicity in a number

of autoimmune settings[186–188]. These and other findings suggest that the interplay between Tfh and Th1 cells may also underlie the emerging role of Tfh cells in type 1 diabetes[189,190], MS/EAE[191], and other autoimmune diseases[169,192].

While self-directed pro-inflammatory immune responses are detrimental to the host in the context of autoimmunity, such responses are critical for the clearance and control of tumors. Th1 cells have long been thought to promote antitumor immunity by supporting the functions of cytotoxic $CD8^+$ T lymphocytes (CTLs), pro-inflammatory macrophages, and DCs[193]. Adoptive transfers of tumor-specific Th1 cells have led to tumor regression and stabilization of disease in human cancer patients, underscoring the central role of these cells in tumor control[194]. Additionally, comparative studies of immune checkpoint blockade (ICB) therapies, which employ antibodies to interfere with signaling through T cell co-inhibitory receptors, found an increase in tumor-infiltrating Th1 cells following administration of anti-CTLA-4[195,196]. Interestingly, these intratumoral Th1 cells expressed high levels of the Tfh-related markers PD-1 and ICOS, but remained negative for Bcl6. More importantly, these Th1 cells were correlated with decreased tumor volume, although assessment of the precise functions of these cells requires further study.

In addition to Th1 cells, a growing body of evidence points to a role for Tfh cells in antitumor immunity. Across multiple cancer types, a subset of patients exhibits tertiary lymphoid structures (TLSs), either within or near established tumors[197]. TLSs form in environments of chronic inflammation and their intratumoral presence is associated with improved prognosis following ICB[198,199]. Tfh cells often represent a large proportion of $CD4^+$ Tconv cells within TLSs and can interact with tumor-infiltrating T and B cells. In a recent report, Cui *et al.* found that B cells were able to uptake and present tumor-derived neoantigens (neoAgs) – whose expression is unique to tumors – to neoAg-specific Tfh cells. The resulting Tfh-B cell interactions occurred

within GCs and led to the production of IL-21, which sustained CTL numbers, promoted expression of the cytotoxic effector granzyme B, and prevented tumor outgrowth[200]. This finding builds upon several other studies linking IL-21 to improved $CD8^+$ T cell responses against tumors[201–203]. In adoptive transfer settings, Tfh cells were also found to elicit TLS formation and tumor regression, suggesting that recognition of tumor-associated antigens (TAAs) by Tfh cells can initiate generation of TLSs and promote the recruitment of additional T and B cells into the tumor microenvironment[204,205].

Understanding how TCR:spMHC-II interactions govern self-directed immune responses

T cell-mediated responses targeting neoAgs are made possible by elevated mutation rates in tumors, which yield immunogenic peptides that are foreign to the host[206,207]. As a result, responses against neoAgs are presumed to be less susceptible to control by mechanisms of T cell tolerance compared to responses against *bona fide* self-peptides[208], meaning that $CD4^+$ and $CD8^+$ T cells exhibiting higher sensitivities to tumor-derived pMHC may more readily arise and mediate tumor eradication. However, the immune system can fail to clear tumors expressing neoAgs and can still generate antitumor responses towards cancers with low somatic mutation burdens, calling into question the necessity and sufficiency of neoAgs for antitumor immunity[208,209]. A more convincing paradigm of antitumor immunity involves a combination of $CD4^+$ and $CD8^+$ T cell responses against TAAs, with the latter comprising both neoAgs and unmutated spMHC ligands[210]. As tumors may evolve mechanisms of immune evasion while under selective pressure by the immune system, the targeting of multiple self- and tumor-derived antigens likely increases the chance of eliminating neoplasms[211,212].

How, then, does the immune system balance the advantages and disadvantages of maintaining a self-reactive $CD4^+$ Tconv cell population in the periphery? Moreover, how do TCR:spMHC-II interactions affect the phenotypes, functions, and regulation of self-reactive $CD4^+$ Tconv cells, either at steady state or in settings of immune perturbation? Lastly, does the expression pattern of self-antigens shape the relationship between sensitivity to spMCHII and function of self-reactive $CD4^+$ Tconv cells? The work summarized herein seeks to address these questions via an in-depth clonal analysis of $CD4^+$ Tconv cells reactive to either a murine prostate-specific self-antigen or a yet-undefined self-antigen expressed across murine SLOs.

CHAPTER II: MATERIALS AND METHODS

Mice

The following mice were purchased from the Jackson Laboratory: B6 (C57BL/6J; stock no. 000664); *Aire*$^{-/-}$ (B6.129S2-Aire$^{tm1.1Doi}$/J; stock no. 004743); B6.SJL, also known as B6 CD45$^{.1/.1}$ (B6.SJL-*Ptprc*^{a} *Pepc*^{b}/BoyJ; stock no. 002014); *Rag1*$^{-/-}$ (B6.129S7-*Rag1*^{tm1Mom}/J; stock no. 002216); *Tcra*$^{-/-}$ (B6.129S2-*Tcra*^{tm1Mom}/J; stock no. 002116 or 002115); *Foxp3*$^{DTR\text{-}EGFP}$ (B6.129(Cg)-*Foxp3*$^{tm3(DTR/GFP)Ayr}$/J; stock no. 016958); *Foxp3*^{EGFP} (B6.Cg-*Foxp3*^{tm2Tch}/J; stock no. 006772); OT-II (B6.Cg-Tg(TcraTcrb)425Cbn/J; stock no. 004194); *Tcrb*$^{-/-}$ (B6.129P2-*Tcrb*^{tm1Mom}/J; stock no. 002118); TRAMP$^{+/-}$ (C57BL/6-Tg(TRAMP)8247Ng/J; stock no. 003135); *MHCII*$^{-/-}$ (B6.129S2-*H2*$^{dlAb1\text{-}Ea}$/J; stock no. 003584 or 003374); *Mb1*^{Cre} (B6.C(Cg)-*Cd79a*$^{tm1(cre)Reth}$/EhobJ; stock no. 020505); and *Rosa26*$^{LSL\text{-}DTR}$ (C57BL/6-*Gt(ROSA)26Sor*$^{tm1(HBEGF)Awai}$/J; stock no. 007900). B6.CgTg(CD4-cre)1Cwi (*Cd4*^{Cre}; model no. 4196) mice were obtained from Taconic. TCR Vβ3 transgenic (TCRβtg) mice expressing a fixed TCRβ chain of sequence Vβ3-(TRBV26-ASSLGSSYEQY) were generated on a C57BL/6J background at the University of Chicago Transgenics Core Facility, as previously described[65]. TCRβtg and *Foxp3*$^{DTR\text{-}EGFP}$ mice were interbred to obtain TCRβtg *Foxp3*$^{DTR\text{-}EGFP}$ mice. *Cd4*^{Cre}, *Tcra*$^{-/-}$, and TCRβtg mice were interbred to obtain *Cd4*^{Cre} *Tcra*$^{-/-}$ TCRβtg mice. *Cd4*^{Cre} *Tcra*$^{-/-}$ TCRβtg and *Foxp3*$^{DTR\text{-}EGFP}$ mice were interbred to obtain *Cd4*^{Cre} *Tcra*$^{-/-}$ TCRβtg *Foxp3*$^{DTR\text{-}EGFP}$ mice. B6 CD45$^{.1/.1}$ and *Foxp3*$^{DTR\text{-}EGFP}$ mice were interbred to obtain CD45$^{.1/.2}$ *Foxp3*$^{DTR\text{-}EGFP}$ mice. B6 CD45$^{.1/.1}$ and *Rag1*$^{-/-}$ mice were interbred to obtain CD45$^{.1/.1}$ *Rag1*$^{-/-}$ mice. TRAMP$^{+/-}$ mice were interbred to obtain TRAMP$^{+/+}$ mice. TRAMP$^{+/+}$ male mice were crossed to homozygous female *Foxp3*$^{DTR\text{-}EGFP}$ mice to obtain TRAMP$^{+/-}$ *Foxp3*$^{DTR\text{-}EGFP/y}$ mice. TRAMP$^{+/+}$ and TCRβtg

mice were interbred to obtain TRAMP$^{+/-}$ TCRβtg mice. *Mb1*^{Cre} and *Rosa26*$^{LSL\text{-}DTR}$ mice were interbred to obtain *Mb1*^{Cre} x *Rosa26*$^{LSL\text{-}DTR}$ mice. *Tcaf3(C4)*$^{-/-}$ mice were generated as previously described[140]. *H2-DMα*$^{-/-}$ mice on a C57BL/6J background were a generous gift from L. K. Denzin at Rutgers University. C57BL/6J mice housed under germ-free conditions (GF) were generously provided to us by E. B. Chang and B. Jabri at the University of Chicago. All mice were bred and maintained at the University of Chicago under specific-pathogen-free conditions (with the exception of germ-free mice) and in accordance with the guidelines of the Institutional Animal Care and Use Committee.

Preparation and enrichment of cell suspensions

Spleen, lymph nodes, Peyer's patches, and thymi were isolated and mechanically dissociated through 40-μm, 70-μm, or 100-μm filters (Corning) in RPMI (Gibco) supplemented with 10% fetal bovine serum (FBS; Gemini Bio-Products) and 1% penicillin and streptomycin (Gibco), referred to as "cRPMI-10". For the isolation of prostates, whole male genitourinary tracts were first isolated and prostate lobes were separated by microdissection. For the isolation of lymphocytes from non-lymphoid organs, prostate lobes, salivary glands, pancreas, and lacrimal glands were injected and digested with pre-warmed RPMI containing 0.4 mg mL^{-1} Liberase TL (Roche) and 0.2 mg mL^{-1} DNase I (Roche) for 30 min at 37°C. Digested prostate was mechanically disrupted with frosted microscope slides, while salivary glands, pancreas, and lacrimal glands were mechanically dissociated through 70-μm filters in cRPMI-10. Following dissociation, each tissue sample was centrifuged at 700 × *g* for 5 min, resuspended in 5 mL of cRPMI-10, overlaid on 5 mL of Histopaque 1119 (Sigma) or Ficoll Paque Plus (Cytiva), and centrifuged at 700 × *g* for 10 min at room temperature with no brake. Viable lymphocytes were isolated from the interface, then

washed and resuspended in cRPMI-10. For experiments involving cell sorting, or where indicated, cell suspensions underwent further enrichment for $CD4^+$ T cells using the $CD4^+$ T Cell Isolation Kit, mouse (Miltenyi Biotec) or depletion of CD8-biotin-labeled cells using the EasySep Mouse Streptavidin RapidSpheres Isolation Kit (STEMCELL Technologies), in accordance with manufacturer protocols.

Antibodies, flow cytometry, and fluorescence-activated cell sorting (FACS)

Cell suspensions were incubated in staining mixes that consisted of fluorochrome-labeled monoclonal antibodies resuspended in staining buffer (phosphate-buffered saline with 2% FBS, 0.1% NaN_3, 5% normal rat serum, 5% normal mouse serum, 5% normal rabbit serum, and 10 μg mL^{-1} 2.4G2 FcR blocking antibody) for 20 min on ice (all sera from Jackson Immunoresearch). For analyses using spectral flow cytometry, staining mixes were supplemented with 10% BD Horizon Brilliant Stain Buffer Plus (BD Biosciences). Fluorochrome-labeled monoclonal antibodies (clones denoted in parenthesis) against B220 (RA3-6B2), CD3ε (145-2C11), CD4 (GK1.5 or RM4-5), CD5 (53-7.3), CD8α (53-6.7), CD8β (YTS156.7.7), CD11b (M1/70), CD11c (N418), CD25 (PC61), CD38 (90), CD44 (IM7), CD45.1 (A20), CD62L (MEL-14), CD69 (H1.2F3), CD73 (TY/11.8), CD200 (OX-90), CXCR5 (L138D7), F4/80 (BM8), FR4 (12A5), GL-7 (GL7), ICOS (C398.4A), Neuropilin-1 (12C2), NK1.1 (PK136), PD-1 (RMP1-30), TCRβ (H57-597), Thy1.1 (OX-7), and Thy1.2 (53-2.1) were purchased from BioLegend, eBioscience, or BD Biosciences unless otherwise noted. Intracellular staining of Bcl6 (K112-91), cleaved Caspase-3 (D3E9, from Cell Signaling Technology), Eomes (Dan11mag), Ki67 (SolA15), T-bet (4B10), GATA3 (TWAJ), RORγt (Q31-378), and Foxp3 (FJK-16s) was performed using the Foxp3 Staining Buffer Set (eBioscience) at 4°C overnight, after 30 minutes of fixation and

permeabilization. For FACS, cells were sorted using a FACSAria II, FACSAria IIIu, or FACSAria Fusion cell sorter running FACSDiva (BD Biosciences). Flow cytometry data was acquired on an LSRFortessa or LSRFortessa X-20 running FACSDiva version 8.0.2 (BD Biosciences), or on an Aurora spectral cytometer running SpectroFlo 2.2.0.4 (Cytek Biosciences), and analyzed using FlowJo software (Tree Star). Doublets were excluded to remove dead cells when possible. Unless otherwise noted, TCR "retrogenic" cells were sorted via FACS as CD8α^{-} CD45.1^{neg} Thy1.1^{+} or CD4^{+} CD8β^{-} CD45.1^{neg} Thy1.1^{+} cells and identified in flow cytometry analyses as TCRβ^{+} CD4^{+} CD8^{neg} Thy1.1^{+} CD45.1^{neg} cells.

pMHC-II tetramer generation and staining

Allophycocyanin- and phycoerythrin (PE) -conjugated C4/I-Ab tetramers were generated as previously described[140]. CD4^{+} T cells were plated in a 96-well round-bottom plate (Nunc) and washed in minimal staining buffer (PBS with 0.1% NaN3, 2% normal rat serum, and 2% normal mouse serum, all from Jackson ImmunoResearch, and 10 μg/ml 2.4G2 antibody). Cells were resuspended in staining buffer supplemented with dasatinib (AdooQ Bioscience) at a final concentration of 50 nM and incubated for 30 minutes at 37°C. Allophycocyanin- and PE-labeled tetramers were added directly to dasatinib-treated cells in minimal staining buffer (without washing) for 1 h at room temperature. Final tetramer concentrations are indicated on a per-experiment basis. Cells were washed and incubated with unconjugated mouse anti-PE antibody (clone PE001; BioLegend) and mouse anti-allophycocyanin antibody (clone APC003; BioLegend) at a concentration of 10 μg/ml for 20 min at 4°C in minimal staining buffer. Cells were washed and stained for flow cytometric analysis as described above, using minimal staining buffer for cell surface marker labeling.

Bulk and single-cell TCR sequencing and analysis

For bulk TCR sequencing, cell populations of interest were FACS sorted into TRI Reagent (Sigma), frozen in dry ice, and stored at -80°C prior to use. RNA was isolated following a standard chloroform extraction and isopropanol precipitation protocol. Briefly, chloroform was added to each TRI reagent suspension, then vortexed and incubated for 3 min at room temperature. Samples were centrifuged at 12,000 × *g* for 15 min at 4°C, and the upper aqueous phase was extracted into a new tube, while avoiding the interface. RNA was precipitated by adding isopropanol along with 20 μg glycogen, then mixed and stored at -80°C for at least 30 min. Precipitated RNA was pelleted by centrifugation at 12,000 × *g* for 10 min at 4°C, and the pellet was washed with 75% ethanol, then air-dried and resuspended in molecular grade RNase-free water. Purified RNA was subjected to TCRα sequencing using the Amp2Seq service from iRepertoire, a platform based on semi-quantitative multiplex PCR coupled with Illumina sequencing. This approach allows analysis of the complete TCRα repertoire, regardless of variable-region usage. Typically, >8 x 10^5 sequence reads were obtained per sample.

For each TCRα peptide sequence, the sum of the corresponding cDNA sequence reads was divided by the total TCRα sequence reads within a given sample to obtain the frequency of each TCRα peptide sequence per sample. “Recurrent” clones were defined as TCRα clonotypes for which the frequency was non-zero across all five samples sequenced for a given non-lymphoid organ. Typically, the most abundant TCRα clonotypes within a site of interest were determined by ranking recurrent TCRα sequences by median frequency in decreasing order.

For single-cell TCR sequencing of *Lm[C4]*-expanded clones, lymphocytes from the spleens of *Lm*-infected *Foxp3*^{GFP} TCRβtg infected mice were isolated into cell suspensions as described above and sorted as described by Chao *et al*.[213] Briefly, Foxp3$^{GFP\text{-}neg}$ CD4$^+$ Tconv cells were single-cell sorted into catch solution (sterile H_2O with TRIS (pH 8.0, Ambio) and RNase

inhibitor (Promega) in 96 well U-bottom plates and processed for TCRα sequencing analysis, as described in Dash *et al.* with modifications[214]. cDNA synthesis was performed directly from single cells using Maxima First Strand cDNA Synthesis Kit (Thermo Scientific) per manufacturer's instructions with minor modifications. The cDNA synthesis used 6 mL of reaction mix consisting of 3 mL 5X Reaction Mix, 0.5 mL Maxima Enzyme Mix, and 1.25% IGEPAL (Sigma). This was added to the 10 mL single cell-containing solution and incubated at 25°C for 10 min, 50°C for 50 min, and 85°C for 5 min. Following reverse transcription, multiplex PCR was performed to amplify the CDR3α transcripts in a 20 mL reaction mix containing 2 mL cDNA and DreamTaq Green Master Mix (Thermo Scientific). The first round of PCR used a mixture of 23 TRAV forward and 1 TRAC reverse primers. The PCR conditions were 94°C for 5 min followed by 45 cycles of 94°C for 30 s, 56°C for 30 s, and 72°C for 1 min, with a final extension at 72°C for 8 min. The second round of PCR used the product from the first round of PCR as template and a mixture internal 23 TRAV forward and 1 TRAC reverse primers. The PCR conditions were similar to the first round but with 50 cycles. The nested PCR product was purified using EXOSap-IT (Applied Biosystems) per the manufacturer's instructions and sequenced using the internal TRAC reverse primer. TCRα sequences were analyzed and assigned using the international ImMunoGeneTics information system (IMGT) database (http://www.imgt.org).

TCR construct design and cloning

Recombined TRAV sequences of interest were obtained from cDNA sequence reads acquired by the iRepertoire sequencing platform (for bulk TCRα sequencing) or by Sanger sequencing (for single-cell TCRα sequencing). The *Trav* chain and the *Trac* constant region were synthesized into pUC57 plasmids (Genscript) and cloned into a conditional retroviral vector,

pMGflThy1.1, as described below and in ref[20]. The pMGflThy1.1 vector is designed such that expression is conditional on Cre-mediated excision of a lox-flanked STOP inserted 5' of the TCRα coding segment. Downstream of the TCRα coding segment is an IRES followed by mouse Thy1.1, such that positively infected cells could be distinguished by staining for the retrovirally encoded Thy1.1 protein and detected by flow cytometry. The *Trav* and *Trac* segments were PCR amplified using the Phusion high-fidelity polymerase (New England Biolabs) with dNTPs in 5X Phusion HF buffer (New England Biolabs). Primers were designed using the NEBuilder Assembly Tool (New England Biolabs) and obtained from IDT. The pMGflThy1.1 vector was digested with restriction enzymes AgeI and NotI (New England Biolabs) for 12 hr at 37°C. PCR products as well as the AgeI- and NotI-digested pMGflThy1.1 vector were gel purified using a QIAquick Gel Extraction Kit (QIAGEN). Purified TRAV and TRAC products were assembled with the purified AgeI- and NotI-digested pMGflThy1.1 vector using the Gibson Assembly Master Mix (New England Biolabs) for 60-90 min at 50°C. Assembled product was transformed into high-efficiency 5-alpha competent *Escherichia coli* (New England Biolabs), and plasmids carrying the correct insert were purified using an EndoFree Plasmid Maxi Kit (QIAGEN). Plasmid preparations were sequenced to verify the TCR insert. Sequence alignment and proper in-frame sequence expression was confirmed using the Snapgene software (GSL Biotech). Similar methods were used to insert TCR sequences into the pMGflhCD4 vector. The pMGflhCD4 vector is identical to the pMGflThy1.1 vector, except for a replacement of the coding sequence of Thy1.1 with the sequencing encoding the extracellular domain of human CD4.

Retrovirus production, infection, and primary TCR retrogenic mice generation

Conditional retrovirus was produced using Platinum-E (Plat-E; Cell Biolabs, Inc.) cells after the *Tcra* genes were inserted into the conditional retroviral vector, pMGflThy1.1 (or pMGflhCD4). *Tcra* constructs were transfected into Plat-E packaging cells using lipofectamine (Life Technologies). Harvested retroviral supernatant was filtered through a 0.45 μm filter, frozen in a dry ice and ethanol bath, and stored at -80°C prior to use.

TCR Vβ3 transgenic $Cd4^{Cre}$ $Tcra^{-/-}$ mice ($Foxp3^{wt}$ or $Foxp3^{DTR\text{-}EGFP}$) were retro-orbitally injected with 150 mg kg^{-1} 5-fluorouracil (Fresenius Kabi) 3 days prior to bone marrow harvest. Bone marrow was harvested by first cutting the epiphysis on each end of the femur bones, then by flushing the marrow out of each open end using a 30-gauge needle and syringe through a 40-μm filter. After harvest, bone marrow was cultured for 2 days in X-vivo 10 medium (Lonza) supplemented with 15% FBS (Gemini Bio-Products), 1% penicillin and streptomycin (Gibco), 100 ng mL^{-1} mouse SCF, 10 ng mL^{-1} mouse IL-3, and 20 ng mL^{-1} mouse IL-6 (all from BioLegend). Cultures were maintained at 37°C with 5% CO_2 in a CO_2 incubator (Sanyo Electric). Stimulated cells were infected with *Tcra*-encoding retrovirus in the presence of 4 μg mL^{-1} polybrene (EMD Millipore) by centrifugation at 900 × *g* for 90 min at 37°C. After 24 hr of additional culture in X-vivo 10 medium (supplemented as described above), transduced bone marrow cells were harvested and mixed with 5×10^6 freshly harvested "filler" bone marrow cells from $CD45^{.1/.1}$ $Rag1^{-/-}$ mice prior to injection. 24 hr prior to injection, recipient mice ($CD45^{.1/.1}$ or $CD45^{.1/.2}$ $Foxp3^{DTR}$) were subjected to lethal total-body irradiation using a dose of 850-900 rads. Irradiation was performed using irradiators with either an X-ray or cesium-137 source. 24 hr after irradiation, recipient mice were retro-orbitally injected with the mixture of infected and filler $CD45^{.1/.1}$ $Rag1^{-/-}$ bone marrow to generate "primary TCR retrogenic" mice. Typically, primary TCR retrogenic (TCRrg) mice were analyzed 6-8 weeks after bone marrow reconstitution. Prior to analysis, proper expression of

the transduced TCRα chains by donor cells was confirmed by staining peripheral blood leukocytes with antibodies specific for CD45.1, Thy1.1, TCRβ, and CD4. In select cases where primary TCRrg mice were generated in CD45$^{.1/.2}$ *Foxp3*$^{DTR\text{-}EGFP}$ recipients, filler bone marrow cells were obtained from the recipient strain.

In vitro T cell stimulation assays

All experiments were performed in RPMI containing 10% FBS (Atlanta Biologicals), 1% penicillin and streptomycin, 0.1% β-mercaptoethanol (Gibco), and 100 U mL^{-1} recombinant mouse interleukin-2 (IL-2) (Miltenyi Biotec), unless absence of IL-2 was specified. In addition, all cell cultures were maintained in 96- or 384-well clear round bottom ultra-low attachment spheroid microplates (Corning) at 37°C with 5% CO_2 in a CO_2 incubator (Sanyo Electric). Pooled spleen and lymph nodes were isolated from primary TCRrg hosts, enriched for CD4$^+$ T cells using the mouse CD4$^+$ T Cell Isolation Kit (Miltenyi Biotec), and stained with antibodies against CD8β, CD45.1, and Thy1.1 prior to FACS sorting. T cells expressing the TCRα chains of interest ("TCR retrogenic cells") were isolated by FACS sorting CD4-enriched lymphocytes as described above. Isolated TCRrg cells were labeled using the CellTrace Violet (CTV) Cell Proliferation Kit (Invitrogen) following manufacturer's protocol, with slight modifications. In brief, sorted cells were resuspended in pre-warmed phosphate-buffered saline containing 0.625 μM CTV and incubated for 20 min at 37°C. The reaction was quenched by the addition of 10 mL cold cRPMI-10, then washed with cRPMI-10. To obtain splenic dendritic cells (DCs), spleens were isolated from various genetic mouse strains (B6 CD45$^{.1/.1}$, GF, *H2-DM*$^{-/-}$, and *MHCII*$^{-/-}$), injected and digested with pre-warmed RPMI containing 0.4 mg mL^{-1} Liberase TL (Roche) and 0.2 mg mL^{-1} DNase I (Roche) for 20 min at 37°C, mechanically dissociated through a 100-μm filter (Corning),

and enriched for $CD11c^+$ cells using the mouse CD11c MicroBeads UltraPure kit (Miltenyi Biotec). In select instances in which DCs from other anatomical sites were used, the same procedures were followed for cells isolated from the indicated sites. 1-2.5 × 10^4 of CTV-labeled TCRrg cells were co-cultured *in vitro* with 5 × 10^4 $CD11c^+$ DCs for 5 days. When specified, anti-MHC-II blocking antibody (clone M5/114.15.2, BD Biosciences) or IgG2b, κ isotype control antibody (BD Biosciences) was added to indicated cultures at a final concentration of 5 μg mL^{-1}. As a positive control, CTV-labeled TCRrg T cells were co-cultured with anti-CD3ε/anti-CD28 MACSiBead particles at a 1:1 ratio using the mouse T Cell Activation/Expansion Kit (Miltenyi Biotec) following manufacturer's protocol. For all experiments, dilution of CTV and total T cell number were assessed by flow cytometry on day 5.

Lymphodepletion of TRAMP mice

To ablate endogenous lymphocytes in prostate tumor-bearing mice, TRAMP mice were subjected to intraperitoneal injections of 100 mg/kg fludarabine (Leucadia Pharmaceuticals) and 200 mg/kg cyclophosphamide (Baxter Healthcare Corporation or Sandoz) based on the regimen described by Koike *et al*.[215] Each reagent was obtained in lyophilized pharmaceutical-grade form and stored at 4°C until use. For preparation, each compound was weighed separately using an analytical balance, resuspended in sterile Dulbecco's Phosphate-Buffered Saline (DPBS) lacking calcium or magnesium, and passed through a polyethersulfone membrane with pore size of 0.22 μm into a 50 mL conical tube (Steriflip; EMD Millipore). Fludarabine alone was given on day -3, and both fludarabine and cyclophosphamide were administered on days -2 and -1, with adoptive cell transfers occurring on day 0.

Adoptive T cell transfers

For transfers of peripheral TCRrg $CD4^+$ T cells, pooled spleen and lymph nodes were isolated from primary TCRrg hosts, enriched for $CD4^+$ T cells, and isolated by FACS sorting as described above. When specified, TCRrg cells were further sorted for the naïve conventional T (Tconv) cell subset by sorting on $CD44^{lo}$ $Foxp3^{DTR\text{-}EGFP\text{-}neg}$ cells. Sorted cells were resuspended in RPMI (Gibco) and retro-orbitally injected into the specified recipients. In experiments involving co-transfer with "filler" splenocytes, spleens were isolated from 6- to 12-week-old mice and processed as described above. Splenocytes were resuspended in 1 mL Red Blood Cell Lysing Buffer (Sigma) and incubated for 5 min at room temperature to lyse red blood cells. The reaction was quenched by the addition of ≥5 mL cold RPMI containing 10% FCS (RPMI-10), then washed with RPMI-10 and resuspended in RPMI prior to injection. Typically, 10 x 10^6 bulk filler cells were co-injected retro-orbitally with sorted TCRrg T cells, such that TCRrg T cells constituted ~1% of the inoculum. In instances in which sort yield was low, the amount of bulk filler cells was reduced such that the proportion of TCRrg T cells would remain as ~1% of the total inoculum.

For intrathymic transfers of TCRrg thymocytes, 10 x 10^6 bulk thymocytes from primary TCRrg mice in ~30 µL were injected into the thymi of into 4- to 6-week-old recipient mice anesthetized with 2-4% isoflurane in medical gas (21% oxygen, 79% nitrogen) in an acrylic chamber. No ultrasound guidance was used. Recipient mice were euthanized for analysis 7 d after transfer. For analysis of CD4SP thymocytes, 95% of whole thymus was depleted of $CD8^+$ cells to enrich for CD4SP thymocytes via column-free magnetic separation using biotin-conjugated anti-CD8α (53-6.7; BioLegend) or biotin-conjugated anti-CD8β (YTS156.7.7; BioLegend) and mouse streptavidin beads (STEMCELL Technologies) per the manufacturer's protocol.

Analysis of cytokine production

For assessment of cytokine production by intracellular staining, cells were cultured in RPMI (Gibco) containing 10% FBS (Gemini Bio-Products), 50 ng mL^{-1} PMA, and 500 ng mL^{-1} Ionomycin in U-bottom 96-well plates (Corning) for 1 hr at 37°C, followed by addition of 2 μM monensin (eBioscience) for another 4 hr at 37°C. Cells were then permeabilized using the Foxp3 Staining Buffer Set (eBioscience), and stained for intracellular cytokines at 4°C overnight. Fluorochrome-labelled monoclonal antibodies (clones denoted in parenthesis) against IFN-γ (XMG1.2), IL-4 (11B11), and IL-10 (JES5-16E3) were purchased from BD Biosciences, IL-17 (TC11-18H10.1) was purchased from BioLegend, and IL-21 (mhalx21) from eBioscience. Flow cytometry data was acquired on an LSRFortessa or LSRFortessa X-20 (BD Biosciences), or on an Aurora spectral flow cytometer (Cytek Biosciences).

Genetic engineering of *Listeria monocytogenes*

All *L. monocytogenes* strains were engineered using the pPL6-myc shuttle vector as described in Yan *et al*.[216] with modifications in some strains as follows. The peptide or protein of interest to be expressed in *L. monocytogenes* was codon-optimized for expression in *L. monocytogenes* (Genscript), and the coding sequence was synthesized and inserted into the pUC18 vector immediately flanked by BamHI restriction sites (Genscript). Coding sequence fragments were amplified with a Phusion PCR (New England Biolabs) using M13 universal forward and reverse primers (IDT) and gel-purified using the QIAquick Gel Extraction Kit (Qiagen) via the manufacturer's protocol. Amplified fragments and pPL6-myc vector, obtained as a generous gift from N. E. Freitag, were digested with 1ul BamHI in Cutsmart Buffer (New England Biolabs) for 1 hr at 37°C, gel-purified, and ligated with 1 μl T4 Ligase in Ligation Buffer (New England

Biolabs) overnight at 16°C using a 1:6 vector:fragment molar ratio. DH5-alpha *E. coli* were heat-transformed using the ligation reaction mix via the manufacturer's protocol (New England Biolabs), and transformed colonies were selected on LB agar plates (Sigma) containing 25 μg/ml chloramphenicol (CAM) (Sigma) overnight at 37°C. DNA from selected colonies was purified with the QIAprep Spin Miniprep Kit (Qiagen) using the manufacturer's protocol. Sequence integration and directionality was confirmed via Sanger sequencing using the pPL6-Myc_Seq primer (TATTCCTATCTTAAAGTTACTTTTATGTGGAGGC). Correctly integrated plasmids were subsequently transformed into electrocompetent SM10 *E. coli* (Freitag Lab) via electroporation using a Gene-pulser and 0.1cm Gene-pulser cuvettes (Bio-Rad Laboratories), applying the following settings: capacitance 25μF, resistance 200Ω, voltage 1.8kV. Electroporated SM10 were selected overnight in LB broth (Gibco) supplemented with 25 μg/ml CAM at 37°C shaking, subsequently incubated overnight on LB agar plates supplemented with 25 μg CAM @ 37C, and selected colonies were expanded. For conjugation into *L. monocytogenes*, transformed SM10 and *L. monocytogenes* parent strains (*Lm[parent]*) were grown to lawns overnight at 37°C on agar plates under the following conditions: LB agar + 25ug/ml CAM and BHI agar (BD Biosciences) + 200 μg/ml streptomycin (Strep), respectively. The following day, SM10 was re-plated in ~1 in square on antibiotic-free BHI agar plates, *Lm[parent]* was replated directly on top of SM10, and conjugation proceeded for 4 hrs at 37°C. Following incubation, conjugation mix was selected overnight at 37°C shaking in BHI broth (BD Biosciences) containing 7.5ug/ml CAM and 200ug Strep. Cultures were further selected overnight @ 37C on BHI agar plates containing 7.5ug/ml CAM and 200ug Strep. Colonies were isolated, expanded, and stored as 15% glycerol stocks at -80°C.

Infection with *L. monocyogenes*

L. monocytogenes strains used in this study are referred to in Yan *et al.*[216] Attenuated strains were derived from the 10403S prfA(G155S) ΔactA parent strain (NF-L974 in reference). Non-attenuated strains were derived from the 10403S actA gus plcB prfA(G155S) parent strain (NF-L943 in reference). The day before infection, glycerol stock of the infecting strain was scraped, dropped in starter culture, and grown overnight at 37°C shaking (225rpm) in BHI broth (Difco) under Chloramphenicol (CAM) (Sigma) selection (7.5μg/ml). On the day of infection, starter culture was diluted 1:20 in BHI+CAM and grown under analogous conditions and expanded to the experimentally determined logarithmic growth phase (~3hrs). Culture was removed and placed on ice for a minimum of 30 min to stall growth. Optical density (OD_{600}) of culture was measured and concentration was calculated using the following experimentally determined equation: For attenuated strains; $Log_{10}[CFU/ml] = 0.6245(OD_{600}) + 8.707$. For non-attenuated strains; $Log_{10}[CFU/ml] = 0.3134(OD_{600}) + 8.585$. Culture was diluted in PBS inoculum to desired concentration, and mice were infected intravenously with 10^7 CFU (attenuated strains) or 5×10^3 CFU (non-attenuated strains) in 400 μl. To confirm infecting dose, following the infection, limiting dilutions of inoculum were plated on antibiotic-free BHI agar plates, and grown overnight at 37°C. Doses were quantified the following day.

Systemic Treg cell ablation

Diphtheria toxin (Sigma) was reconstituted at 5 μg/mL in sterile molecular grade water following manufacturer's protocol and stored at -80°C prior to use. Diphtheria toxin aliquots were frozen and thawed once and 50 μg/kg of diphtheria toxin was injected intraperitoneally on days 0

and 1, then every other day until day 12. Mice were monitored for signs of terminal autoimmune disease and were sacrificed once moribund.

Bulk RNA sequencing preparation, quality control and quantification

Sample processing, sequencing, and analysis

Spleen and lymph nodes were isolated from primary TCRrg mice 17-25 weeks after bone marrow reconstitution and processed for FACS as described above. At least 1 x 10^4 TCRrg $CD4^+$ T cells were FACS sorted from each sample using a FACSAriaII cell sorter (BD Biosciences) and resuspended in TRI Reagent (Sigma). TCRrg T cells were selected by gating on $Dump^{neg}$ ($B220^{neg}CD11b^{neg}CD11c^{neg}F4/80^{neg}$), followed by $CD4^+CD8\beta^{neg}$, then by $Thy1.1^+CD45.1^{neg}$. Biological samples containing at least 1 x 10^5 TCRrg $CD4^+$ T cells were subjected to RNA sequencing (RNA-seq). Total RNA was isolated following a standard chloroform extraction and isopropanol precipitation protocol as described above (see Materials & Methods, Bulk & single-cell TCR sequencing and analysis). RNA quality and quantity was assessed using the Agilent bio-analyzer. Strand-specific RNA-seq libraries were prepared using the TruSEQ mRNA RNA-seq library protocol (Illumina). Library quality and quantity was assessed using the Agilent bio-analyzer. Sequencing of RNA-seq libraries was performed on the NovaSeq 6000, running 100 bp paired-end reads (PE100) and generating approximately 60 million reads per sample. Raw reads were aligned to reference genome mm10 using the STAR aligner[217]. ENSEMBL genes were quantified using FeatureCounts[218]. Differential expression statistics (fold-change and p-value) and normalized expression values were computed using edgeR using the exactTest() function[219,220]. *P*-values were adjusted for multiple testing using the false discovery rate (FDR) correction of

Benjamini and Hochberg[221]. Significant genes were determined based on a FDR threshold of 5% (0.05).

Enrichment against custom gene list

Up- and down-regulated genes were compared to a custom list of 25 genes that have been implicated in T follicular helper cell differentiation, maintenance, and function, curated from the literature[167,169,222,223]. Enrichment log ratios and *p*-values were computed using Fisher's Exact test, with the set of all expressed genes as a background.

Immunofluorescence microscopy

Spleens were isolated from primary TCRrg hosts and washed in DPBS at 4°C. Spleens were directly frozen in embedding medium for optimal cutting temperature (Tissue-Tek OCT, Sakura Finetek) using cryomold trays placed on dry ice, then stored at -80°C prior to use. Spleen samples were sectioned at a thickness of 6 μm using a cryostat (University of Chicago Human Tissue Resource Center). Tissue sections were washed with PBS and incubated in solution containing 10% normal donkey serum and 1:200 dilution of anti-mouse Fc antibody (Sigma-Aldrich). Sections were stained with antibodies against B220, Bcl6, CD4, CD45.2 (or Thy1.1), and TCR Vβ3 (clones and manufacturers indicated under "Antibodies, flow cytometry, and fluorescence-activated cell sorting (FACS)"). Following staining, tissue sections were mounted onto glass microscope slides using ProLong Gold Antifade Mountant (Invitrogen) and visualized 24-48 h later by confocal microscopy using either the Stellaris (40x / 1.25 oil objective) or SP8 (20x / 0.7 oil objective) (Leica Microsystems). Images were processed using Fiji (version 2.3.0/1.53q, open-source software)[224].

B cell depletion

For systemic ablation of B cells in *Mb1*^{Cre} x *Rosa26*$^{LSL\text{-}DTR}$ mice, diphtheria toxin (Sigma) was reconstituted at 5 μg/mL in sterile molecular grade water following manufacturer's protocol and stored at -80°C prior to use. Diphtheria toxin aliquots were frozen and thawed once and 50 μg/kg of diphtheria toxin was injected intraperitoneally on experiment days 0, 1, 4, and 7. Mice were euthanized for analysis on experiment day 8.

For antibody-mediated B cell depletion, InVivoPlus anti-mouse CD20 (clone MB20-11, IgG2c, BioXCell) was resuspended in sterile PBS to a final concentration of 250 μg per 200 μL. In parallel, InVivoPlus rat IgG2a isotype control, anti-trinitrophenol (clone 2A3, BioXCell) was also diluted in PBS to a final concentration of 250 μg per 200 μL. Mice were injected intraperitoneally with 250 μg of anti-CD20 or isotype control solution and monitored daily for one week.

Statistical analyses

Except for data from RNA or TCR sequencing experiments, data were analyzed using Prism software (GraphPad). For the comparison of two groups, the Welch's t-test was used unless otherwise indicated[225]. For the comparison of paired groups, the paired t-test was used. For comparison of multiple groups, one-way ANOVA was employed, coupled with Tukey's HSD post-hoc tests when appropriate. *$p < 0.05$; **$p < 0.01$; ***$p < 0.001$, unless otherwise specified.

CHAPTER III: RESULTS PART I – THE ENDOGENOUS REPERTOIRE HARBORS SELF-REACTIVE CD4$^+$ T CELL CLONES THAT ADOPT A T FOLLICULAR HELPER-LIKE PHENOTYPE AT STEADY STATE[*]

Overview

Prior to seeding secondary lymphoid organs (SLOs), αβ T cells navigate multiple developmental checkpoints in the thymus to ensure their functionality and specify their fate. One such checkpoint involves the somatic recombination of T cell receptor (TCR) gene segments to form exons encoding antigen receptors. While this process enables the development of a diverse αβ TCR repertoire, this diversity comes with a cost: the generation of TCRs that confer overt reactivity to major histocompatibility complex (MHC) molecules bearing self-derived peptides[19]. Thymocytes with such TCRs experience strong and/or persistent signaling following TCR ligation of self-peptide/MHC complexes (spMHC). If CD4$^+$ T cells with strong reactivity to spMHC-II are allowed to egress into the periphery, these cells may trigger autoimmune responses directed against host tissues.

To mitigate autoimmune threat to the host, mechanisms of central tolerance prevent self-reactive MHC-II-restricted thymocytes from entering the conventional CD4$^+$ T (Tconv) cell pool. Following agonist interactions with spMHC-II, self-reactive thymocytes may undergo negative selection, skewing into the immunosuppressive Foxp3$^+$ regulatory T (Treg) cell lineage, and/or diversion into alternative T cell fates[21]. Several studies have shown that recognition of self-antigens in the thymus is required for these fates to occur. For example, in the absence of the transcriptional regulator, Aire, ectopic expression of many tissue-specific antigens (TSAs) by

[*] Much of this section is reproduced, with modifications, from Lee & Rodriguez *et al.* The endogenous repertoire harbors self-reactive CD4$^+$ T cell clones that adopt a T follicular helper-like phenotype at steady state. In revision.

medullary thymic epithelial cells (mTECs) is abrogated, resulting in autoimmune infiltration of multiple host tissues[64,65,71]. Secondly, genetic ablation of a defined TSA increases the pathogenicity of $CD4^+$ Tconv cells reactive to that self-antigen upon adoptive transfer into TSA-sufficient mice. Thymocytes that would have otherwise undergone clonal deletion of thymic Treg (tTreg) cell differentiation instead develop as $CD4^+$ Tconv cells and may contribute to autoimmune processes[72,141,226,227]. In line with this, naïve $CD4^+$ T cells bearing Treg-derived TCRs reactive to myelin oligodendrocyte glycoprotein (MOG) were found to cause more severe disease upon induction of experimental autoimmune encephalomyelitis (EAE) compared to cells bearing TCRs derived from MOG-reactive $CD4^+$ Tconv cells. Collectively, these findings support the notion that the immune system avoids autoimmunity by eliminating potentially pathogenic clones from the T cell repertoire via clonal deletion or diverting such clones into the Treg cell lineage during thymic development.

Interestingly, in multiple studies of murine $CD4^+$ T cell responses towards transgenically expressed or *bona fide* self-antigens, Treg and $CD4^+$ Tconv cells with shared antigen specificities co-exist in the endogenous T cell repertoire[72,136,140]. Such findings corroborate earlier reports of self-reactive $CD4^+$ Tconv cells in the SLOs of healthy human individuals[228,229]. Moreover, these observations shed light on genome-wide association studies linking distinct human leukocyte antigen (HLA) class II alleles with increased risk for several autoimmune diseases, which implicate $CD4^+$ T cells in the pathogenesis of autoimmunity[230,231]. In autoinflammatory settings, self-reactive $CD4^+$ T cells may either fail to restrain inflammation (as in the case of Treg cells) and/or promote inflammatory responses (as for $CD4^+$ Tconv cells). As such, it is critical to understand the factors that govern the development of self-reactive $CD4^+$ Tconv cells, as well as these cells' activation and autoimmune potential in peripheral SLOs.

Several lines of evidence indicate that, if unleashed, self-reactive $CD4^+$ Tconv cells in the endogenous T cell repertoire can promote autoimmunity. First, adoptive transfer of naïve $CD4^+$ $CD25^{neg}$ Tconv cells into T cell-deficient mice leads to autoimmune destruction of multiple non-lymphoid organs, as well as the production of autoantibodies[232]. Second, mice whose $CD8^+$ regulatory T cells are unable to engage with the nonclassical MHC molecule Qa-1 demonstrate an expansion of $CD4^+$ Tconv cells bearing the T follicular helper (Tfh) phenotype concomitant with autoantibody production[233]. Third, sustained administration of diphtheria toxin (DT) to *Foxp3*^{DTR} mice, which express the human diphtheria toxin receptor (DTR) in all Foxp3-expressing cells, leads to systemic ablation of Treg cells, multiorgan lymphocytic infiltration by $CD4^+$ Tconv cells, and increased mortality[93]. Similar findings were observed in Treg-ablated mice housed in either specific pathogen-free (SPF) or germ-free (GF) conditions, as well as in mice fed a diet lacking peptide antigens, implying that $CD4^+$ Tconv cells that remain following systemic Treg cell depletion mediate disease through recognition of spMHC-II ligands[89,234].

Despite these findings, the prevalence, antigen specificities, developmental trajectories, and functional properties of potentially pathogenic self-reactive $CD4^+$ Tconv cells all remain poorly understood. To address this knowledge gap, we utilized TCR sequencing to identify putative self-reactive $CD4^+$ Tconv clones within the endogenous repertoire that are recurrently enriched in non-lymphoid organs following sustained Treg cell ablation. Through the study of monoclonal TCR "retrogenic" mice, we demonstrate that several $CD4^+$ Tconv cell clones identified in this screen exhibit common properties at steady state, including widespread activation across various SLOs, *ex vivo* reactivity to endogenous MHC-II-restricted self-ligands displayed by splenic dendritic cells, adoption of a $Bcl6^{hi}$ PD-1^{hi} phenotype, and a propensity to localize within B cell follicles. Thus, our collective work identifies a naturally occurring population of overtly

self-reactive Tfh-like $CD4^+$ T cells that populate the endogenous repertoire of healthy mice and infiltrate non-lymphoid organs when released from Treg cell-mediated suppression.

Recurrent $CD4^+$ Tconv clones are detected in non-lymphoid organs of Treg cell-depleted mice

Given that multiple non-lymphoid organs exhibit autoimmune infiltration by $CD4^+$ Tconv cells following systemic Treg cell ablation, we first sought to understand whether $CD4^+$ Tconv cell recruitment into such tissues occurred in an antigen-specific fashion. To address this question, we generated mice expressing the *Foxp3*$^{DTR\text{-}EGFP}$ allele as well as a transgenic TCRβ chain (TCRβtg). The *Foxp3*$^{DTR\text{-}EGFP}$ allele enables systemic Treg cell ablation upon DT administration, as well as identification of $CD4^+$ Tconv cells lacking EGFP expression. Use of a fixed TCRβ chain allows for complete characterization of the TCR repertoire by deep sequencing of endogenous TCRα chains. Male *Foxp3*$^{DTR\text{-}EGFP/y}$ TCRβtg mice were subjected to systemic Treg cell ablation by DT administration over 12 days (Figure 1a), leading to pronounced $CD4^+$ Tconv cell infiltration of several organs, including the prostate, pancreas, salivary gland, and lacrimal gland (Figure 1b). We purified $CD4^+$ Tconv cells from the prostates of DT-treated mice via fluorescence-activated cell sorting (FACS) and performed TCRα sequencing to characterize the frequency and recurrence of organ-infiltrating clonotypes. We conducted the same approach with $CD4^+$ Tconv cells isolated from the salivary glands of Treg-ablated mice as a comparative control. We isolated an average of ~7.22×10^4 cells per prostate and ~1.08×10^5 cells per salivary gland. Following TCRα sequencing, we obtained an average of ~8.96×10^5 in-frame *Tcra* sequence reads per sample (data not shown). Collectively, the prostatic repertoire contained 17,154 distinct TCRα clonotypes (defined by the amino acid sequence of the TCRα complementarity determining region 3, or

CDR3α), of which 265 TCRα clonotypes were recurrently detected across all five prostate samples sequenced. For TCRα nomenclature, a recurrent TCRα clonotype is denoted using a three-letter code that reflects the amino acids at positions 3-5 of the CDR3α. For example, a clonotype with CDR3α sequence AVSRPGGGSNYKLT is denoted "SRP".

Analysis of the 20 most abundant prostate-associated $CD4^+$ Tconv cell clones demonstrated that these clones were found recurrently in all five prostate samples (Figure 1c) and accounted for ~23.9% ± 6.7% of all Tconv cells within the prostate, suggestive of TCR-dependent enrichment of select clones. We next compared the frequency of these top 20 prostate-associated TCRs within the SLOs of unmanipulated male TCRβtg mice. In doing so, we found that these clonotypes were generally present at low frequencies in the Treg and/or $CD4^+$ Tconv cell repertoires, arguing against these clones' infiltration into non-lymphoid tissues as a byproduct of elevated clonal frequencies within SLOs (Figure 1d). Surprisingly, following Treg cell depletion, many of the most abundant prostate-associated TCRs were also observed among $CD4^+$ Tconv cells that had infiltrated the salivary glands of the same mice (Figure 1d). Indeed, multiple $CD4^+$ Tconv cell clones isolated from the prostates of Treg-ablated mice were also detected in the salivary gland and vice-versa, although some clones preferentially infiltrated one non-lymphoid organ or the other. Collectively, these findings indicate that, in the setting of systemic Treg cell ablation, $CD4^+$ Tconv cell clones recurrently infiltrate both the prostate and salivary gland – albeit to differing extents.

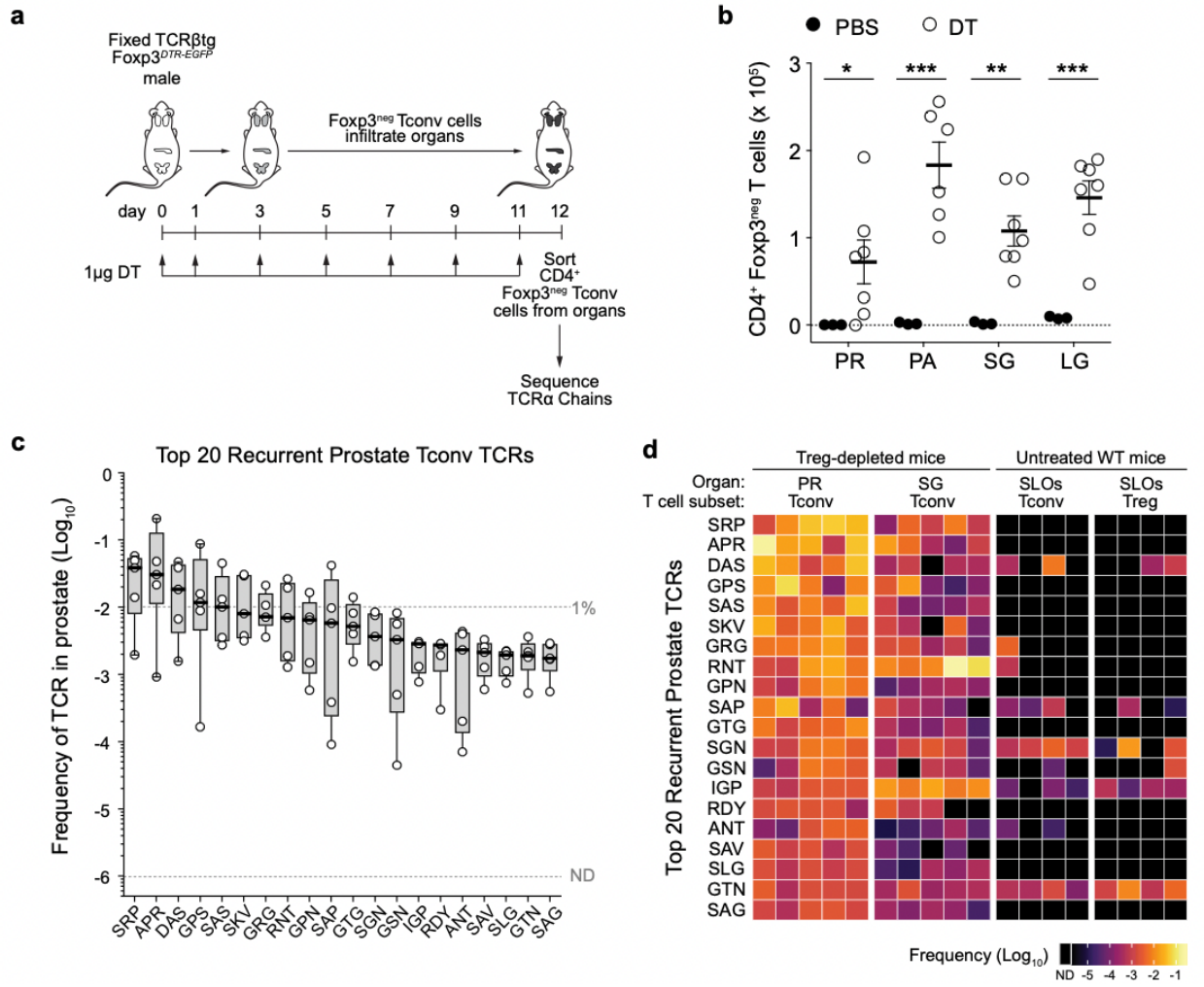

Figure 1 | Recurrent CD4⁺ Tconv clones are detected in non-lymphoid organs of Treg cell-depleted mice.

a, Experimental schematic. 6-8 week-old male TCRβtg *Foxp3*$^{DTR\text{-}EGFP}$ mice ($n = 7$) were subjected to sustained Treg cell ablation via administration of diphtheria toxin (DT). At day 12, CD4⁺Foxp3^{neg} T conventional (Tconv) cells were purified from select non-lymphoid organs by fluorescence-activated cell sorting (FACS). Samples from five mice were then subjected to deep sequencing of transcripts encoding TCRα chains using the iRepertoire platform (see Materials & Methods).

b, Absolute numbers of CD4⁺Foxp3^{neg} Tconv cells recovered from the prostate (PR), pancreas (PA), salivary glands (SG), and lacrimal glands (LG) of Treg cell-depleted mice (open circles; $n = 7$) shown in **a**. Data from control mice treated with PBS (closed circles; $n = 3$) are also shown. Error bars represent means ± SEM.

c, Box plots displaying the $\log_{10}$ frequency of the top 20 most abundant recurrent TCRα sequences expressed by Tconv cells in the prostate of Treg cell-depleted mice ($n = 5$). Each TCRα chain is denoted using a 3-letter code representing residues 3-5 of the predicted CDR3α chain. TCRα sequence information is listed in Table 1.

Figure 1, continued.
Boxes represent interquartile ranges (IQRs; Q1-Q3 frequencies), bold horizontal lines represent median values. Whiskers represent maximum and minimum values. A frequency of 1% is denoted by a horizontal dashed line.
d, Heat map displaying the 20 TCRα sequences from **c** and their corresponding $\log_{10}$ frequency in four groups of samples, as indicated. From left to right, these groups are Tconv cells from the prostate (PR) of Treg-depleted *Foxp3*$^{DTR\text{-}EGFP}$ males (n = 5), Tconv cells from the salivary glands (SG) of Treg-depleted *Foxp3*$^{DTR\text{-}EGFP}$ males (n = 5), Tconv cells from the pooled secondary lymphoid organs (SLOs) of untreated wild-type *Foxp3*^{GFP} males (n = 4), and Treg cells from the SLOs of untreated wild-type *Foxp3*^{GFP} males (n = 4). Data from the latter two groups are taken from ref[65]. Each column represents one biological sample. ND = not detected.

TCR	Vα Gene	Jα Gene	TCRα CDR3 Sequence	Category	Group
APR	TRAV6-7/DV9	TRAJ9	ALAPRNMGYKLT	No self-reactivity	1
DAS	TRAV8D-1	TRAJ50	ATDASSSFSKLV	No self-reactivity	1
ANT	TRAV7D-2	TRAJ40	AAANTGNYKYV	No self-reactivity	1
GPS	TRAV6-7/DV9	TRAJ9	ALGPSNMGYKLT	Low-level self-reactivity	2
GRG	TRAV9D-4	TRAJ32	AVGRGGSSGNKLI	Low-level self-reactivity	2
GPN	TRAV6-2	TRAJ42	VLGPNSGGSNAKLT	Low-level self-reactivity	2
SAP	TRAV14-2	TRAJ30	AASAPPNAYKVI	Low-level self-reactivity	2
GSN	TRAV9D-3	TRAJ34	ALGSNTNKVV	Low-level self-reactivity	2
IGP	TRAV14-2	TRAJ49	AAIGPGYQNFY	Low-level self-reactivity	2
SRP	TRAV9D-4	TRAJ53	AVSRPGGGSNYKLT	Overt self-reactivity	3
SKV	TRAV9D-4	TRAJ53	AVSKVGGGSNYKLT	Overt self-reactivity	3
SAS	TRAV9D-4	TRAJ9	AVSASTMGYKLT	Overt self-reactivity	3
GTG	TRAV14D-3/DV8	TRAJ12	ASGTGGYKVV	Overt self-reactivity	3

Table 1 | Selection of recurrent prostate-infiltrating CD4$^+$ Tconv clones isolated from Treg-ablated mice for TCR retrogenic studies.

13 of the top 20 most abundant recurrent TCRα sequences expressed by CD4$^+$ Tconv cells in the prostate of Treg cell-depleted mice were selected for TCR retrogenic studies. TCRs were selected based on differential TRAV and TRAJ usage. Each TCRα chain is denoted using a 3-letter code representing residues 3-5 of the predicted CDR3α chain. The full TCRα sequence information is listed, including TRAV and TRAJ usage. The 13 selected TCRα clonotypes can be binned into three groups based on hallmarks of steady-state activation and reactivity to MHC-II-restricted self-ligands (see Figure 2).

Multiple recurrent prostate-infiltrating CD4$^+$ Tconv cell clones display overt reactivity to endogenous spMHC-II ligands

The presence of recurrent CD4$^+$ Tconv cell clones in both the prostate and salivary glands of Treg-ablated mice raised questions regarding the nature of the self-antigens these clones recognize. To gain insights into these clones' antigen specificities, we selected 13 of these for further study using our TCRrg approach, prioritizing clones using unique combinations of Vα and Jα gene segments (Table 1). After generating primary TCRrg mice for each TCR of interest (see Materials & Methods and refs[140,141]), we characterized the localization and phenotype of TCRrg CD4$^+$ T cells across SLOs and non-lymphoid tissues of TCRrg mice. In performing this analysis for each of the 13 TCRs under study, we observed that clones could be broadly categorized into three groups (see Table 1). The first group ("Group 1") consisted of three clones, which yielded TCRrg CD4$^+$ T cells that remained phenotypically naïve in the SLOs of primary TCRrg mice (Figure 2a-b for ANT and DAS; data not shown for APR). Group 2 contained six clones, which yielded TCRrg CD4$^+$ T cells whose expression of CD69 varied but remained low across SLOs of primary TCRrg mice (data not shown). Interestingly, the four clones in Group 3 upregulated similarly high levels of CD69 and PD-1 across all SLOs examined, indicative of sensitivity to spMHC-II ligands present throughout the body (Figure 2a-b). We next assessed proliferation of our prostate-associated CD4$^+$ Tconv cell clones following co-culture of CTV-labeled TCRrg CD4$^+$ T cells with CD11c$^+$ splenocytes and IL-2. These analyses validated the TCR grouping strategy and patterns of reactivity described from characterizations of primary TCRrg mice. Specifically, Group 1 TCRrg CD4$^+$ T cells showed no proliferation over background when co-cultured with splenic APCs and IL-2 (Figure 2c-d). Addition of microbeads coated with anti-CD3/anti-CD28 antibodies induced proliferation of Group 1 TCRrg CD4$^+$ T cells, demonstrating that these cells

were not inherently dysfunctional. Group 2 TCRrg $CD4^+$ T cells exhibited variable extents of low-level proliferation in *in vitro* co-cultures, reflecting variable CD69 positivity in primary TCRrg hosts (data not shown). On the other hand, Group 3 TCRrg $CD4^+$ T cells expanded robustly in the presence of splenic APCs and IL-2 alone (Figure 2c-d). Group 3 TCRrg $CD4^+$ T cells also proliferated when splenic APCs from GF mice were used (Figure 2e-f), arguing against a role for recognition of antigens derived from commensal bacteria. Notably, proliferation of Group 3 TCRrg $CD4^+$ T cells was abrogated when splenic APCs from *H2-DMa*$^{-/-}$ mice were used (Figure 2e-f). H2-M-deficient APCs predominantly present MHC-II molecules loaded with the invariant chain-derived CLIP peptide as a result of impaired peptide exchange[235]. The lack of response by Group 3 TCRrg $CD4^+$ T cells to H2-M-deficient APCs showed that these cells react to specific self-derived peptides rather than MHC-II itself. Moreover, the finding that Group 3 TCRrg $CD4^+$ T cells proliferate in the absence of exogenous peptide indicates that the antigenic peptide is endogenously presented by splenic APCs at steady state.

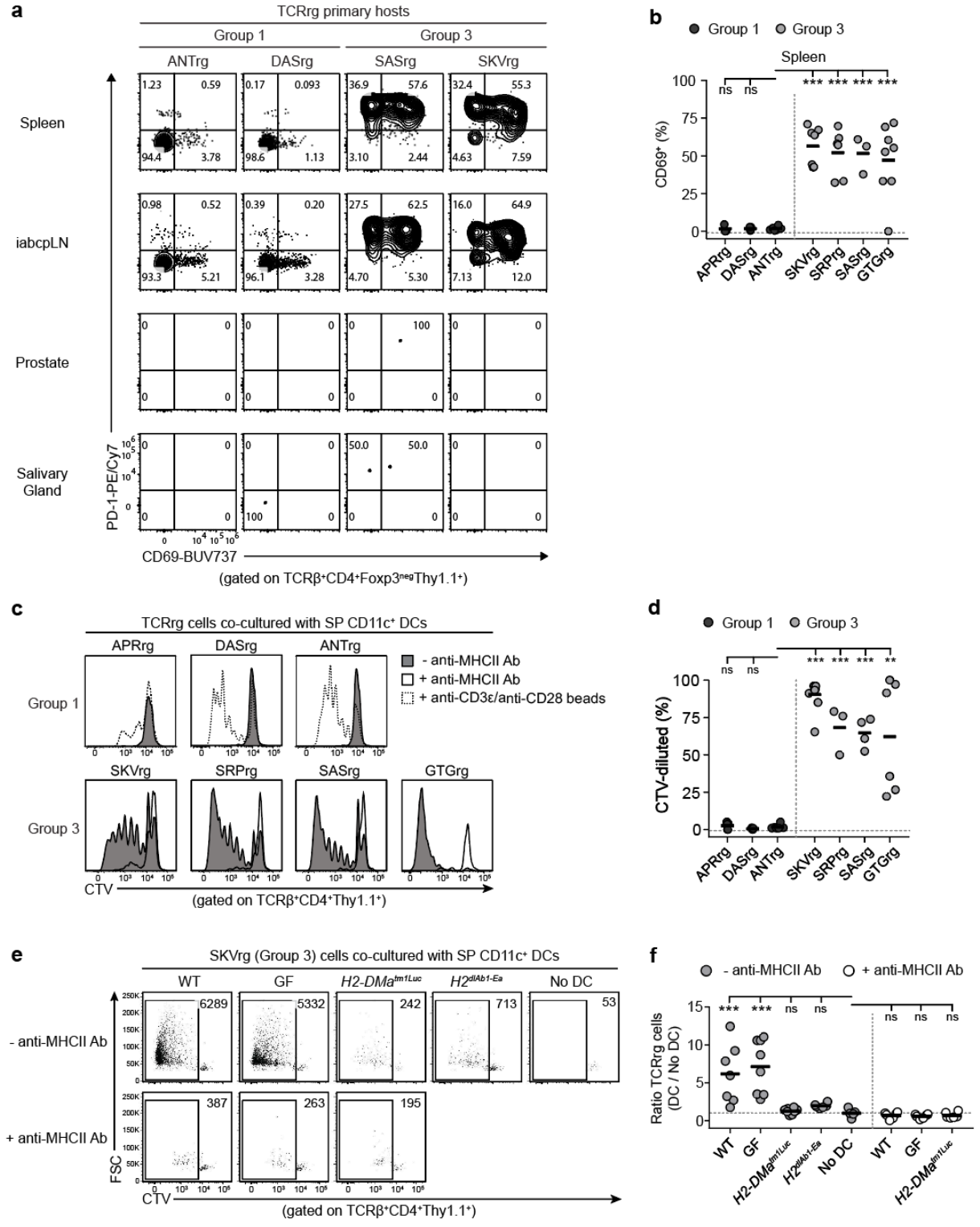

Figure 2 | Multiple recurrent prostate-infiltrating CD4$^+$ Tconv clones exhibit hallmarks of steady-state activation and reactivity to MHC-II-restricted self-ligands.

Figure 2, continued.
Group 1 and Group 3 TCRs as defined in Table 1 were cloned and expressed as TCRrg mice (see Materials & Methods). >6 weeks after bone marrow reconstitution, TCRrg T cells were purified and directly phenotyped using flow cytometry (**a**,**b**) or subjected to *in vitro* reactivity assays (**c-f**).
a, Representative flow cytometric analysis of CD69 and PD-1 expression by Group 1 clones ANT and DAS and Group 3 clones SAS and SKV isolated from the spleen, pooled lymph nodes (iabcpLN), prostate and salivary glands of primary male TCRrg mice.
b, Summary plot of data from **a** showing the percentage of splenic Group 1 (black symbols) and Group 3 (gray symbols) TCRrg T cells ($TCR\beta^+CD4^+Thy1.1^+$) expressing CD69. Each symbol depicts cells from an individual TCRrg mouse. $n \geq 3$ per TCR. Data are pooled from eleven independent experiments.
c, Purified $TCR\beta^+CD4^+Thy1.1^+$ TCRrg T cells expressing the indicated Group 1 (top) and Group 3 (bottom) clones were labeled with CellTrace Violet (CTV) and co-cultured with splenic $CD11c^+$ dendritic cells (DCs) and mouse recombinant IL-2 (mrIL-2) ± anti-MHCII blocking antibody for 5 days (see Methods). Representative flow cytometric analyses of CTV dilution are shown. TCRrg cells co-cultured with anti-CD3ε/anti-CD28 MACSiBead particles (1:1) and mrIL-2 served as positive controls, indicated by dashed histograms.
d, Summary plot of data from **c** depicting the percentage of CTV-diluted Group 1 (black symbols) and Group 3 (gray symbols) TCRrg T cells. Each symbol represents an individual co-culture. $n \geq 3$ per condition. Data are pooled from eight independent experiments.
e, Histograms displaying representative flow cytometric analysis of proliferation by Group 3 CTV-labeled TCRrg cells ($TCR\beta^+CD4^+Thy1.1^+$) co-cultured with splenic $CD11c^+$ DCs and mrIL-2 ± anti-MHC-II blocking antibody for 5 days. DCs were isolated from various mouse strains: WT, B6 $CD45^{.1/.1}$; GF, germ-free; *H2-DMa*^{tm1Luc}, H2-DM-deficient mice; *H2*$^{dlAb1\text{-}Ea}$, MHC class II $I\text{-}A^b$-deficient mice (see Methods). TCRrg cells co-cultured with mrIL-2 in the absence of $CD11c^+$ DCs served as negative controls.
f, Summary plot of data from **e** depicting the absolute number of Group 3 TCRrg cells recovered at the culture endpoint, displayed as a ratio of total TCRrg cell count within each DC-containing co-culture sample divided by the mean of TCRrg cell counts within cultures lacking DCs in a given experiment. Symbols represent individual co-cultures. $n \geq 5$ per condition. Data are pooled from two independent experiments.
TCRrg T cells are denoted by the TCRα CDR3 amino acid sequence at positions 3-5 (see Table 1), followed by "rg." Bold horizontal lines represent means. *p* values were calculated by two-tailed Student's t-test. *ns*, not significant; $*p < 0.05$; $**p < 0.01$; $***p < 0.001$.

Group 3 clones express common hallmarks of T follicular helper cells

Despite overt self-reactivity to self-antigens and widespread availability of spMHC-II ligands, $CD4^+$ T cells bearing Group 3 TCRs were not found to promote spontaneous autoimmunity, as shown by a lack of organ infiltration in TCRrg primary hosts (Figure 2a). To understand how such cells are regulated at steady state, we FACS-purified TCRrg $CD4^+$ T cells expressing the Group 3 TCR SAS and performed transcriptional profiling of these cells via bulk RNA sequencing (RNAseq; Figure 3a). We also performed the same analysis for TCRrg $CD4^+$ T cells expressing the Group 1 TCR ANT, which do not show hallmarks of activation in response to self-antigens. Principal component analysis (PCA) revealed right clustering of samples by TCR, with pronounced separation of Group 1 ANT and Group 3 SAS samples along PC1 (Figure 3b). In comparing transcripts expressed by Group 3 SAS cells and Group 1 ANT cells, we found 5,085 differentially expressed genes (DEGs) at a false discovery rate (FDR) cut-off of $q \leq 0.05$. Of these, 2,851 genes were upregulated in Group 3 SAS cells relative to Group 1 ANT cells (Figure 3c).

We first focused on genes upregulated by Group 3 SAS cells to determine if these cells were adopting a particular T helper (Th) cell program at steady state. We performed gene set enrichment analysis (GSEA) comparing the genes upregulated by Group 3 SAS cells to previously published gene sets associated with various Th subsets[236]. Unsurprisingly, as many established gene sets are derived from analysis of $CD4^+$ T cells undergoing *in vitro* polarization or active *in vivo* immunization, Group 3 SAS cells at steady state did not exhibit statistically significant enrichment of these predefined Th gene sets relative to Group 1 ANT cells (data not shown). However, closer examination of the 100 most upregulated and 100 most downregulated transcripts in Group 3 SAS cells relative to Group 1 ANT cells yielded valuable insights. Group 3 SAS cells were distinguished by decreased expression of *Ly6c1* (Ly6c) and *Prdm1* (Blimp-1), as well as

increased expression of *Cxcr5*, *Pdcd1* (PD-1), and *Slamf7*. These features are shared by Tfh cells, which are specialized to interact with B cells and potentiate antibody responses[169,223]. Further curation of DEGs revealed that Group 3 SAS cells were enriched for additional hallmarks of Tfh cells, including *Bcl6*, *Cd200*, *Icos*, and *Tox2* (Figure 3d)[222,237,238]. At the protein level, Group 3 TCRrg $CD4^+$ T cells were found to express Bcl6, PD-1, CXCR5, and ICOS via flow cytometry (Figure 3e-h). In contrast, Group 1 clones showed minimal protein expression of these markers, consistent with their naïve phenotype in the periphery (Figure 3e-h). In sum, Group 3 TCRrg $CD4^+$ T cells display several canonical features of the Tfh cell phenotype at steady state.

Group 3 clones exhibit signs of agonist signaling during thymic development

In observing the adoption of a Tfh-like phenotype by Group 3 clones, we asked whether this phenotype is imparted upon thymocytes expressing Group 3 TCRs during thymic development, or whether this phenotype is imposed upon Group 3 $CD4^+$ T cells once in the periphery. We first isolated thymi from Group 1 and Group 3 TCRrg mice and profiled TCRrg thymocytes *ex vivo*. CD4 single-positive (CD4SP) thymocytes expressing Group 3 TCRs (SAS or SKV) remained predominantly negative for Bcl6 and CXCR5 expression (Figure 4a). Importantly, a greater fraction of Group 3 TCRrg CD4SP thymocytes expressed PD-1, suggestive of strong TCR signaling in response to spMHC-II ligands in the thymus (Figure 4a-b)[20]. In line with this finding, Group 3 TCRrg thymocytes at the double-positive (DP) stage of thymic development exhibited downregulation of both the CD4 and CD8 co-receptors, a phenomenon termed “DP dulling” that is considered a readout of agonist ligand sensing[239] (Figure 4b). Despite this, expression of Foxp3 and active caspase-3 remained minimal among Group 3 TCRrg CD4SP

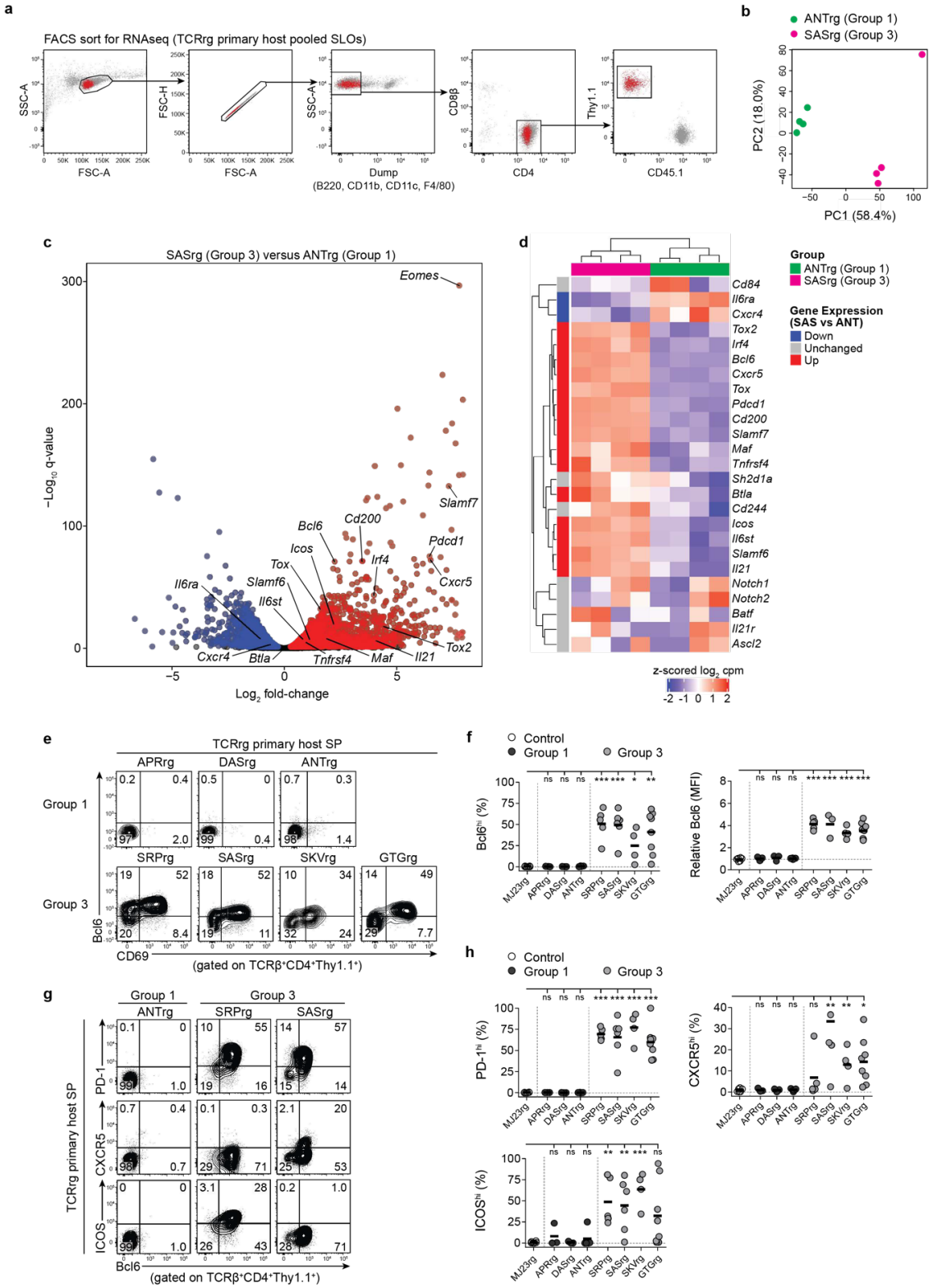

Figure 3 | Group 3 clones express common hallmarks of T follicular helper cells.

Figure 3, continued.
a-d, Comparative RNA-Seq analysis of Group 3 SAS and Group 1 ANT TCRrg cells. The SAS and ANT TCRs were cloned and expressed as TCRrg mice (see Methods). >6 weeks after bone marrow reconstitution, TCRrg T cells were purified from the pooled secondary lymphoid organs (SLOs) of primary TCRrg mice and subjected to bulk RNA sequencing (see Methods). Only biological samples containing ≥ 1 x 10^5 TCRrg T cells were included for analysis (n = 4 mice per TCR).
a, Gating strategy schematic for the fluorescence-activated cells sorting (FACS) of TCRrg T cells for RNA sequencing. TCRrg T cells were selected by gating on $Dump^{neg}$ ($B220^{neg}CD11b^{neg}CD11c^{neg}F4/80^{neg}$), followed by $CD4^+CD8\beta^{neg}$, then by $Thy1.1^+CD45.1^{neg}$.
b, Principal component analysis (PCA) of mRNA expression in Group 1 ANT and Group 3 SAS TCRrg T cells, presented as log-scaled normalized expression (log_2 CPM). Each dot corresponds to an independent biological sample. Green and magenta dots denote samples isolated from Group 1 ANT and Group 3 SAS TCRrg mice, respectively. n = 4 per TCR. Data are pooled from two independent experiments.
c, RNA-seq volcano plot depicting differential gene expression for Group 3 SAS and Group 1 ANT TCRrg cells. The $-log_{10}$ q-value versus log_2 fold-change is depicted for genes with average log_2 CPM ≥ -1. Blue and red dots denote genes over-represented in Group 1 ANTrg and Group 3 SASrg T cells, respectively, with a false discovery rate (FDR) of 5%. Labels denote select up- and down-regulated genes implicated in T follicular helper (Tfh) cell differentiation and function, as defined in **b**. Data are pooled from two independent experiments. q values were generated using edgeR (see Methods). For the 25 Tfh-related genes highlighted in **d**, genes that are significantly under- or overexpressed by Group 3 SAS TCRrg cells relative to Group 1 ANT TCRrg cells are indicated. Also indicated is the gene Eomes, relevant to later figures.
d, RNA-seq heatmap displaying differential expression of select genes, shown as z-scored expression values (log_2 CPM), for Group 3 SAS vs. Group 1 ANT TCRrg cells. The 25 genes depicted represent a curated list of genes previously implicated in Tfh cell differentiation and function[169,222,223,238]. Group 3 SAS TCRrg cells were enriched for the gene set shown (Fisher's exact test, $p = 4 \times 10^{-8}$).
e-h, Flow cytometric analysis of TCRrg T cells expressing Group 1 and Group 3 TCRs. TCRrg female mice expressing the prostate-specific MJ23 TCR (MJ23rg) served as additional negative controls. $n \geq 3$ per TCR.
e, Representative flow cytometric analysis of Bcl6 vs. CD69 expression by splenic Group 1 (top) and Group 3 (bottom) TCRrg T cells ($TCR\beta^+CD4^+Thy1.1^+$). SP, spleen.
f, Left, summary plot of data from **c** showing the percentage of splenic Group 1 (black symbols), Group 3 (gray symbols), and MJ23 (white symbols) TCRrg T cells ($TCR\beta^+CD4^+Thy1.1^+$) expressing Bcl6. Right, summary plot of data from **c** depicting relative Bcl6 expression, displayed as a ratio of mean fluorescence intensity (MFI) in Group 1 (black symbols) and Group 3 (gray symbols) TCRrg T cells ($TCR\beta^+CD4^+Thy1.1^+$) divided by MFI in control MJ23 TCRrg T cells (MJ23rg, white symbols) in a given experiment. Each symbol depicts cells from an individual TCRrg mouse. Data are pooled from six independent experiments.
g, Representative flow cytometric analysis of PD-1 (top row), CXCR5 (middle row), and ICOS (bottom row) vs. Bcl6 expression by splenic Group 1 and Group 3 TCRrg T cells ($TCR\beta^+CD4^+Thy1.1^+$). SP, spleen.
h, Summary plots of data from **e** showing the percentage of splenic Group 1 (black symbols), Group 3 (gray symbols), and MJ23 (white symbols) TCRrg T cells ($TCR\beta^+CD4^+Thy1.1^+$)

expressing PD-1 (top left), CXCR5 (top right), and ICOS (bottom left). Each symbol depicts cells from an individual TCRrg mouse. Data are pooled from six independent experiments.
TCRrg T cells are denoted by the TCRα CDR3 amino acid sequence at positions 3-5 (see Table 1), followed by "rg." Bold horizontal lines represent means. *p* values were calculated by two-tailed Student's t-test. *ns*, not significant; *$p < 0.05$; **$p < 0.01$; ***$p < 0.001$.

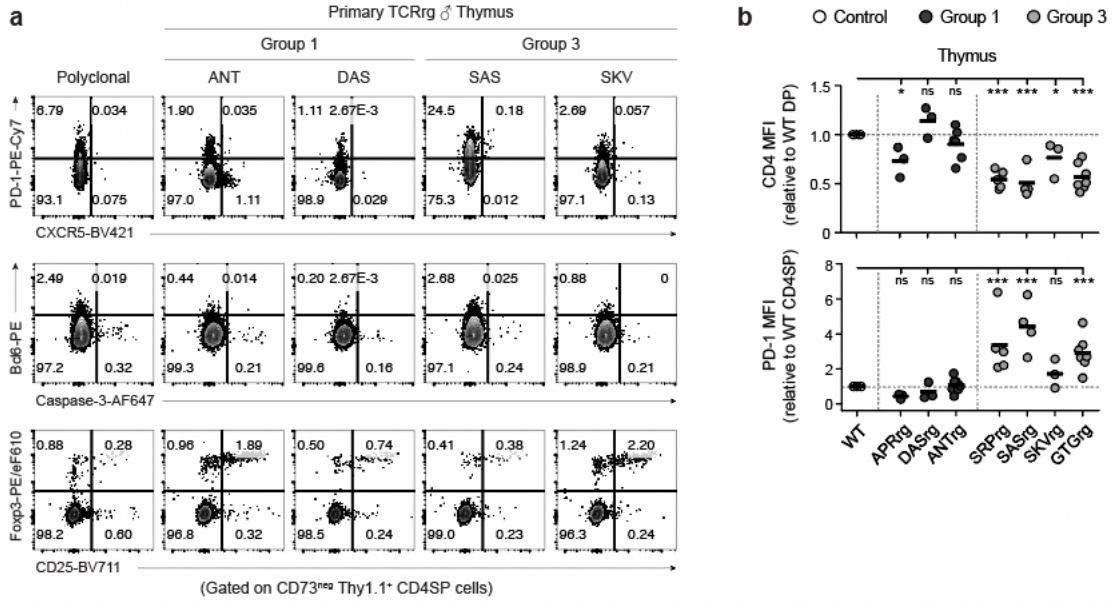

Figure 4 | Thymocytes expressing Group 3 TCRs do not show overt hallmarks of negative selection, tTreg cell differentiation, or intrathymic Tfh cell induction.

a-c, Assessment of thymocyte fate in TCRrg mice. TCRrg mice were generated for the indicated Group 1 and Group 3 TCRs. ≥6 weeks post-generation, thymi were isolated from TCRrg mice for phenotypic analysis.
a, Flow cytometric plots showing expression of PD-1 and CXCR5 (top), Bcl6 and cleaved caspase-3 (middle), and Foxp3 and CD25 (bottom) among TCRrg CD4SP thymocytes.
b, Top, quantification of the mean fluorescence intensity (MFI) of CD4 among Group 1 (black symbols) and Group 3 (gray symbols) TCRrg thymocytes, normalized to CD4 MFI of $CD4^+CD8\alpha^+$ double-positive (DP) thymocytes from control wild-type (WT) mice. Bottom, quantification of PD-1 MFI among Group 1 (black symbols) and Group 3 (gray symbols) TCRrg thymocytes, normalized to PD-1 MFI of $CD4^+CD8^{neg}$ single-positive (CD4SP) thymocytes from control WT mice.

thymocytes (Figure 4a), indicating that signaling in response to agonist TCR:spMHC-II interactions does not culminate in tTreg cell differentiation or clonal deletion of these clones. Moreover, Group 3 TCRrg CD4$^+$ T cells displayed only a subset of their Tfh-like phenotype in the thymus, suggesting that additional cues in SLOs shape these cells' differentiation, expansion, and/or maintenance in the periphery.

Group 3 clones are poised to interface with B cells

Classical Tfh cells are thought to develop and be maintained by TCR:pMHC-II and ICOS-ICOSL interactions facilitated by both dendritic cells (DCs) and B cells. As such, B cell deficiency is associated with impaired Tfh cell differentiation and/or maintenance in settings of immunization and acute infection[240–242]. To determine whether peripheral B cells are required for the induction of a more complete Tfh-like program in Group 3 TCRrg CD4$^+$ T cells, we transferred CD4SP thymocytes from Group 3 SAS TCRrg mice into secondary recipients pre-treated with either an anti-CD20 or isotype control antibody. Anti-CD20 administration led to the depletion of most, but not all, B cells in spleen and lymph nodes by day 7 post-treatment (Figure 5a-b), in line with previous reports[243]. Group 3 SAS TCRrg thymocytes were still found to upregulate Bcl6, CD200, and CXCR5 following transfer into anti-CD20-treated mice (Figure 5c-d), suggesting that B cells are dispensable for Group 3 clones to adopt a Tfh-like program in the periphery.

In a similar experiment, we sought to determine the extent to which CD4$^+$ Tconv cells expressing Group 3 TCRs maintained their Tfh-like phenotype in the absence of B cells. Group 3 SAS CD4$^+$ Tconv cells were isolated from the SLOs of primary SAS TCRrg mice and transferred

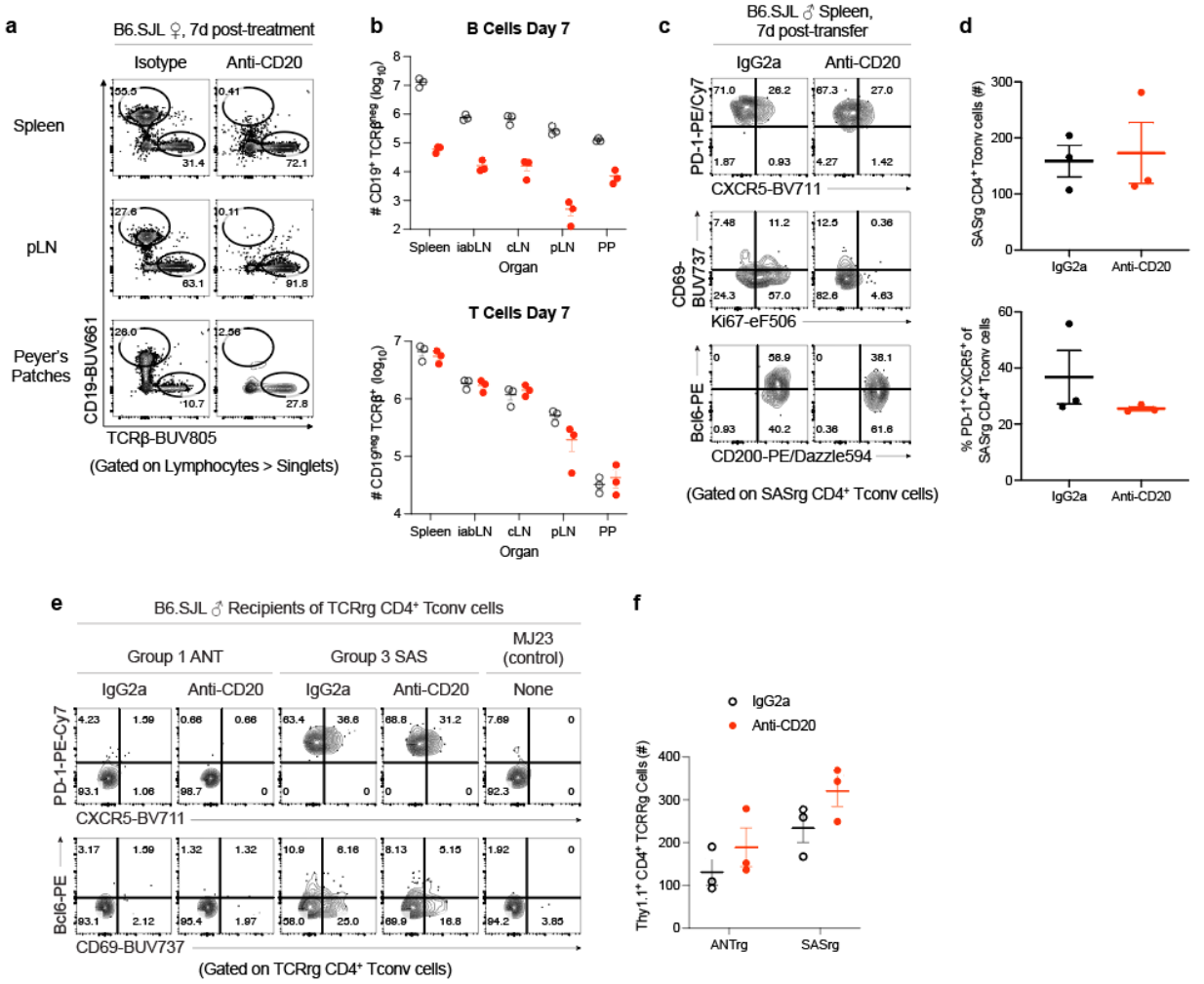

Figure 5 | Group 3 TCRrg CD4$^+$ Tconv cells express signature markers of Tfh cells in settings of B cell depletion.

a-b, Effect of anti-CD20 antibody administration (clone MB20-11, see Materials & Methods) on endogenous B and T cells in the spleen, periaortic lymph nodes (pLN), and Peyer's Patches 7 days post-treatment.

a, Representative flow cytometric plots showing frequencies of CD19$^+$ B cells and TCRβ$^+$ T cells isolated from the indicated sites of mice injected intraperitoneally (i.p.) 7 days earlier with 250μg anti-CD20 or IgG2a isotype control antibody.

b, Quantification of B and T cell counts as shown in **a**.

c-d, CD8β-depleted thymocytes from Group 3 SAS TCRrg mice were transferred into secondary recipients that had been treated 7 days earlier with 250μg anti-CD20 or IgG2a isotype control antibody. Group 3 SAS TCRrg CD4$^+$ Tconv cell numbers and phenotype were assessed 7 days post-transfer.

c, Representative flow cytometric plots showing Group 3 SAS TCRrg CD4$^+$ Tconv cell expression of Tfh cell markers PD-1 and CXCR5 (top), activation markers CD69 and Ki67 (middle), and markers that facilitate interactions with B cells (Bcl6 and CD200, bottom).

Figure 5, continued.
d, Top, quantification of Group 3 SAS TCRrg CD4$^+$ Tconv cell counts recovered from recipient spleens. Bottom, quantification of the frequency of Group 3 SAS TCRrg CD4$^+$ Tconv cells expressing canonical Tfh cell markers following transfer.
e-f, FACS-purified TCRrg CD4$^+$ Tconv cells were transferred into secondary recipients that had been treated 7 days earlier with 250µg anti-CD20 or IgG2a isotype control antibody. Donor cell numbers and phenotype were assessed 7 days post-transfer.
e, Representative flow cytometric plots showing TCRrg CD4$^+$ Tconv cell expression of PD-1 and CXCR5 (top), and CD69 and Bcl6 (bottom).
d, Quantification of Group 3 SAS TCRrg CD4$^+$ Tconv cell counts recovered from recipient spleens.

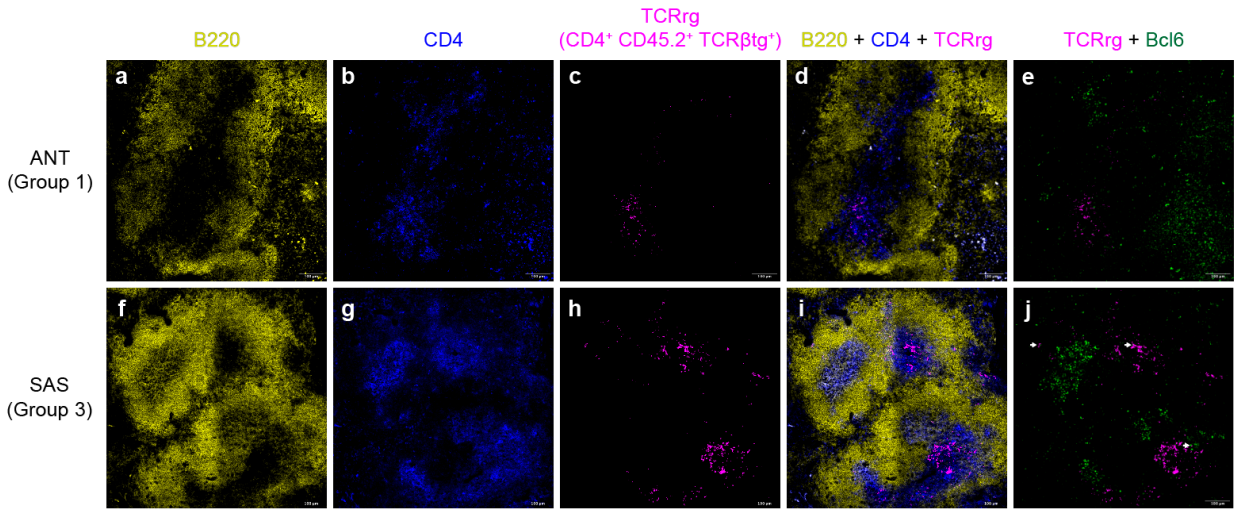

Figure 6 | Group 3 TCRrg CD4$^+$ T cells are localized near and within B cell follicles at steady state.

a-h, Immunofluorescence (IF) microscopy of TCRrg spleen sections to assess localization of TCRrg CD4$^+$ T cells. Spleens from primary TCRrg hosts were isolated, embedded in OCT, and frozen for sectioning and IF microscopy (see Materials & Methods). Sections were stained with antibodies against B220, CD4, CD45.2, TCRβtg, and Bcl6. Representative images are shown for the Group 1 ANT clone (**a-e**) and the Group 3 SAS clone (**f-j**). Data are from two independent experiments, $n = 6$ per clone.
a, Positioning of B220-expressing cells in the spleen of a Group 1 ANT TCRrg mouse.
b, Positioning of CD4-expressing cells in the spleen of a Group 1 ANT TCRrg mouse.
c, Positioning of splenic ANT TCRrg cells, defined as CD45.2$^+$ CD4$^+$ TCRβtg$^+$ cells.
d, Overlay of images shown in **a-c**.
e, Overlay of **c** with superimposed Bcl6 staining.
f, Positioning of B220-expressing cells in the spleen of a Group 3 SAS TCRrg mouse.
g, Positioning of CD4-expressing cells in the spleen of a Group 3 SAS TCRrg mouse.
h, Positioning of splenic SAS TCRrg cells, defined as in **c**.
i, Overlay of images shown in **e-g**.
j, Overlay of **h** with superimposed Bcl6 staining. White arrowheads indicate Bcl6$^+$ TCRrg cells.

into anti-CD20-treated or control mice. Seven days following transfer, mice given anti-CD20 or isotype control showed no notable differences with regards to Group 3 SAS $CD4^+$ Tconv cell numbers or expression of Tfh cell markers (Figure 5e-f). These findings suggest that, at least for a period of 7 days, B cells are not required for Group 3 clones to persist or to adopt their Tfh-like phenotype. Alternatively, the few B cells that remain following αCD20 treatment may support the differentiation and/or maintenance of Group 3 clones.

While B cells may not be required for Group 3 clones to survive or upregulate Tfh-related markers, the latter's expression of Bcl6, CXCR5, and ICOS may still enable these cells to interact with B cells near the B cell follicle. To assess this possibility, we isolated spleens from primary TCRrg mice expressing either the Group 1 ANT TCR or the Group 3 SAS TCR, and then analyzed the localization of TCRrg cells in these samples using immunofluorescence (IF) microscopy. TCRrg $CD4^+$ T cells were distinguished from endogenous B6 $CD45^{.1/.1}$ cells using the combination of CD4, CD45.2, and TCR Vβ3. Our imaging analysis revealed that Group 1 ANT TCRrg $CD4^+$ T cells were predominantly confined to T cell zones and excluded from B cell follicles (Figure 6a-d). In contrast, individual Group 3 SAS TCRrg $CD4^+$ T cells could be observed near the edges of B cell follicles and in close proximity to B cells (Figure 6f-i). Moreover, individual $Bcl6^+$ TCRrg cells were readily in spleens from Group 3 SAS TCRrg mice, but less so in samples from Group 1 ANT TCRrg mice, mirroring our flow cytometric characterizations of these clones (Figure 6e, j).

Group 3 clones infiltrate non-lymphoid tissues and switch to a Th1 cell phenotype following systemic Treg cell ablation

In addition to upregulating multiple markers associated with Tfh cells, Group 3 clones highly expressed the transcription factor eomesodermin (Eomes) in the spleens of TCRrg mice

(Figure 7a). Eomes is involved in multiple facets of $CD8^+$ T cell differentiation and function, including in these cells' production of IFN-γ[244] and in their adoption of a memory phenotype[245]. In $CD4^+$ T cells, the function of Eomes remains incompletely understood, with recent reports linking its expression to $CD4^+$ T cell secretion of IFN-γ, IL-10, and/or granzyme B[246]. In our RNAseq analysis of Group 3 SAS cells, both *Eomes* and *Ifng* were found to be among the most highly upregulated transcripts relative to Group 1 ANT cells (Figure 3c and data not shown). Despite this, Group 3 SAS TCRrg $CD4^+$ Tconv cells did not produce IFN-γ at steady state (Figure 7b, PBS histograms), suggesting that pro-inflammatory cytokine production by Group 3 clones may be limited to inflammatory contexts. To test this, we generated TCRrg male mice expressing Group 1 or Group 3 TCRs, in which both host and TCRrg cells harbored the *Foxp3*$^{DTR\text{-}EGFP}$ allele. DT administration over the course of 12 days (as in Figure 1a) led to lymphoproliferation and T cell infiltration of non-lymphoid organs. Notably, in this setting, Group 3 clones readily infiltrated both the prostate and salivary gland, whereas minimal organ infiltration was observed for Group 1 clones (Figure 7c). Moreover, in the SLOs and non-lymphoid tissues of Treg-ablated animals, Group 3 clones produced IFN-γ upon PMA/ionomycin stimulation (Figure 7b, DT histograms), concomitant with a loss of Bcl6 (data not shown). Taken together, these findings suggest that, at steady state, Group 3 clones are diverted into a Tfh-like fate to curb their pathogenic potential. Once tolerance is broken, as in the case of systemic Treg cell ablation, Group 3 clones lose their Tfh-like phenotype, adopt a Th1 cell program, and mediate autoimmune responses against host tissues.

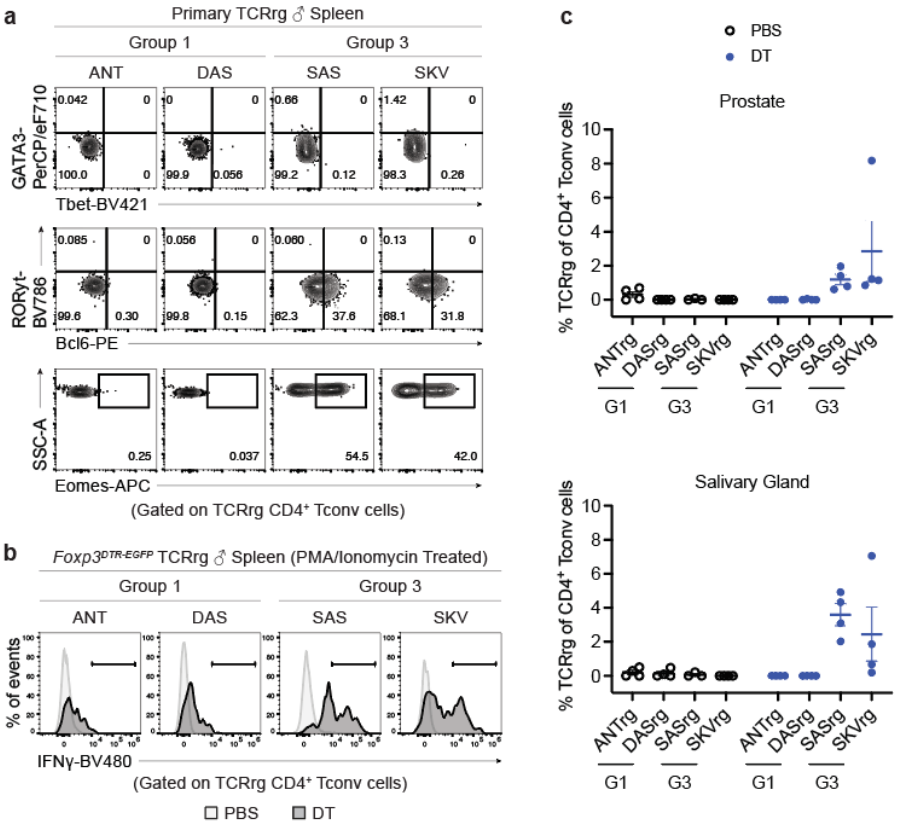

Figure 7 | Upon systemic Treg cell ablation, Group 3 clones produce IFNγ and infiltrate non-lymphoid tissues.

TCRrg mice expressing Group 1 or Group 3 TCRs were generated in *Foxp3*$^{DTR\text{-}EGFP/y}$ hosts using bone marrow from "retrogenic donor" mice that also harbored the *Foxp3*$^{DTR\text{-}EGFP}$ allele (see Materials & Methods). ≥ 8 weeks post-generation, TCRrg mice were treated with diphtheria toxin (DT) to ablate endogenous and TCRrg-derived Treg cells as in Figure 1a. PBS-treated TCRrg mice were included as controls. On experiment day 12, TCRrg CD4$^+$ Tconv cells were isolated from spleen, pooled lymph nodes (not shown), prostate, and salivary gland for phenotypic analysis.

a, Top and middle, expression of T helper (Th) lineage-defining transcription factors by TCRrg CD4$^+$ Tconv cells recovered from the spleens of PBS-treated *Foxp3*$^{DTR\text{-}EGFP/y}$ TCRrg mice. Bottom, expression of Eomes by TCRrg CD4$^+$ Tconv cells recovered from the spleens of PBS-treated *Foxp3*^{DTR} TCRrg mice.

b, Assessment of IFNγ production by splenic TCRrg CD4$^+$ Tconv cells following DT (dark gray histogram) or PBS treatment (light gray histogram). Cells were stimulated for 5 h with PMA & ionomycin, supplemented with monensin for the final 4 h of culture (see Materials & Methods).

c, Summary plots showing the frequency of TCRrg cells among all CD4$^+$ Tconv cells recovered from the prostates (top) and salivary glands (bottom) of PBS or DT-treated *Foxp3*^{DTR} TCRrg mice (open white and closed blue dots, respectively). Data are compiled from two independent experiments, n ≥ 3 per TCR per condition.

The endogenous CD4$^+$ Tconv repertoire harbors T cells displaying hallmarks of Group 3 clones

Given the potential danger that Group 3 clones pose to the host, we aimed to identify polyclonal CD4$^+$ T cells within the endogenous repertoire that display similar phenotypic hallmarks of Group 3 clones. Based on our transcriptional and phenotyping profiling of Group 3 SAS TCRrg cells, we defined PD-1^{hi} Bcl6$^+$ Eomes$^+$ CD4$^+$ Tconv cells as "Group 3-like" cells (Figure 8a). The combined use of these markers allowed us to identify a measurable population of polyclonal CD4$^+$ T cells from unmanipulated WT mice that phenotypically mirror Group 3 SAS TCRrg cells (Figure 8b). Notably, polyclonal Group 3-like cells and Group 3 SAS TCRrg cells expressed similar extents of CD69, suggesting that polyclonal Group 3-like cells had also recently undergone TCR stimulation in response to spMHC-II ligands (Figure 8c). Moreover, PD-1$^+$ Bcl6$^+$ Eomes$^+$ CD4$^+$ Tconv cells were phenotypically distinct from other previously defined populations of antigen-experienced CD4$^+$ T cells, including Foxp3$^+$ Treg cells, CD44^{hi} CD62L^{lo} "memory-phenotype" Tconv cells[247], and CD44^{hi} CD73^{hi} FR4^{hi} "anergic phenotype" Tconv cells[248,249] (Figure 8c). Thus, polyclonal T cells exhibiting numerous features of Group 3 clones can be readily identified within the endogenous repertoire.

The frequency of polyclonal Group 3-like cells is diminished following inducible depletion of B cells

Lastly, we investigated whether B cells were required for the differentiation or maintenance of polyclonal CD4$^+$ Tconv cells displaying the Group 3-like PD-1$^+$ Bcl6$^+$ Eomes$^+$ phenotype. To do so, we generated *Mb1^{Cre} x Rosa26$^{LSL-DTR}$* mice, which harbor a Cre-inducible DTR inserted in

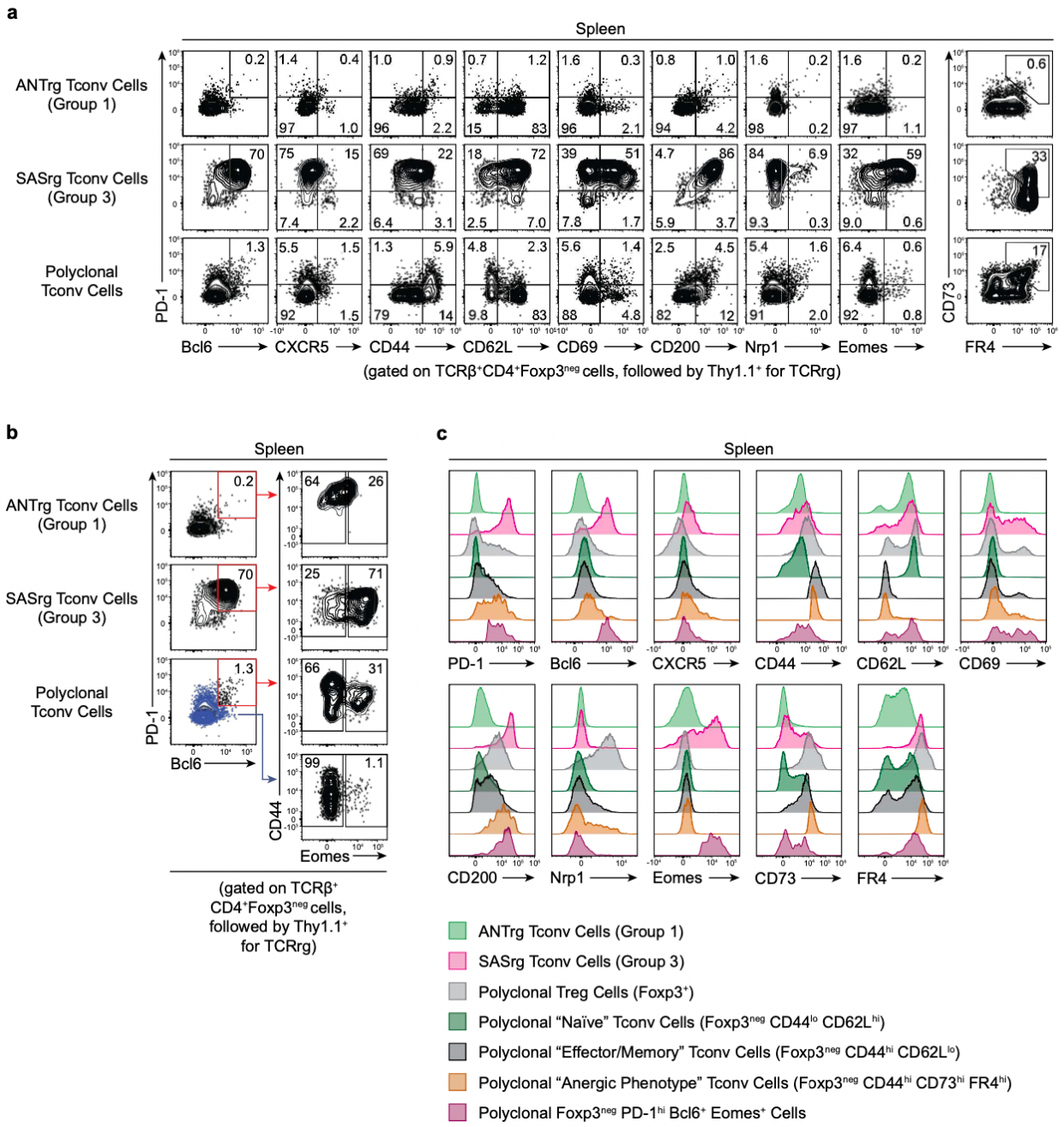

Figure 8 | The endogenous CD4$^+$ Tconv repertoire harbors T cells displaying hallmarks of Group 3 clones

Flow cytometric analysis of Group 1 ANT TCRrg, Group 3 SAS TCRrg, and polyclonal CD4$^+$ Tconv cells. (Continued on next page.)

Figure 8, continued.

a, TCRrg T cells (TCRβ^{+} CD4^{+} Thy1.1^{+}) from Group 1 ANT and Group 3 SAS TCRrg mice were analyzed using flow cytometry. Representative flow cytometric analysis of PD-1 expression vs. expression of the indicated markers (left columns), or CD73 vs. FR4 expression (far right column) by splenic ANTrg or SASrg T cells. Splenic CD4^{+} T cells (TCRβ^{+} CD4^{+}) isolated from untreated B6 mice served as controls (polyclonal, bottom row).
b, Gating strategy for the identification of polyclonal CD4^{+} Foxp3^{neg} Tconv cells from untreated B6 mice displaying common features of Group 3 clones. Group 3-like cells were identified by gating on PD-1^{hi}Bcl6^{+} (red gate) cells, followed by Eomes^{+} cells. PD-1^{lo} Bcl6^{neg} cells from untreated B6 mice served as negative controls (blue dot plot and arrow).
c, Histograms displaying representative flow cytometric analysis of expression of Tfh-associated markers (PD-1, Bcl6, and CXCR5), markers of T cell antigen experience (CD44, CD62L, CD69, CD200), and other relevant phenotypic markers (Nrp1, Eomes, CD73, and FR4) by the following cell populations: Group 1 ANTrg and Group 3 SASrg T cells (TCRβ^{+}CD4^{+}Thy1.1^{+}), polyclonal Treg cells (Foxp3^{+}), polyclonal "naïve" Tconv cells (Foxp3^{neg}CD44^{lo}CD62L^{hi}), polyclonal effector/memory Tconv cells (Foxp3^{neg}CD44^{hi}CD62L^{lo}), polyclonal "anergic phenotype" cells (Foxp3^{neg}CD44^{hi}CD73^{hi}FR4^{hi}), and polyclonal Group 3-like cells (Foxp3^{neg}PD-1^{hi}Bcl6^{+}Eomes^{+}).

the *Rosa26* locus[250] and express Cre in all B cells beginning at the pro-B cell developmental stage[251]. As a result, these mice exhibit inducible depletion of B cells upon DT administration (Figure 9a). Systemic B cell ablation led to the reduction of PD-1^{+} Bcl6^{+} Eomes^{+} CD4^{+} Tconv cells, but not of other antigen-experienced CD4^{+} Tconv cell subsets, including memory-phenotype CD44^{hi} CD62L^{lo} and anergic-phenotype CD44^{hi} CD73^{hi} FR4^{hi} cells (Figure 9b-c). The PD-1^{+} CXCR5^{+} CD4^{+} Tconv cell population, which overlaps with our polyclonal Group 3-like cells of interest, also experienced a slight decrease in frequency following B cell depletion, albeit below the threshold of statistical significance. Similar results were observed when anti-CD20 antibody administration was used to deplete B cells (data not shown). Collectively, these data indicate that endogenous polyclonal Group 3-like cells are dependent on the continued presence of B cells for adoption and/or maintenance of the PD-1^{+} Bcl6^{+} Eomes^{+} phenotype, suggesting a critical dependence on B cells or B cell-dependent factors.

Conclusion

Through in-depth clonal analyses of CD4^{+} Tconv cells recovered from non-lymphoid organs following systemic Treg cell ablation, our work defines a previously unidentified class of self-reactive CD4^{+} Tconv cells that, despite their overt responses to self-antigens, subvert central T cell tolerance and egress into the periphery. There, under steady-state conditions, CD4^{+} Tconv cells expressing Group 3 TCRs adopt signature features of the Tfh cell program, including elevated expression of Bcl6 and PD-1, as well as proximity to B cell follicles within the spleens of TCRrg mice. Expression of CD62L and Eomes distinguishes Tfh-like cells from other antigen-experienced CD4^{+} T cell subsets, including the effector/memory and anergic phenotype CD4^{+} Tconv cell populations previously described in the literature. However, in the setting of systemic

Treg cell ablation, these self-reactive $CD4^+$ Tconv cells transition away from a Tfh-like phenotype, produce the Th1 lineage-defining cytokine IFN-γ, and infiltrate multiple non-lymphoid tissues. Altogether, we show that potentially pathogenic self-reactive $CD4^+$ Tconv cell clones populate the peripheral repertoire, regularly sense self-antigens, are controlled by Treg cells, and promote autoimmunity if released from Treg cell-mediated suppression.

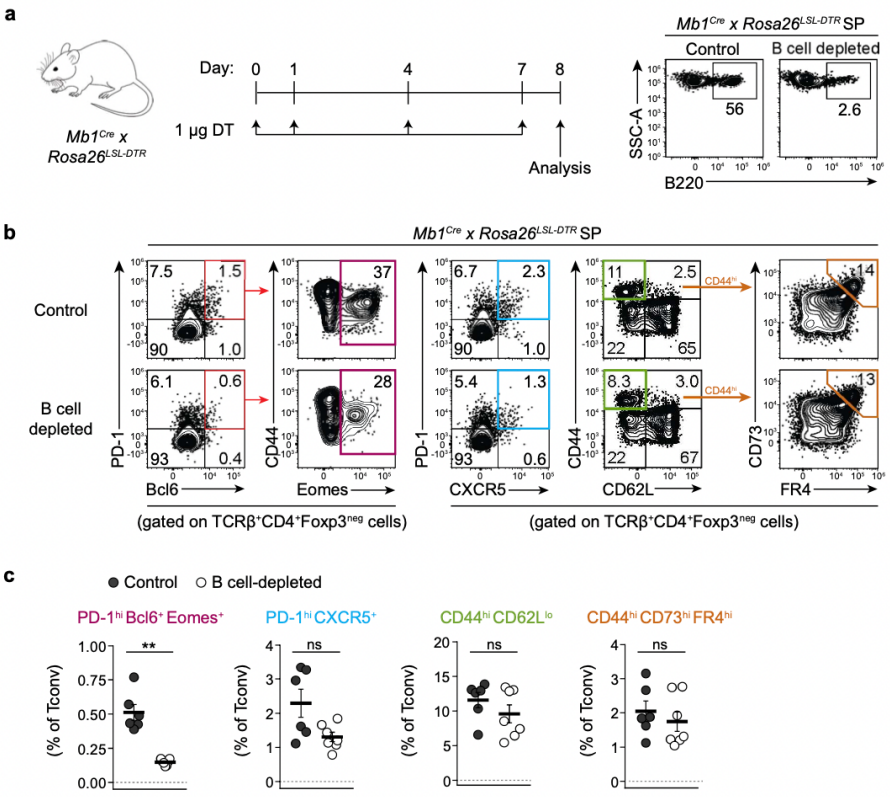

Figure 9 | The frequency of polyclonal Group 3-like cells is diminished following inducible depletion of B cells

Flow cytometric quantification of polyclonal Group 3-like and other antigen-experienced CD4$^+$ Tconv cells following inducible ablation of B cells.

a, Left, experimental schematic. *Mb1^{Cre} x Rosa26$^{LSL\text{-}DTR}$* mice were subjected to sustained B cell ablation via intraperitoneal administration of diphtheria toxin (DT) or were treated with PBS. On experiment day 8, cells from the secondary lymphoid organs of B-cell-depleted mice and control littermates were isolated and analyzed via spectral flow cytometry. Right, representative flow cytometric analysis of B220 expression by splenic lymphocytes in B-cell-depleted mice and control littermates.

b, Representative flow cytometric analysis of splenic CD4$^+$ Tconv cells exhibiting a PD-1^{hi} Bcl6$^+$ Eomes$^+$ Group 3-like phenotype. For comparison, gating on additional antigen-experienced Tconv cell populations is also shown, including PD-1$^+$ CXCR5$^+$, T effector/memory (CD44^{hi} CD62L^{lo}), and "anergic phenotype" (CD44^{hi} CD73^{hi} FR4^{hi}) cells. Plots for PBS-treated controls (top row) and B cell-depleted mice (bottom row) are depicted.

c, Summary plot of data from **b** showing the frequency of Group 3-like (PD-1^{hi} Bcl6$^+$ Eomes$^+$), PD-1$^+$ CXCR5$^+$, T effector/memory (CD44^{hi} CD62L^{lo}), and "anergic phenotype" (CD44^{hi} CD73^{hi} FR4^{hi}) cells in B-cell-depleted mice (white symbols) and control littermates (black symbols). Data are pooled from two independent experiments, $n \geq 7$ mice per group. Error bars represent means ± SEM. p values were calculated by Mann-Whitney test. *ns*, not significant; *$p < 0.05$; **$p < 0.01$; ***$p < 0.001$.

CHAPTER IV: RESULTS PART II –

IMPACT OF T CELL RECEPTOR – PEPTIDE/MHC CLASS II SENSITIVITY ON THE DEVELOPMENT & PATHOGENICITY OF PROSTATE-REACTIVE CD4$^+$ T CELLS

Overview

Through somatic recombination of T cell receptor (TCR) gene segments, the immune system gives rise to pathogen-reactive T cells capable of defending the host against infection, as well as self-reactive T cells capable of mediating pathogenic responses against host tissues[97,252]. Self-reactive Foxp3^{neg} CD4$^+$ conventional T (Tconv) cells have been implicated in multiple autoimmune disorders, highlighting the importance of understanding the thymic development and peripheral activity of these cells[230,231]. With regards to development of self-reactive CD4$^+$ Tconv cells, a common paradigm of thymopoiesis suggests that the affinity with which a thymocyte's TCR binds self-pMHC-II (spMHC-II) dictates whether that cell undergoes positive selection into the CD4$^+$ Tconv cell compartment, differentiation into the Foxp3$^+$ CD4$^+$ regulatory T (Treg) cell lineage, or removal from the repertoire by clonal deletion[49,66,253,254]. Per the affinity model of thymic development, thymocytes bearing TCRs exhibiting low or high affinities to spMHC-II ligands undergo egress as CD4$^+$ Tconv cells or negative selection, respectively. Moreover, intermediate TCR:pMHC-II affinities – at the threshold between positive and negative selection – are thought to promote optimal thymic Treg (tTreg) development, allowing Treg cell clones to differentiate while also evading clonal deletion. Thus, in prevailing models of thymic development, TCR:pMHC-II affinity is regarded as the primary determinant of thymocyte fate and the key factor governing the development of self-reactive CD4$^+$ T cell clones.

However, these proposed principles largely stem from the study of foreign-reactive CD4$^+$ T cell clones reactive to engineered model antigens transgenically expressed in murine thymi. In

these engineered systems, recognition of agonist peptide in the thymus induces coincident clonal deletion and tTreg cell differentiation among model antigen-specific thymocytes, with the efficiency of both processes increasing as TCR:pMHC-II affinity increases[135,136]. In contrast, recent developmental studies of naturally occurring Treg cell clones reactive to *bona fide* self-antigens have shown that these clones undergo tTreg cell differentiation with no evidence of coincident clonal deletion[137,139–141]. As the expression patterns, ligand densities, TCR:pMHC-II affinities, and immune recognition of engineered antigens may not reflect those of endogenous self-antigens, it remains unclear whether the predictions of the affinity model fully apply to Treg and $CD4^+$ Tconv cell clones reactive to natural self-ligands. Moreover, factors beyond TCR:pMHC-II affinity – including the number, quality, and duration of TCR:pMHC-II bonds (encapsulated by T cell avidity); the contributions of cell adhesion molecules (affecting T cell senstivity); and the nature of the antigen-presenting cells (APCs) displaying self-antigens – have also been shown to modulate the development of self-reactive Treg and $CD4^+$ Tconv cells[70,137,255]. These findings suggest that a broad examination of T cell sensitivity to self-antigens is required to understand how TCR interactions with self-antigens govern the fate of self-reactive MHC-II-restricted thymocytes.

While TCR:spMHC-II interactions are also expected to shape the peripheral function of self-reactive $CD4^+$ Tconv cells, the relationship between $CD4^+$ Tconv cell sensitivity to self-antigens and such cells' pathogenic potential remains unclear. Under the affinity model of thymic development, only thymocytes exhibiting lower TCR affinities for spMHC-II ligands are expected to develop as $CD4^+$ Tconv cells. In contrast, the majority of Treg cells are thought to emerge from the thymus following agonist interactions with self-antigens, meaning that the Treg cell repertoire is enriched for clones exhibiting greater sensitivities to spMHC-II relative to the repertoire of $CD4^+$

Tconv cells[49]. Treg cells may leverage this improved sensitivity to spMHC-II to prevent activation of $CD4^+$ Tconv cells of matched antigen specificity, disrupt ongoing interactions between self-reactive $CD4^+$ Tconv cells and APCs[110], and mitigate autoimmune responses[72].

However, recent studies have questioned the extent to which immune homeostasis relies on Treg cells successfully outcompeting self-reactive $CD4^+$ Tconv cells for the same spMHC-II complexes. In one, Sprouse *et al.* generated mixed TCR "retrogenic" bone marrow chimeras in T cell-deficient non-obese diabetic (NOD) mice to assess the extent of disease control exerted by insulin-reactive Treg cells bearing high- or low-affinity TCRs. The authors demonstrated that Treg cells expressing a lower-affinity TCR could still delay diabetes onset in mice whose $CD4^+$ Tconv cells expressed high-affinity TCRs[256]. In another, immunization with the self-antigen myelin oligodendrocyte glycoprotein (MOG) led to induction of experimental autoimmune encephalomyelitis (EAE), even in mice prophylactically receiving Treg cells engineered to express a high-avidity MOG-specific TCR[72]. Thus, while Treg cells may partially limit self-reactive $CD4^+$ Tconv cells through differential sensitivity to spMHC-II, self-reactive $CD4^+$ Tconv cells still exhibit sensitivities to self-antigens that enable them to promote disease. Work by the Vignali group reinforces this point by showing that insulin-reactive $CD4^+$ Tconv cells bearing higher- or lower-affinity TCRs induced similar extents of insulitis when transferred into lymphopenic NOD.*scid* mice[151]. The findings of Bettini *et al.* demonstrate that a broad range of sensitivity to self-antigens can confer pathogenic potential, and that other factors, such as spMHC-II availability, likely contribute to self-reactive $CD4^+$ Tconv cell responses.

The present study seeks to understand the mechanisms by which the immune system regulates self-reactive $CD4^+$ Tconv cells that exhibit varying sensitivities to self, using a panel of $CD4^+$ T cell clones reactive to the same endogenous tissue-specific antigen (TSA). Here, we pair

deep TCRα repertoire profiling with in-depth analyses of individual self-reactive CD4$^+$ Tconv cell clones in tumor-free and prostate tumor-bearing mice. In doing so, we found that self-reactive CD4$^+$ Tconv cell clones with lower sensitivities to self-antigens could still infiltrate non-lymphoid tissues in some – but not all – contexts, indicative of susceptibility to cell-extrinsic modes of peripheral T cell tolerance. In contrast, clones with higher sensitivities to self-antigens were more vulnerable to T cell-intrinsic mechanisms of tolerance, particularly when spMHC-II ligands were more readily available. By defining the characteristics of the self-reactive CD4$^+$ Tconv cell clones that pose the greatest danger of autoimmunity, this work elucidates the ways in which the immune system leverages TCR:spMHC-II interactions to impose immune tolerance.

spMHC-II tetramers identify endogenous prostate-reactive CD4$^+$ Tconv cells in *Aire*$^{-/-}$ mice

Recently, the Savage and Adams groups described two naturally occurring murine Treg cell clones reactive to distinct I-A^b-restricted peptides from the same protein, Tcaf3[140]. Tcaf3 is an endogenous protein whose expression in the periphery is limited to the anterior and dorsolateral lobes of the mouse prostate, and whose expression in the thymus is mediated by Aire in medullary thymic epithelial cells (mTECs)[65,68,140]. Of the Tcaf3-specific Treg cell clones identified, one – termed MJ23 – recognizes a peptide corresponding to residues 646-658 of Tcaf3 (hereafter referred to as C4 peptide). TCR transgenic (TCRtg) thymocytes expressing the MJ23 TCR upregulate Foxp3 when transferred into wild-type (WT) C57BL/6J (B6) mice – yet fail to do so when transferred into mice with targeted deletion of the C4 peptide (*Tcaf3(C4)*$^{-/-}$). In C4-deficient mice, MJ23tg thymocytes instead develop as CD4$^+$ Tconv cells, indicating that the C4 peptide is required for tTreg differentiation but not positive selection of MJ23tg CD4$^+$ T cells. Considering these

findings, it became of great interest to characterize the endogenous $CD4^+$ T cell repertoire reactive to the Treg-inducing self-ligand, C4/I-A^b.

To do so, we utilized fluorescently labeled C4/I-A^b tetramers to identify C4-reactive $CD4^+$ T cells in the prostates and prostate-draining lymph nodes (pLNs) of *Aire*$^{-/-}$ TCRβtg mice. *Aire*$^{-/-}$ mice develop a robust T cell infiltrate within the prostate and other non-lymphoid organs. Use of a transgene encoding the TCRβ chain of MJ23 enabled complete profiling of the TCR repertoire by deep TCRα sequencing. Of the $CD4^+$ T cells derived from the prostates and pLNs of these mice, a fraction bound both allophycocyanin- and PE-conjugated tetramers, indicative of reactivity to C4/I-A^b (Figure 10a). C4/I-A^b tetramer-positive cells were purified from five mice via fluorescence-activated cell sorting (FACS) and subjected to TCRα sequencing using the iRepertoire platform. This yielded 1,436 distinct TCRα clonotypes, as determined by unique sequences in the complementarity determining region 3 (CDR3α). Of these 1,436 clonotypes, 17 were observed across all five mice examined. Of note, this list of recurrent clones included the MJ23 TCRα, suggesting that the TCRs within this group were enriched for sensitivity to C4/I-A^b.

To validate this, we selected the three most abundant recurrent C4/I-A^b tetramer-binding clonotypes for further study (Table 2). Figure 10b displays the frequencies of selected clonotypes within the population in which these clones were identified. Unless otherwise indicated, TCR names are abbreviated using the amino acid sequence corresponding to positions 3 to 5 of the CDR3α region. For example, the TCR with CDR3α sequence AMRETWSNYNVLY is referred to as "RET." For each of the TCRs listed in Figure 10b, we generated TCR "retrogenic" (TCRrg) mice; these mice develop $CD4^+$ T cells bearing an individual TCR of interest, which can be used to perform both *in vivo* and *ex vivo* studies. TCRrg $CD4^+$ T cells for each TCR were

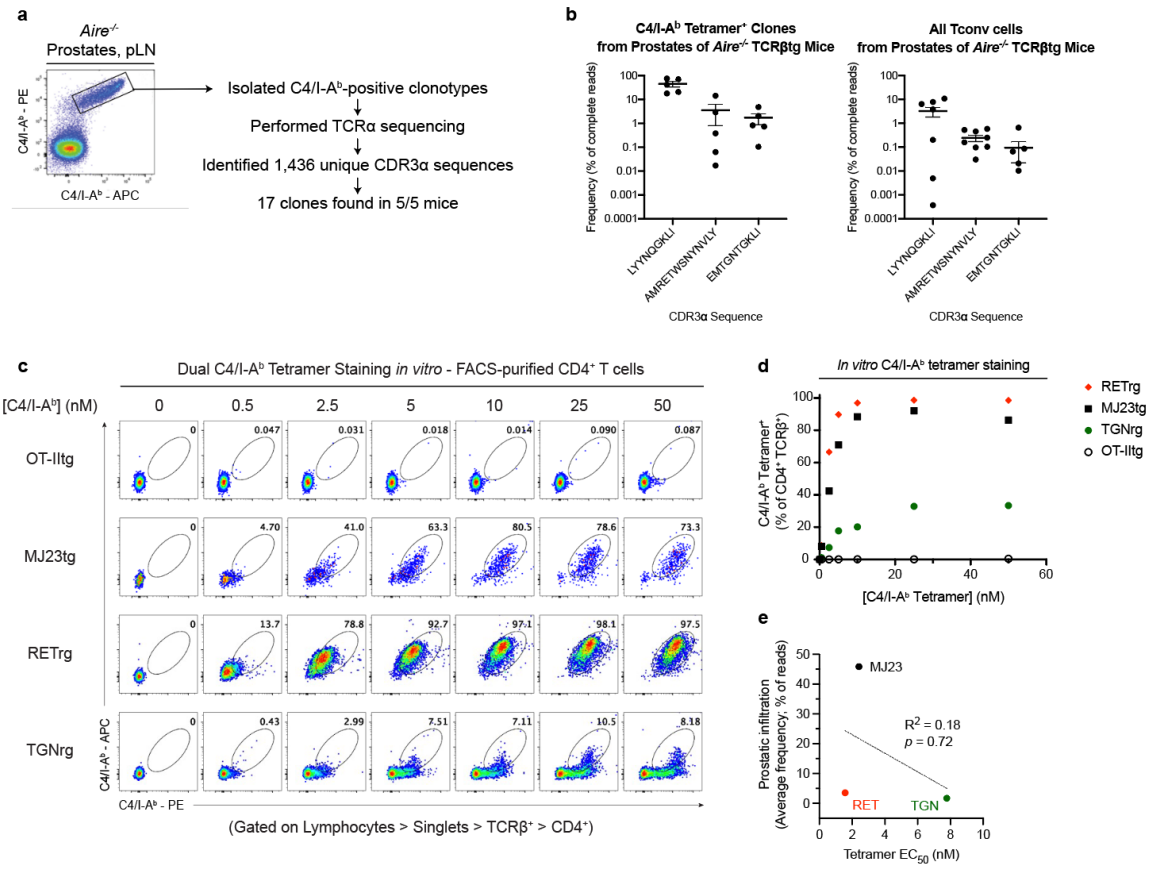

Figure 10 | pMHC-II tetramers identify prostate-infiltrating CD4$^+$ T cell clones with differing avidities for the prostate-derived C4/I-A^b self-ligand.

a. Isolation of putative C4-reactive clones. CD4$^+$ T cells were isolated from the prostates and prostate-draining lymph nodes of >8-week-old *Aire*$^{-/-}$ TCRβtg male mice and stained with dual C4/I-A^b tetramer reagents. Tetramer-positive cells were subjected to TCRα sequencing (iRepertoire).

b. Plots showing the average frequency of selected TCRs among all C4/I-A^b tetramer-positive CD4$^+$ T cells (left) and among all Foxp3^{neg} CD4$^+$ T cells (right) recovered from the prostates and prostate-draining lymph nodes of >8-week-old *Aire*$^{-/-}$ TCRβtg male mice.

c. Flow cytometric analysis of TCRrg (or TCRtg) CD4$^+$ T cells stained *ex vivo* with C4/I-A^b tetramers. For the indicated TCRs, TCR "retrogenic" (TCRrg) mice were generated as previously described[140]. TCRrg CD4$^+$ T cells were purified via FACS from pooled spleen and lymph nodes, plated at 10^4 cells/well, and stained with the indicated concentrations of C4/I-A^b tetramer (per fluorophore). Where indicated, cells from TCR transgenic (TCRtg) mice were used as a substitute for TCRrg cells.

d. Summary plot for data shown in **c**.

e. Plot showing the concentration of C4/I-A^b tetramer yielding half-maximal staining per clone (EC_{50}) versus the frequency of each clone among prostate-associated C4/I-A^b tetramer-positive CD4$^+$ T cells from *Aire*$^{-/-}$ TCRβtg mice. Data in **c** and **d** are representative of two independent experiments.

CDR3	TRAV	TRAJ	Average Freq.	Median Freq.
LYYNQGKLI (MJ23)	14-2	23	0.4582994459	0.4237347543
AMRETWSNYNVLY (RET)	16 or 16D/DV11	21	0.0355272356	0.0038421823
EMTGNTGKLI (TGN)	7-6	37	0.0172251881	0.0082604580
PYYNQGKLI	14-2 or 14D-3/DV8	23	0.0012641459	0.0008337953
LYCNQGKLI	14-2	23	0.0004297051	0.0004619943
LYHNQGKLI	14-2	23	0.0003709236	0.0004014570
LCYNQGKLI	14-2	23	0.0002709708	0.0003346892
VYYNQGKLI	14-2	23	0.0000651806	0.0000200728
EVTGNTGKLI	7-6	37	0.0000620365	0.0000329640
LNYNQGKLI	14-2	23	0.0000503252	0.0000633067
ETTGNTGKLI	7-6	37	0.0000468208	0.0000242382
LYFNQGKLI	14-2	23	0.0000310542	0.0000245121
LFYNQGKLI	14-2	23	0.0000190416	0.0000185288
LYNNQGKLI	14-2	23	0.0000178689	0.0000143732
LYSNQGKLI	14-2	23	0.0000121854	0.0000102665
LYDNQGKLI	14-2	23	0.0000064300	0.0000061763
LSYNQGKLI	14-2	23	0.0000059250	0.0000030881

Table 2 | List of C4/I-A^{b} tetramer-binding CD4^{+} Tconv clones recurrently detected within the prostates and draining lymph nodes of *Aire*$^{-/-}$ TCRβtg mice.

17 TCRα sequences were found in all five *Aire*$^{-/-}$ TCRβtg mouse samples. Full TCRα sequence information is listed, including TRAV and TRAJ usage, for each clone. Additionally, the average and median frequency of each TCRα sequence across all five samples are provided. Of these, the three most abundant were selected for TCR retrogenic studies. Selected TCRα chains are denoted using a 3-letter code representing residues 3-5 of the predicted CDR3α chain.

FACS-purified, plated at a defined number per well, and subjected to dual C4/I-A^b tetramer staining across a range of tetramer concentrations. The majority of RET TCRrg $CD4^+$ T cells were C4/I-A^b tetramer-positive, even at limiting tetramer doses, reflecting the high avidity of this clone for C4/I-A^b (Figure 10c-d). A similar staining pattern was observed for TCRrg $CD4^+$ T cells bearing the MJ23 TCR. In contrast, for TGN TCRrg $CD4^+$ T cells, C4/I-A^b tetramer binding was not saturated across the range of tetramer concentrations tested, indicating that this clone exhibits lower avidities for C4/I-A^b (Figure 10c-d). On their own, these data do not support the existence of a linear relationship between T cell avidity for spMHC-II and organ infiltration, as all three clones were highly prevalent among $CD4^+$ T cells recovered from the prostates and pLNs of *Aire*$^{-/-}$ TCRβtg mice, despite their varying avidities for C4/I-A^b (Figure 10e).

$CD4^+$ Tconv cell clones that recurrently infiltrate the prostates of *Aire*$^{-/-}$ mice display differing sensitivities for the C4/I-A^b self-ligand

Next, we sought to confirm that our C4/I-A^b tetramer-binding clones truly exhibited reactivity to C4/I-A^b. First, we performed *ex vivo* phenotyping of TCRrg $CD4^+$ T cells isolated from distinct SLOs of TCRrg male mice. In TCRrg mice generated to express the MJ23, RET, or TGN TCRs, TCRrg $CD4^+$ T cells were enriched in the pLNs relative to other SLOs, suggestive of preferential accumulation at the site of antigen expression (Figure 11a). Next, for these three clones, we generated primary TCRrg hosts using female mice, in which C4-reactive $CD4^+$ T cells are expected to remain phenotypically naïve due to the lack of Tcaf3 expression in the periphery. We isolated TCRrg $CD4^+$ Tconv cells from the pooled SLOs of these mice by sorting on $CD44^{lo}$ $Foxp3^{DTR\text{-}EGFP\text{-}neg}$ cells, and then transferred these cells into WT male mice. 24 hours later, TCRrg $CD4^+$ Tconv cells upregulated CD69 and Egr2 in the pLNs, but not within distal sites (Figure 11b).

Upregulation of these markers was abrogated upon transfer of TCRrg $CD4^+$ Tconv cells into *Tcaf3(C4)*$^{-/-}$ male recipients (Figure 11b), indicating that these self-reactive $CD4^+$ T cells sense the C4/I-A^b antigen and experience TCR signaling as a result. Transferred cells also remained $Foxp3^{neg}$ regardless of the TCR expressed, demonstrating minimal conversion of MJ23, RET, or TGN TCRrg $CD4^+$ T cells into peripherally induced Treg (pTreg) cells (Figure 11c). Based on these results, these clones' responses to C4/I-A^b were not drastically restrained by antigen ignorance or pTreg cell differentiation. When FACS-purified TCRrg $CD4^+$ T cells were labeled with the proliferation dye CellTrace Violet (CTV), co-cultured *in vitro* with $CD11c^+$ splenocytes (as a source of APCs), and supplemented with interleukin-2 (IL-2) and exogenous C4 peptide across a range of C4 concentrations, all three clones proliferated upon addition of C4 peptide, demonstrating that these clones' ability to respond to C4/I-A^b remained intact despite antigen sensing in the periphery (Figure 11d). Interestingly, compared to cells expressing the MJ23 or RET TCRs, TGN TCRrg $CD4^+$ T cells required approximately tenfold greater C4 peptide doses in order to achieve half-maximal proliferation, in line with this clone's lower sensitivity to C4/I-A^b. As a final measure to confirm reactivity to C4/I-A^b, we transferred TCRrg $CD4^+$ Tconv cells into secondary WT recipients and infected the latter with 10^7 colony-forming units (CFU) of *Listeria monocytogenes* (*Lm*) engineered to express the C4 peptide (*Lm[C4]*; see Materials & Methods and Figure 11e). MJ23, RET, and TGN TCRrg $CD4^+$ Tconv cells expanded robustly in *Lm[C4]*-infected animals, but not in mice infected with the parental strain of *Lm*, which lacks C4 expression (Figure 11f). Collectively, these data show that $CD4^+$ Tconv cells beaing the MJ23, RET, and TGN TCRs react to C4/I-A^b, albeit with differing sensitivities.

Clones with higher sensitivities to C4/I-A^b infiltrate the prostates of tumor-free mice

The release of C4-reactive $CD4^+$ T cell clones from regulation in settings of inflammation raised an important question: are clones with differing sensitivities to C4/I-A^b similarly capable of promoting prostate-directed autoimmunity? To address this question, we adoptively transferred C4-reactive TCRrg $CD4^+$ Tconv cells into *Tcrb*$^{-/-}$ recipients. T cells transferred into lymphopenic environments undergo homeostatic proliferation (HP) and activation as a result of excess availability of cytokines and spMHC-II ligands[257]. Following transfer into *Tcrb*$^{-/-}$ recipients, TCRrg $CD4^+$ Tconv cells bearing the higher-sensitivity MJ23 and lower-sensitivity TGN TCRs infiltrated the prostate to similar extents (Figure 12a). When C4-reactive TCRrg $CD4^+$ Tconv cells were co-transferred with filler splenocytes to curb the effects of HP, prostatic infiltration of MJ23 and RET TCRrg $CD4^+$ Tconv cells was partially abrogated (Figure 12b). Notably, few TGN TCRrg $CD4^+$ Tconv cells were recovered from the prostates of *Tcrb*$^{-/-}$ mice following co-transfer with filler splenocytes. Altogether, these findings suggest that, compared to their higher-sensitivity counterparts, $CD4^+$ Tconv cell clones exhibiting lower sensitivities to TSAs may rely more heavily on sensing inflammatory cues or cytokine signals in order to subvert tolerance to host tissues.

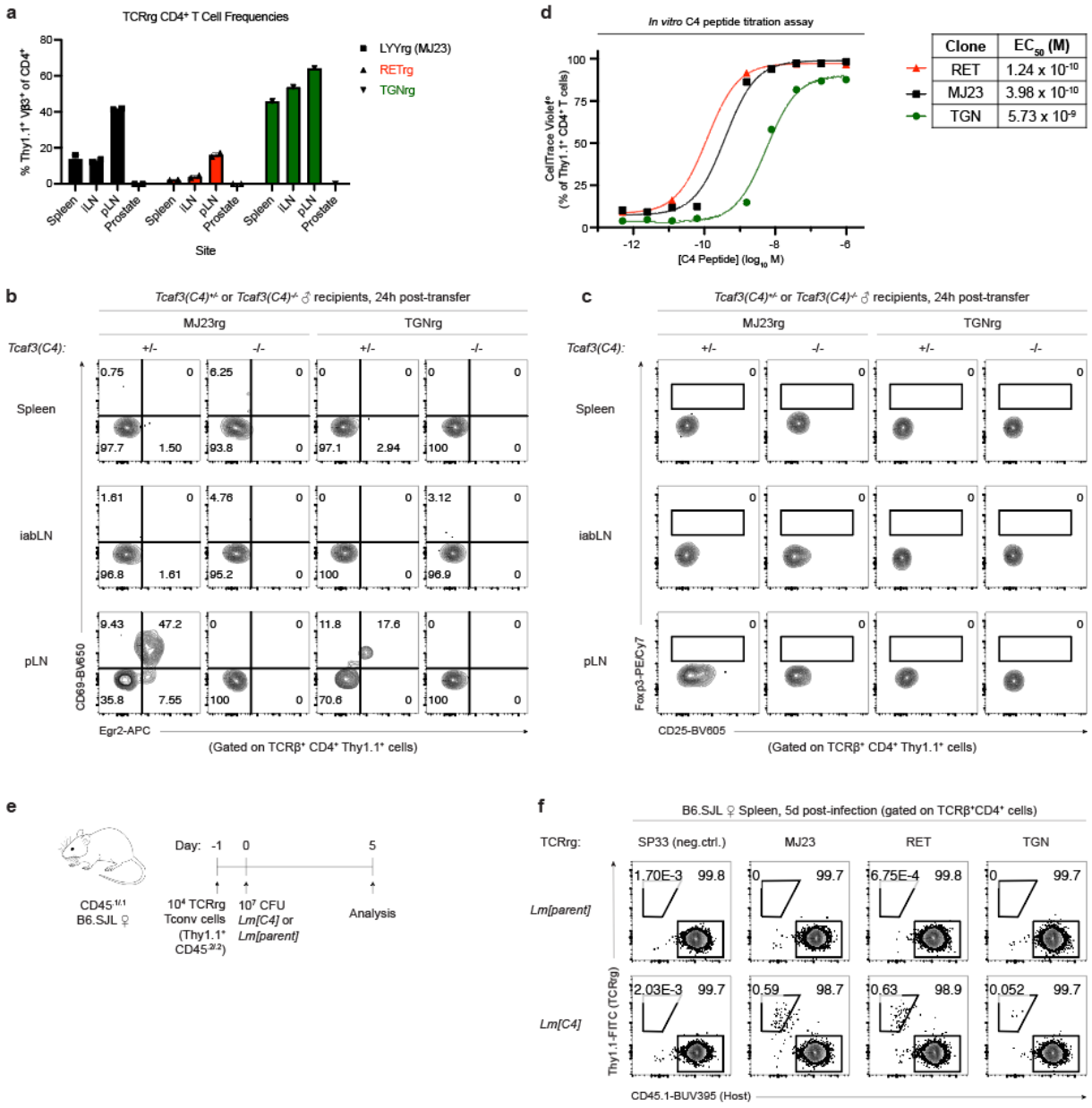

Figure 11 | The MJ23, RET, and TGN TCRs confer reactivity to C4/I-A^b.

a. Distribution of MJ23, RET, and TGN TCRrg CD4$^+$ T cells within TCRrg male mice. Primary TCRrg mice were analyzed >8 weeks post-generation. Frequencies of TCRrg CD4$^+$ T cells in the prostate and indicated SLOs are shown.

Primary TCRrg hosts were generated using female mice to yield monoclonal populations of naïve C4-reactive CD4$^+$ T cells. TCRrg CD4$^+$ Tconv cells from the SLOs of female TCRrg mice were purified and transferred into C4-sufficient *Tcaf3(C4)*$^{+/-}$ or C4-deficient *Tcaf3(C4)*$^{-/-}$ male recipients. Recipients were euthanized 24 h post-transfer and donor cell localization and phenotype were assessed (**b-c**). Data are representative of two independent experiments.

Figure 11, continued.
b. Flow cytometric analysis of CD69 and Egr2 expression among transferred Thy1.1$^+$ TCRrg CD4$^+$ Tconv cells bearing the MJ23 (MJ23rg) or TGN (TGNrg) TCR.
c. Flow cytometric analysis of Foxp3 and CD25 expression among transferred MJ23rg and TGNrg CD4$^+$ Tconv cells.
For the indicated TCRs, TCRrg CD4$^+$ T cells were isolated, labeled with CellTrace Violet, and co-cultured with CD11c$^+$ splenocytes at a 1:5 ratio. Cultures were supplemented with varying concentrations of C4 peptide, and proliferation was assessed after 72 hours.
d. Left, summary plot of CTV dilution versus concentration of C4 peptide added to co-cultures. Right, list of C4 peptide concentration required for each clone to achieve half-maximal proliferation (EC_{50} values). Data are representative of three independent experiments.
Naïve TCRrg CD4$^+$ Tconv cells isolated from female TCRrg hosts were transferred into congenically disparate female recipients. One day post-transfer, recipients were infected with L. monocytogenes expressing or lacking C4 peptide (*Lm[C4]* or *Lm[parent],* respectively) (**e-f**).
e. Experimental schematic for *Lm* infection system to assess reactivity to C4/I-A^b.
f. Flow cytometric plots showing the frequency of donor-derived Thy1.1$^+$ TCRrg cells and recipient CD45.1$^+$ cells among splenic CD4$^+$ T cells isolated from recipient mice 5 d post-infection. As a control, TCRrg CD4$^+$ Tconv cells expressing the SP33 TCR, reactive to a different peptide derived from Tcaf3, were transferred[140,141]. Data are representative of two independent experiments.

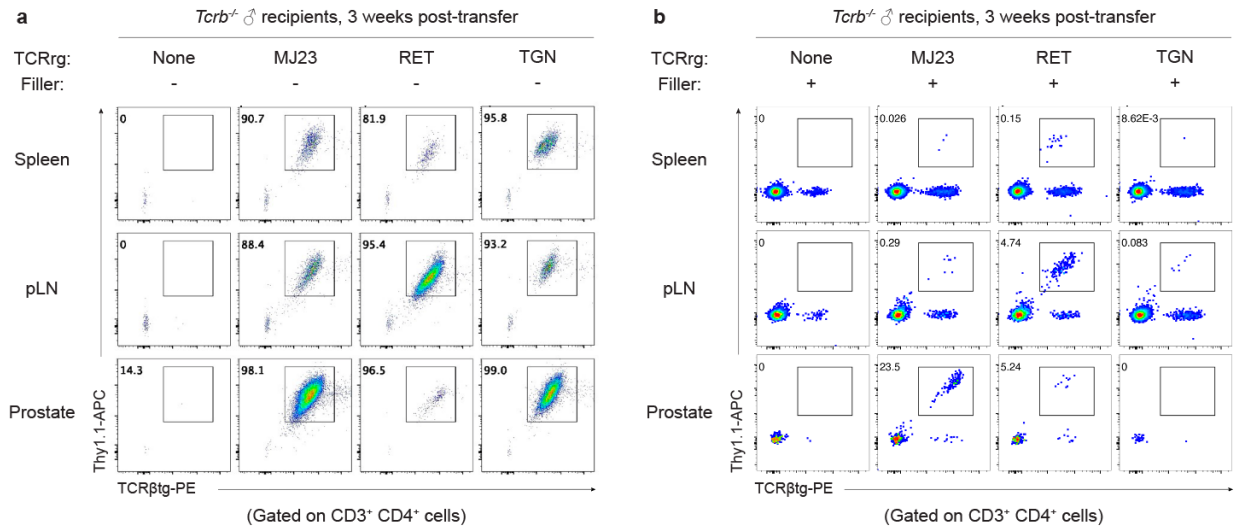

Figure 12 | Clones with higher sensitivities to C4/I-A^b infiltrate the prostates of tumor-free mice

Naïve TCRrg CD4$^+$ Tconv cells were isolated from pooled SLOs of female TCRrg mice and transferred into *Tcrb*$^{-/-}$ mice with (**a**) or without (**b**) co-transfer of "filler" splenocytes. Each recipient received 10^5 FACS-sorted TCRrg CD4$^+$ Tconv cells (CD45$^{.2/.2}$) ± 10^7 CD45$^{.1/.1}$ splenocytes. Donor cell localization and phenotype were assessed 3 weeks post-transfer.

Clones with lower sensitivities to C4/I-A^b are more readily observed among prostate tumor-infiltrating CD4$^+$ Tconv cells

In this vein, we next probed whether TGN TCRrg CD4$^+$ Tconv cells could more readily infiltrate established prostate tumors, as cancers are frequently associated with increased inflammatory triggers and availability of self-antigens. We leveraged the Transgenic Adenocarcinoma of Mouse Prostate (TRAMP) model, in which oncogenic SV40 T antigens are expressed under the control of the rat probasin promoter[258]. This leads to oncoprotein expression in prostatic epithelial cells of the dorsolateral and ventral lobes, subsequent inactivation of the tumor suppressors Rb and p53, and invasive neoplasia by 20 weeks of age. Importantly, the involvement of the dorsolateral lobe in tumorigenesis makes C4/I-A^b a tumor-associated antigen (TAA) in TRAMP mice. To enable engraftment of adoptively transferred T cells into tumor-bearing mice, we optimized a lymphodepletion regimen based on the chemotherapeutic agents fludarabine (Flu) and cyclophosphamide (Cy). In the clinic, these reagents are administered to patients undergoing preconditioning ahead of chimeric antigen receptor (CAR) T cell therapy. Flu/Cy treatment of TRAMP$^{+/+}$ mice led to transient ablation of B and T cells – including Treg cells – in the blood and SLOs, with lymphocyte numbers starting to recover at 3 days post-treatment. TRAMP$^{+/+}$ mice treated with Flu/Cy or PBS displayed similar tumor masses 8 weeks post-treatment, indicating that Flu/Cy itself did not alter tumor mass (Figure 13a). Engraftment of transferred donor CD4$^+$ T cells was superior in TRAMP$^{+/+}$ mice preconditioned with Flu/Cy versus a sublethal dose of total body irradiation, an additional regimen used to promote the success of bone marrow transplantation or adoptive cell therapies (Figure 13b). Thus, to mirror currently approved clinical therapies, Flu/Cy treatment was used for all adoptive T cell transfers into tumor-bearing TRAMP mice unless otherwise indicated.

This preconditioning and adoptive transfer system allowed us to address a longstanding debate in the field of cancer immunotherapy surrounding the antitumor efficacy of low- versus high-avidity tumor-reactive $CD4^+$ Tconv cells. Monoclonal C4-reactive TCRrg $CD4^+$ Tconv cells were administered to Flu/Cy-treated $TRAMP^{+/+}$ mice, and the frequency, localization, and phenotype of donor cells were assessed 2-3 weeks post-transfer (Figure 13c). Interestingly, TGN TCRrg $CD4^+$ Tconv cells robustly infiltrated prostate tumors following transfer into lymphodepleted $TRAMP^{+/+}$ mice (Figure 13d). Moreover, TGN cells experienced greater extents of proliferation in the tumor-draining pLN compared to the higher-sensitivity clone RET, as shown by greater dilution of CTV (Figure 13e). These findings suggest that $CD4^+$ Tconv cells with lower sensitivities to self-antigens are kept in check when needing to compete for limited antigen, co-stimulatory and/or cytokine-derived signals. Alternatively, clones bearing high sensitivities to self-antigens may be more prone to mechanisms of peripheral T cell tolerance.

In Flu/Cy-treated mice, adoptively transferred C4-reactive TCRrg $CD4^+$ Tconv cells briefly predominate over endogenous Treg cells, as the latter are temporarily removed following chemotherapy. To what extent does the endogenous Treg cell population regulate $CD4^+$ Tconv cell clones with differing sensitivities to C4/I-A^b? To test this, we generated $TRAMP^{+/-}$ *Foxp3*$^{DTR\text{-}EGFP/y}$ mice, which express the human diphtheria toxin receptor (DTR) in all Treg cells. In these mice, a short course of DT administration leads to transient yet systemic Treg cell ablation, followed by repopulation of the Treg cell compartment by 3 weeks post-treatment. As a result, these mice experience lymphoproliferation due to temporary release from Treg-mediated suppression, but do not succumb to multiorgan autoimmunity. Non-Flu/Cy-treated $TRAMP^{+/-}$ *Foxp3*$^{DTR\text{-}EGFP/y}$ mice received C4-reactive TCRrg $CD4^+$ Tconv cells followed by DT administration for 5 days (Figure 13f). Three weeks post-transfer, intratumoral TGN TCRrg $CD4^+$ Tconv cells were recovered at

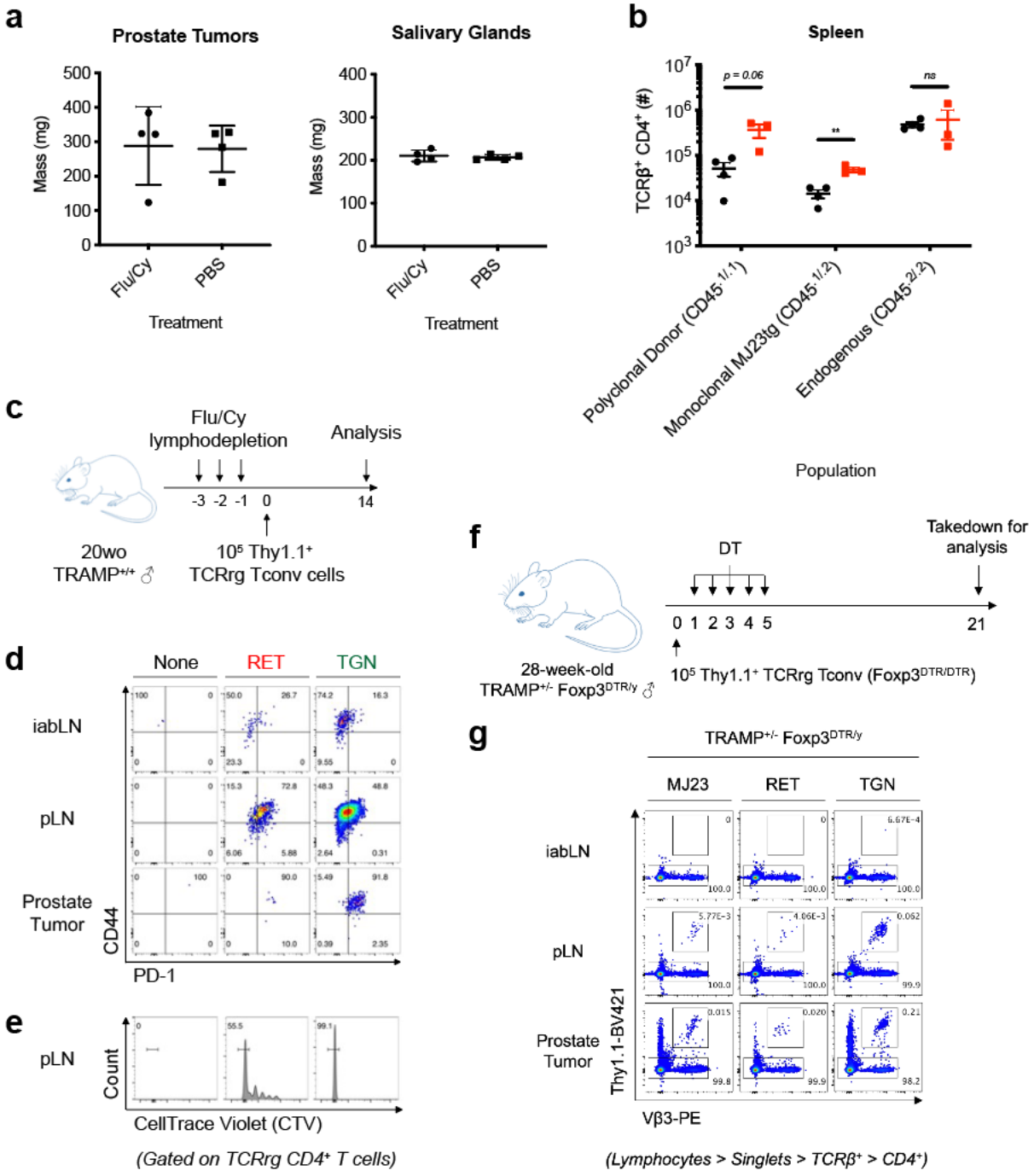

Figure 13 | TGN TCRrg CD4$^+$ Tconv cells exhibiting lower sensitivity to C4/I-A^b outperform higher-sensitivity cells for access to oncogene-drive prostate tumors.

a-b, Development of a nonmyeloablative lymphodepletion strategy to promote engraftment of adoptively transferred T cells into TRAMP mice.

Figure 13, continued.
a, ≥20-week-old TRAMP$^{+/+}$ male mice were injected intraperitoneally (i.p.) with 10 mg/kg fludarabine (Flu) and 200 mg/kg cyclophosphamide (Cy) as described in Materials & Methods. Lymphodepleted animals were euthanized 8 weeks following the completion of Flu/Cy treatment, and masses of prostate tumors (left) and salivary glands, as a control (right), were measured.
b, ≥20-week-old TRAMP$^{+/+}$ male mice were injected i.p. with Flu/Cy as in **a** or were subjected to 500 rads of X-ray total body irradiation. One day following treatment, lymphodepleted mice received 2 x 10^5 CD4$^+$ T cells from *Aire*$^{-/-}$ male donors and 3 x 10^5 CD4$^+$ T cells from female MJ23tg donors. Donor cell engraftment was assessed two weeks following adoptive transfer.
c-e, Assessment of prostate tumor infiltration by clones bearing distinct sensitivities to the tumor-associated antigen, C4/I-A^b. Data are representative of two independent experiments, n ≥ 4 per TCR.
c, Experimental setup for adoptive transfer of CTV-labeled TCRrg CD4$^+$ Tconv cells into Flu/Cy-treated TRAMP$^{+/+}$ mice. Donor cell localization and phenotype, as well as prostate tumor masses, were assessed 2 weeks post-transfer.
d, Flow cytometric plots showing the presence and phenotype of RET and TGN TCRrg CD4$^+$ Tconv cells in the pooled skin-draining lymph nodes (iabLN), the prostate-draining lymph node (pLN), and the prostate tumor.
e, Analysis of CTV dilution as a measure of proliferation by TCRrg CD4$^+$ Tconv cells recovered from the pLNs of tumor-bearing TRAMP$^{+/+}$ mice.
f-g, Mobilization of C4-reactive TCRrg CD4$^+$ Tconv cells in tumor-bearing TRAMP$^{+/-}$ *Foxp3*$^{DTR/y}$ mice following transient Treg cell ablation. Data are representative of three independent experiments, n ≥ 6 per TCR.
f, Experimental schematic. CTV-labeled TCRrg CD4$^+$ Tconv cells were transferred into lymphoreplete TRAMP$^{+/-}$ *Foxp3*$^{DTR/y}$ mice. Recipients were subjected to daily i.p. injections of DT (see Materials & Methods) for 5 days. Donor cell localization and phenotype, as well as prostate tumor masses, were assessed 3 weeks post-transfer.
d, Flow cytometric plots showing the presence of MJ23, RET, and TGN TCRrg CD4$^+$ Tconv cells at the indicated sites.

greater numbers compared to their MJ23 or RET counterparts (Figure 13g). This result prompts consideration of two non-mutually exclusive possibilities. First, transient Treg cell ablation likely diminished the endogenous C4-reactive Treg cell population, granting TGN TCRrg $CD4^+$ Tconv cells greater access to C4/I-A^b within TRAMP prostate tumors and pLNs. Second, increased TSA availability may have led to increased exhaustion or deletion of $CD4^+$ Tconv cells bearing higher sensitivities to C4/I-A^b. Support for this second point stems from observations of decreased proliferation of RET TCRrg $CD4^+$ Tconv cells (Figure 13e) and increased expression of the co-inhibitory receptor PD-1 by RET and MJ23 TCRrg $CD4^+$ Tconv cells (shown for RET in Figure 13d) in the pLNs of tumor-bearing $TRAMP^{+/+}$ mice.

$CD4^+$ Tconv cells bearing the high-sensitivity MJ23 TCR show limited ability to control prostate tumor growth

Next, we hypothesized that, if $CD4^+$ Tconv cells bearing the MJ23 TCR were more susceptible to cell-intrinsic mechanisms of peripheral T cell tolerance, such cells would fail to control prostate tumor burden in TRAMP mice. We returned to our Flu/Cy preconditioning and adoptive transfer system (Figure 14a), instead infusing large numbers of MJ23 TCRtg $CD4^+$ Tconv cells preactivated *in vitro* with $CD11c^+$ cells and exogenous C4 peptide. Eight weeks post-transfer, tumor masses were comparable between $TRAMP^{+/+}$ mice receiving MJ23tg $CD4^+$ Tconv cells and control $TRAMP^{+/+}$ mice (Figure 14b). In contrast, lymphodepleted $TRAMP^{+/+}$ mice that received polyclonal $CD4^+$ Tconv cells from *Aire*$^{-/-}$ donors exhibited reduced prostate tumor burden (Figure 14c). Moreover, $TRAMP^{+/-}$ *Aire*$^{-/-}$ mice, which experience early prostatic infiltration of MJ23 and several other $CD4^+$ Tconv cell clones, demonstrated reduced prostate tumor burden at 28 weeks

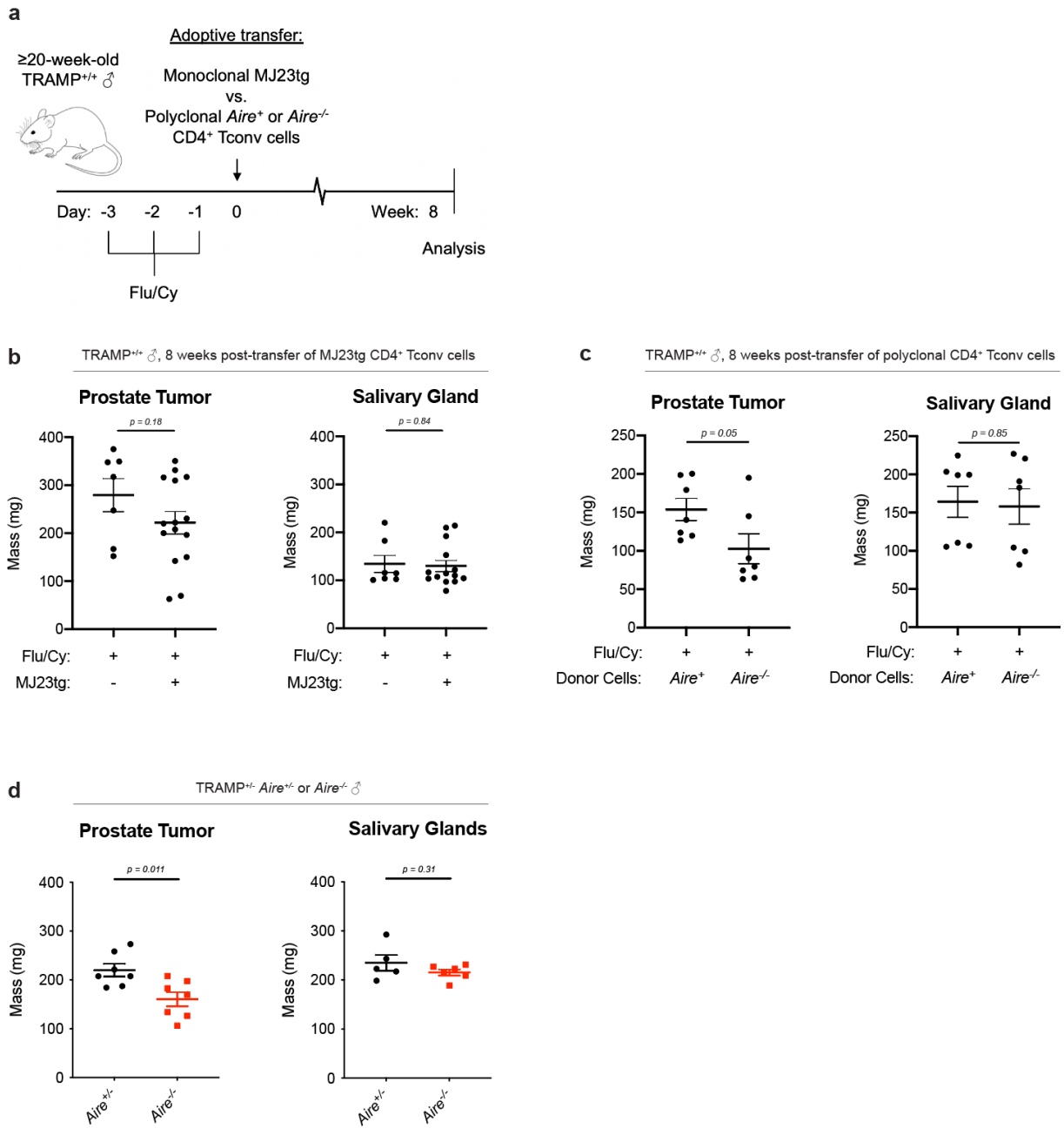

Figure 14 | Presence of polyclonal *Aire*$^{-/-}$, but not monoclonal MJ23, CD4^{+} Tconv cells leads to reduced prostate tumor burden in TRAMP mice.

(**a-c**) 20-week-old TRAMP$^{+/+}$ males were subjected to Flu/Cy-based lymphodepletion, followed by adoptive transfer of 2.5-5 x 10^5 *in vitro* preactivated MJ23 TCRtg CD4^{+} Tconv cells (**b**) or 1-2.5 x 10^6 polyclonal CD4^{+} Tconv cells from the SLOs of *Aire*$^{+/-}$ or *Aire*$^{-/-}$ males (**c**). Recipient mice were euthanized 8 weeks post-transfer and masses of the indicated non-lymphoid tissues were measured. Data are representative of three independent experiments, n ≥ 7 per condition.

Figure 14, continued.
a, Experimental setup for adoptive transfers into TRAMP$^{+/+}$ mice with established prostate tumors. **b.** Comparison of prostate tumor (left) and salivary gland (1 lobe; right) masses of TRAMP$^{+/+}$ mice receiving monoclonal MJ23 TCRtg CD4^{+} Tconv cells versus control mice receiving lymphodepletion treatment alone.
c. Comparison of prostate tumor (left) and salivary gland (1 or 2 lobes; right) masses of TRAMP$^{+/+}$ mice receiving polyclonal CD4^{+} Tconv cells from *Aire*$^{+/-}$ versus *Aire*$^{-/-}$ donors.
d. TRAMP$^{+/+}$ mice and *Aire*$^{-/-}$ were intercrossed to generate TRAMP$^{+/-}$ *Aire*$^{+/-}$ and TRAMP$^{+/-}$ *Aire*$^{-/-}$ mice, which were analyzed for prostate tumor mass and T cell infiltration (not shown) at 28 weeks of age. Data are representative of three independent experiments, n ≥ 5 per condition.

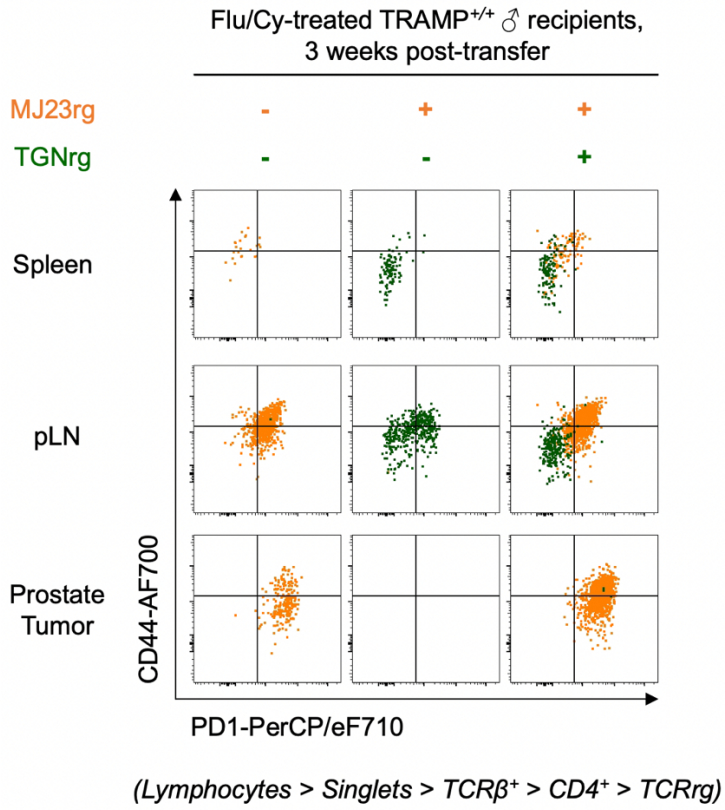

Figure 15 | MJ23 TCRrg CD4^{+} Tconv cells may promote the autoimmune infiltration of their lower-sensitivity counterparts.

20-week-old TRAMP$^{+/+}$ males were subjected to Flu/Cy-based lymphodepletion, followed by adoptive transfer of 10^5 Thy1.1^{+} MJ23 TCRrg CD4^{+} Tconv cells (first column), 10^5 hCD4^{+} TGN TCRrg CD4^{+} Tconv cells (second column), or 5 x 10^4 CD4^{+} Tconv cells of each clone (third column). Recipient mice were euthanized 3 weeks post-transfer and the localization and phenotype of each transferred population were assessed. Flow cytometric plots show the presence and CD44 versus PD-1 expression of TCRrg CD4^{+} Tconv cells (MJ23 in orange, TGN in green). Data are representative of one experiment, n ≥ 2 per condition.

of age compared to Aire-sufficient TRAMP$^{+/-}$ mice (Figure 14d). Combined, these findings suggest that, once tolerance is broken, self-reactive CD4^{+} Tconv cell clones require continuous replenishment and/or collaboration with other such clones to mediate prolonged and effective immune responses against host tissues.

Clones bearing greater sensitivity to C4/I-A^{b} may promote the prostatic infiltration of less sensitive C4-reactive clones

To address the latter point of collaboration between self-reactive CD4^{+} Tconv cell clones, we generated MJ23 TCRrg mice expressing the Thy1.1 reporter on TCRrg cells, as well as TGN TCRrg mice whose TCRrg cells expressed a truncated human CD4 (hCD4) reporter. This enabled tracking of two distinct C4-reactive clones following co-transfer into the same tumor-bearing TRAMP mouse. Based on previous studies of CD8^{+} T cells, we originally predicted that the clone with higher sensitivity to C4/I-A^{b}, MJ23, would outcompete the lower-sensitivity TGN clone for access to self-antigen, preventing TGN TCRrg CD4^{+} Tconv cells from infiltrating prostate tumors[109]. Surprisingly, while TGN TCRrg CD4^{+} Tconv cells failed to enter prostate tumors on their own, co-transfer with MJ23 TCRrg CD4^{+} Tconv cells enhanced the recovery of intratumoral TGN TCRrg CD4^{+} Tconv cells 3 weeks post-transfer (Figure 15). Of note, TGN TCRrg CD4^{+} Tconv cells generated with the hCD4 reporter displayed lower TCR expression compared to those bearing the Thy1.1 reporter (data not shown), which may explain divergent results in Figure 13 and Figure 15. Interestingly, compared to the single-transfer setting, TGN TCRrg CD4^{+} Tconv cells co-transferred with MJ23 cells showed decreased expression of CD44 and PD-1 (Figure 15). However, MJ23 TCRrg CD4^{+} Tconv cells displayed similar extents of CD44 and PD-1 expression in the presence or absence of co-transferred TGN cells. Based on this dichotomy, CD4^{+} Tconv

cells with higher sensitivities to TSAs may more readily infiltrate non-lymphoid tissues at early timepoints. In doing so, these cells promote organ infiltration of $CD4^+$ Tconv cells with lower sensitivities to the same TSAs. As the former peter out, the latter may remain within host tissues and retain pathogenic potential.

Thymocytes exhibiting higher sensitivities to C4/I-A^b undergo tTreg cell differentiation

As shown thus far, $CD4^+$ Tconv cell clones with higher sensitivities to C4/I-A^b increase autoimmune risk by infiltrating the prostate and facilitating prostatic infiltration by other C4-reactive $CD4^+$ Tconv cells. Given a limited role for anergy, ignorance, or pTreg induction in the regulation of MJ23 and RET TCRrg $CD4^+$ Tconv cells, the immune system may primarily avert disease by directing such clones into the tTreg cell fate during thymopoiesis. Doing so would limit the prevalence of potentially pathogenic C4-reactive clones within the $CD4^+$ Tconv cell compartment and yield tTreg cells capable of competing with clones like TGN for access to spMHC-II ligands. To assess the extent to which the MJ23, RET, and TGN TCRs facilitate tTreg cell differentiation, we transferred bulk thymocytes from TCRrg mice into new hosts via intrathymic injection. This enabled the introduction of TCRrg T cell precursors at low clonal frequencies, thereby reducing intraclonal competition for niches that facilitate tTreg development[139]. Seven days following transfer, a fraction of thymocytes bearing either the MJ23 or RET TCR upregulated Foxp3 (Figure 16). In contrast, negligible Foxp3 expression was observed among TGN TCRrg thymocytes (Figure 16). The ability of MJ23 and RET TCRrg thymocytes to undergo tTreg cell differentiation was dependent on expression of C4/I-A^b, as shown by minimal Foxp3 upregulation upon intrathymic injection into *Tcaf3(C4)*$^{-/-}$ recipients

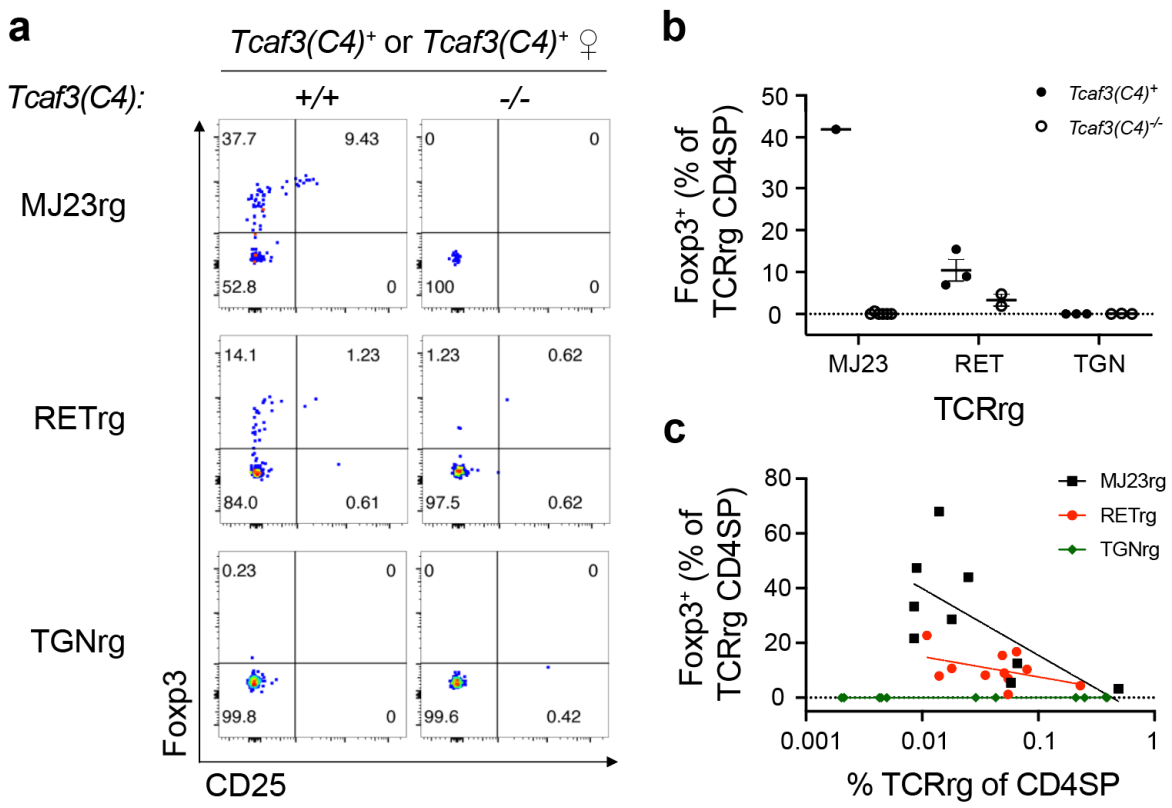

Figure 16 | Following intrathymic injection, thymocytes exhibiting higher sensitivities to C4/I-A^b undergo tTreg cell differentiation in a C4-dependent manner.

Female TCRrg primary host mice were generated as previously described. 10^7 bulk thymocytes from TCRrg primary hosts were injected directly into the thymi of female mice expressing or lacking C4 peptide (*Tcaf3(C4)*$^+$ or *Tcaf3(C4)*$^{-/-}$ mice, respectively). Injections were performed using a nonsurgical technique under isoflurane anesthesia. Seven days post-injection, Thy1.1$^+$ TCRrg thymocyte frequency and phenotype were assessed (**a-c**).

a. Flow cytometric plots showing Foxp3 versus CD25 expression of Thy1.1$^+$ CD4 single-positive cells.

b. Quantification of flow cytometric data shown in **a**. Data are representative of one experiment, n ≥ 3 per TCR.

c. Efficiency of thymic Treg cell differentiation exhibited by TCRrg thymocytes following transfer into C4-sufficent B6.SJL recipients. Data are representative of three independent experiments, n ≥ 8 per TCR.

(Figure 16). In all, this data support diversion into the tTreg cell lineage as one mechanism by which tolerance is maintained towards the C4/I-A^b self-antigen.

Infection with C4-expressing *L. monocytogenes* expands additional putative C4-reactive $CD4^+$ Tconv cell clones and promotes prostatic infiltration of C4-reactive $CD4^+$ Tconv cells

Treg cell-mediated control of C4-reactive $CD4^+$ Tconv cells may contribute to the prevention of prostate-directed immune responses, as prostatic infiltration of TCRrg $CD4^+$ T cells was rarely observed in TCRrg male mice (Figure 11a). However, while TGN $CD4^+$ Tconv cells are detected at lower frequencies within the prostates of mice following sustained Treg cell ablation, C4/I-A^b tetramer-binding TCRs are not among the most prevalent prostate-associated clonotypes recovered from Treg-ablated animals (Figure 1c, Table 2, and data not shown). These observations suggest that the combination of Treg cell-mediated suppression and limiting antigen availability may prevent prostatic infiltration by C4-reactive $CD4^+$ Tconv cells.

To address this possibility, we sought to assess functional responses of polyclonal C4-reactive $CD4^+$ Tconv cells following infection with *Lm[C4]*, as this tool allows us to provide additional C4 peptide and potentially break tolerance to C4/I-A^b *in vivo* (Figure 17a). Male *Foxp3*^{GFP} TCRβtg mice were infected with 10^7 CFU *Lm[C4]*. Seven days post-infection, $CD4^+$ T cells from the spleens of *Lm[C4]*-infected mice were isolated and subjected to dual C4/I-A^b tetramer staining. Foxp3$^{GFP\text{-}neg}$ $CD44^{hi}$ tetramer-positive cells were single-cell sorted via FACS and subjected to TCRα sequencing to identify clonotypes that had likely expanded following *Lm[C4]* infection (Figure 17b). Intriguingly, TCRα sequencing identified recurrent clonotypes whose CDR3α sequences varied from those of the "canonical" RET and TGN TCRs by one or two amino acid residues (Figure 17c). Notably, these amino acid substitutions fell within or near the

non-germline-encoded junctional regions of the CDR3α, suggesting that these newly identified TCRs may exhibit differential binding properties to C4/I-A^b, yet retain some degree of reactivity to C4/I-A^b based on their detection among activated $CD4^+$ Tconv cells in *Lm[C4]*-infected mice.

In light of the above, we referred back to our original TCRα sequencing results from C4/I-A^b tetramer-binding $CD4^+$ T cells recovered from *Aire*$^{-/-}$ TCRβtg mice, mining this dataset for additional variants of the MJ23, RET, and TGN TCRs. From this analysis, we selected 10 variant TCRs for further assessment of their reactivity to C4/I-A^b using our TCR retrogenic approach (Table 3). In preliminary work, we focused on the RET variant TCR, RETTA. FACS-purified TCRrg $CD4^+$ Tconv cells bearing the RET, RETTA, or TGN TCR were transferred into congenically disparate mice. Recipients were infected one day later with 10^7 CFU *Lm[C4]*, and donor cell phenotype and localization were assessed 8 days post-infection (Figure 17d). For all three TCRs, $CD4^+$ Tconv cells expanded in *Lm[C4]*-infected animals, but not in *Lm[parent]*-infected mice (Figure 17e). Moreover, RET, RETTA, and TGN TCRrg $CD4^+$ Tconv cells were recovered from the prostates of *Lm[C4]*-infected male mice, indicating that microbial infection and/or increases in antigen availability facilitated entry of C4-reactive $CD4^+$ Tconv cells into the prostate. However, the degree of prostatic infiltration varied among the three clones under investigation, with many TGN but few RETTArg $CD4^+$ Tconv cells recovered from the prostates of *Lm[C4]*-infected mice. Ongoing work will assess the sensitivity of $CD4^+$ Tconv cells expressing the RETTA or other variant TCRs and will continue to dissect how differences in sensitivity relate to pathogenic potential of various C4-reactive clones.

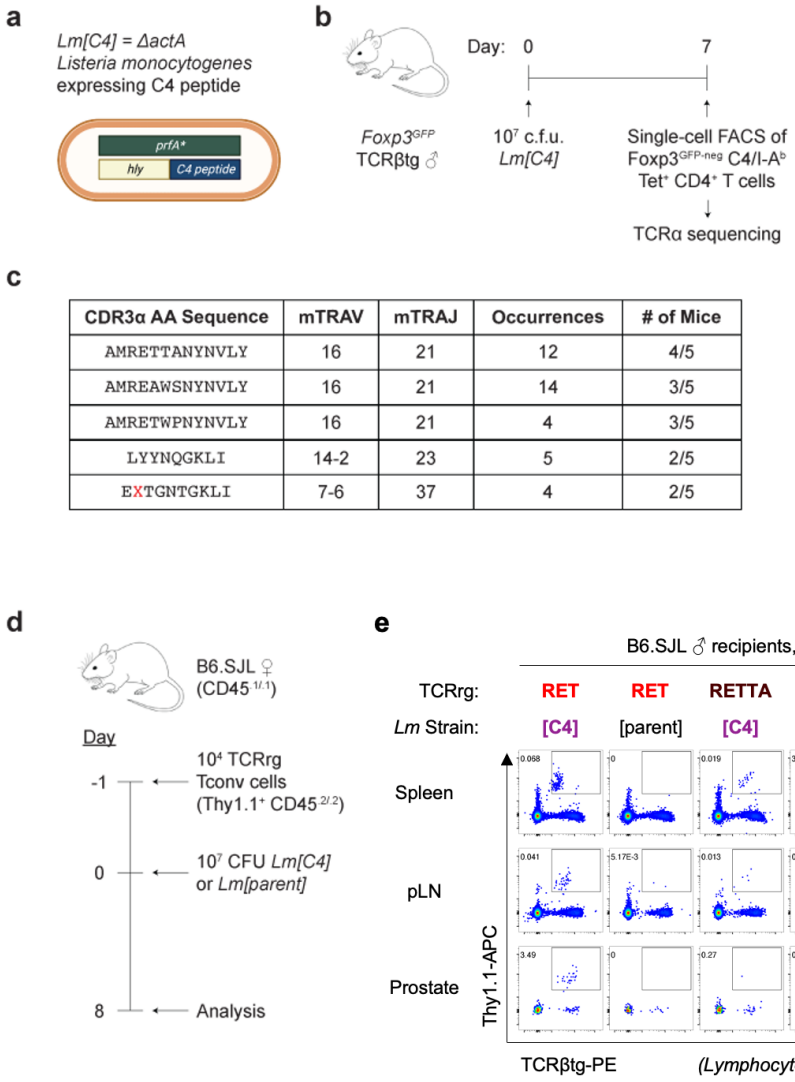

CDR3α AA Sequence	mTRAV	mTRAJ	Occurrences	# of Mice
AMRETTANYNVLY	16	21	12	4/5
AMREAWSNYNVLY	16	21	14	3/5
AMRETWPNYNVLY	16	21	4	3/5
LYYNQGKLI	14-2	23	5	2/5
EXTGNTGKLI	7-6	37	4	2/5

Figure 17 | Variants of known C4-reactive TCRs are expanded following infection with C4-expressing L. monocytogenes.

a, Diagram of attenuated *L. monocytogenes* engineered to express the C4 peptide (see Materials & Methods).
b, Experimental schematic for the discovery of additional C4-reactive TCRs. *Foxp3*^{GFP} TCRβtg male mice were inoculated with 10^7 CFU *Lm[C4]*. Seven days post-infection, splenocytes were isolated from infected animals, magnetically enriched for CD4$^+$ T cells, and subjected to dual C4/I-A^b tetramer staining. CD4$^+$ CD44^{hi} Foxp3$^{GFP\text{-}neg}$ C4/I-A^b tetramer-positive cells were isolated via FACS into individual wells of 96-well plates for single-cell TCRα sequencing (scTCRseq).
c, Partial list of candidate C4-reactive TCRs, alongside their total incidence and recurrence across 5 mice examined. The top three TCRs are variants of the RET TCR (TRAV16 - AMRETWSNYNVLY - TRAJ21). The fourth TCR corresponds to MJ23. The fifth listing refers to TGN variant TCRs, with X indicating any amino acid.

Figure 17, continued.
d, Experimental schematic for the validation of candidate C4-reactive CD4$^+$ T cell clones using *Lm[C4]*. Prior to the experiment, female TCR "retrogenic" (TCRrg) primary hosts bearing the indicated TCRs were generated as previously described (see Materials & Methods). One day prior to infection, Foxp3$^{GFP\text{-}neg}$ TCRrg CD4$^+$ Tconv cells were isolated from the secondary lymphoid organs of TCRrg primary hosts, magnetically enriched for CD4$^+$ T cells, purified via FACS, and labeled with the proliferation dye CellTrace Violet (CTV). 10^4 CTV-labeled TCRrg Tconv cells were then transferred into CD45$^{.1/.1}$ B6.SJL females. The following day, B6.SJL recipients were inoculated with 10^7 CFU *Lm[C4]* or parental *L. monocytogenes* (*Lm[parent]*). Eight days post-infection, spleens, prostate-draining lymph nodes (pLNs), and prostates were harvested from infected mice and analyzed for Thy1.1$^+$ TCRrg CD4$^+$ Tconv cell expansion and localization by flow cytometry.
e, Flow cytometric analysis of donor cells following *Lm[C4]* or *Lm[parent]* infection. Data show the frequency of Thy1.1$^+$ TCRrg CD4$^+$ T cells among all CD4$^+$ Tconv cells at the indicated sites. Data are representative of one experiment, n ≥ 2 per clone and condition.

TCR	mTRAV	CDR3α Sequence	mTRAJ
MJ23	**14-2**	**LYYNQGKLI**	**23**
LNYNQ	"	LNYNQGKLI	"
LYHNQ	"	LYHNQGKLI	"
LYFNQ	"	LYFNQGKLI	"
PYYNQ	"	PYYNQGKLI	"
RET	**16**	**AMRETWSNYNVLY**	**21**
REAWS	"	AMREAWSNYNVLY	"
RETTA	"	AMRETTANYNVLY	"
RETWP	"	AMRETWPNYNVLY	"
TGN	**7-6**	**EMTGNTGKLI**	**37**
EMAGN	"	EMAGNTGKLI	"
ETTGN	"	ETTGNTGKLI	"
GMTGN	"	GMTGNTGKLI	"

Table 3 | List of putative C4-reactive "variant" TCRs under investigation.

Naturally arising clonotypes harboring one to two amino acid substitutions near the underlined non-germline-encoded CDR3α of "canonical" MJ23, RET, and TGN TCRs (highlighted in yellow) were identified following TCRα sequencing of C4/I-A^b tetramer-binding CD4$^+$ T cells from *Aire*$^{-/-}$ TCRβtg mice and *Lm[C4]*-infected *Foxp3*^{GFP} TCRβtg mice. For each TCR, Vα and Jα gene segment usage is shown, along with the CDR3α residue differences indicated in red. TCRrg mice have been generated for all TCRs shown, allowing for downstream validation of reactivity to C4/I-A^b.

Conclusion

By employing a robust clonal analysis of naturally occurring $CD4^+$ T cell clones reactive to an endogenous TSA, C4/I-A^b, our study elucidates the impact of T cell sensitivity on the fate, function, and pathogenic potential of self-reactive $CD4^+$ T cells. C4-reactive clones were readily identified in the endogenous $CD4^+$ Tconv cell repertoire, indicating that the elimination of these clones by clonal deletion is, at best, an imperfect process[76]. Based on our TCRα sequencing data and transfers of TCRrg thymocytes, clones exhibiting higher degrees of sensitivity to C4/I-A^b showed limited evidence of restraint by clonal deletion but preferentially developed as tTreg cells, thereby limiting their pathogenic potential. Furthermore, we showed that, should these highly sensitive C4-reactive clones fail to differentiate into the tTreg cell lineage, they emerge as $CD4^+$ Tconv cells capable of infiltrating the prostate and enhancing prostatic infiltration of other C4-reactive $CD4^+$ Tconv cells, including those with lower sensitivities for the same self-antigen. However, $CD4^+$ Tconv cells exhibiting lower sensitivities to C4/I-A^b still possessed the ability to undergo prostatic infiltration in the contexts of infection, autoimmunity, and neoplasia, indicating that various inflammatory settings can release lower-sensitivity self-reactive $CD4^+$ Tconv cells, especially if such settings involve perturbation of the Treg cell compartment. Ongoing work will continue to leverage our novel and physiologically relevant TCR-ligand system to further assess the relationship between T cell sensitivity to self-antigens and autoimmune potential and better understand the fundamental mechanisms by which immune tolerance is established and enforced.

CHAPTER V: DISCUSSION

Overview

Here, we interrogated the mechanisms by which the immune system restrains naturally occurring $CD4^+$ Tconv cells reactive to endogenous self-antigens. In the case of a prostate-associated antigen, C4/I-A^b, $CD4^+$ Tconv cells exhibiting higher sensitivities to C4/I-A^b were diverted into the thymic Treg cell lineage in an Aire- and C4-dependent manner. In contrast, a C4-reactive clone with lower sensitivity to C4/I-A^b egressed from the thymus into the $CD4^+$ Tconv cell lineage but was kept in check by Treg cells in the periphery of tumor-free mice. In an autochthonous, oncogene-driven model of prostate cancer, lower-sensitivity C4-reactive $CD4^+$ Tconv cells were able to infiltrate established tumors following adoptive transfer, even in the presence of endogenous Treg cells. These findings suggest that, at steady state, competition for access to limited antigenic and/or other inflammatory signals prevents the autoimmune function of self-reactive $CD4^+$ Tconv cells. Such cues become more readily available to lower-sensitivity C4-reactive $CD4^+$ Tconv cells upon systemic Treg cell ablation, indicating that systemic inflammation and/or loss of Treg-specific functions enables robust activation of self-reactive $CD4^+$ Tconv cell clones present within the endogenous repertoire.

Notably, the rarity of C4-reactive clones among prostate-infiltrating $CD4^+$ Tconv cells in Treg-ablated mice revealed another striking finding: the existence of a previously undefined class of self-reactive $CD4^+$ Tconv cells that exhibit overt reactivity to widespread self-ligands. Through in-depth analyses of these cells in our TCR "retrogenic" (TCRrg) system, we found that such clones evade central tolerance, despite experiencing agonist TCR:spMHC-II interactions in the

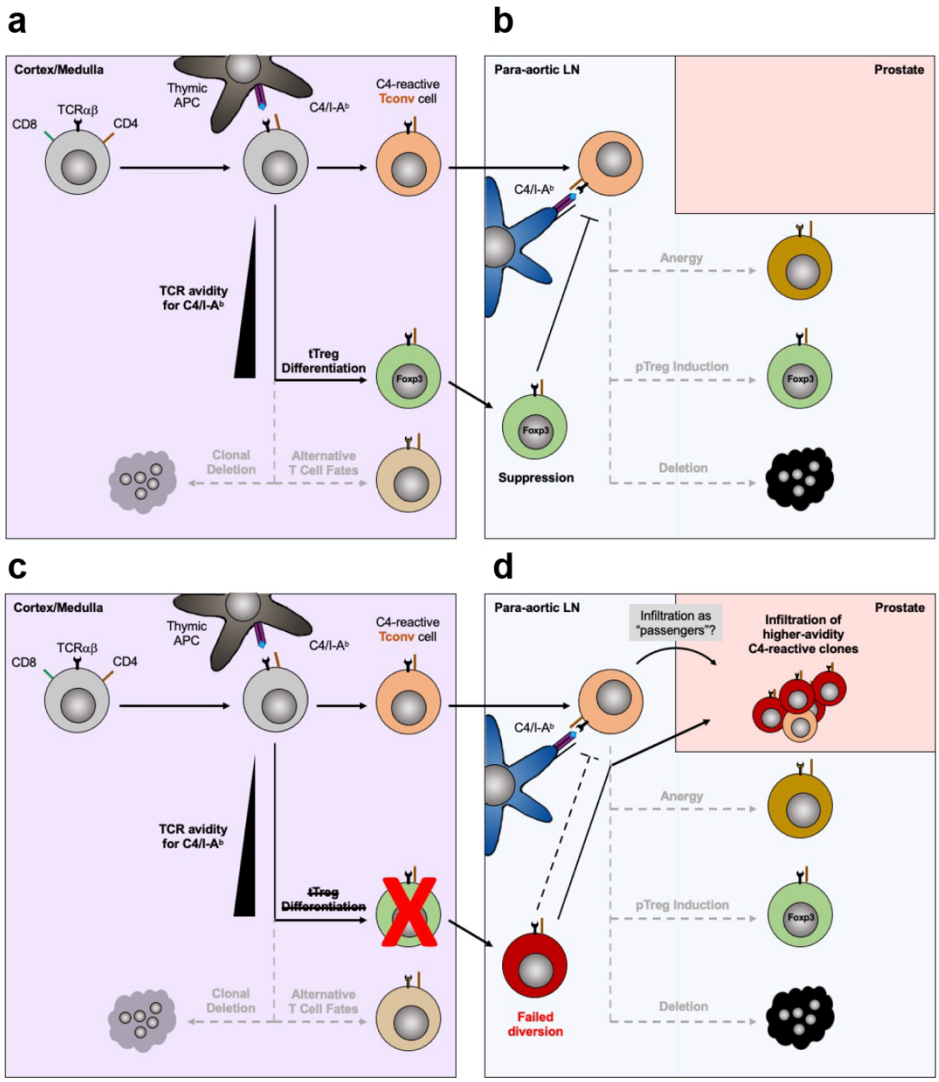

Figure 18 | Working model of immune regulation of CD4$^+$ Tconv cells reactive to the tissue-specific antigen, C4/I-A^b.

Thymocytes bearing TCRs that react to the prostate-derived peptide Tcaf3$_{646\text{-}658}$ ("C4 peptide") encounter this antigen in the thymic medulla. Upon encounter of C4/I-A^b, C4-reactive thymocytes differentiate as either thymic Treg (tTreg) cells or as CD4$^+$ Tconv cells, with clones exhibiting higher avidities or sensitivities to C4/I-A^b preferentially experiencing tTreg cell induction (**a**). The resulting C4-reactive tTreg cells may successfully compete with their CD4$^+$ Tconv cell counterparts for access to C4/I-A^b, thereby restraining the latter's pathogenic potential (**b**). However, if highly sensitive C4-reactive clones are prevented from undergoing tTreg cell differentiation (as in **c**), such cells may egress from the thymus as CD4$^+$ Tconv cells and promote autoimmune infiltration of the prostate in both tumor-free and tumor-bearing mice (**d**). Self-directed immune responses by clones with lower sensitivity to C4/I-A^b may be enhanced by settings in which their access to antigen, cytokines, and/or co-stimulatory molecules is enhanced, such as in the case of systemic Treg cell ablation.

thymus. Instead, these self-reactive CD4$^+$ Tconv cells adopt several features of Tfh cells in the periphery, including apposition to B cell follicles in the spleens of TCRrg mice. Interestingly, at steady state, these self-reactive "natural Tfh-like" (nTfh) cells do not express IL-21 or promote spontaneous GC formation, calling into question their ability to perform common Tfh cell effector functions. However, upon Treg cell depletion, nTfh cells downregulated Bcl6, produced IFN-γ, and infiltrated non-lymphoid organs, indicative of a switch to a pathogenic Th1 cell program. Given the ever-growing connection between Tfh and Th1 cells in autoimmunity, the clones described herein may play a central role in self-directed immune responses.

The relationship between T cell sensitivity for self-antigens and autoimmune potential

Collectively, our results do not support a strictly linear relationship between a CD4$^+$ Tconv cell's sensitivity to spMHC-II and its pathogenic potential. However, such a relationship may appear non-linear due to differential effects at the extremes in polyclonal settings. Specifically, autoimmune functions of clones with higher sensitivities to self-antigens may be blunted by cell-intrinsic mechanisms of peripheral T cell tolerance. While our analyses of MJ23 and RET TCRrg CD4$^+$ Tconv cells did not demonstrate a role for the induction of pTreg cells or anergy, other modes of tolerance, including exhaustion and activation-induced cell death, have yet to be ruled out. Prior studies have implicated these mechanisms in the regulation of CD4$^+$ and CD8$^+$ T cell clones exhibiting high extents of reactivity to foreign antigens[144,259]. With regards to lower-sensitivity self-reactive CD4$^+$ Tconv cells, their organ infiltration and function may be enhanced by the presence of self-reactive clones with greater sensitivities to self-antigens. This point is supported by our co-transfers of C4-reactive clones, which demonstrated enhanced recovery of TGN TCRrg CD4$^+$ Tconv cells when their MJ23 counterparts were also present. Additionally, in

the setting of Treg cell depletion, our observations of diminished organ infiltration by Group 1 clones suggests that their initial discovery amongst prostate-infiltration $CD4^+$ Tconv cells may have been facilitated by the more broadly self-reactive $CD4^+$ Tconv cells comprising Group 3. Thus, we propose that clones with higher extents of self-reactivity represent "drivers" of autoimmunity once tolerance is broken, whereas clones exhibiting lower sensitivities to self-antigens enter non-lymphoid organs as "passengers."

However, the extent to which passenger or "bystander" clones contribute to autoimmune processes remains unclear. This question has been frequently asked with regards to antitumor immunity, as tumor-specific and non-tumor-reactive clones are detected among $CD8^+$ tumor-infiltrating lymphocyte (TIL) populations. In characterizing the antigen specificity of tumor-infiltrating $CD8^+$ T cell clones, Newell and colleagues observe a substantial fraction of clones that display hallmarks of reactivity to viral epitopes, not tumor-derived antigens[260]. These bystander $CD8^+$ TILs exhibited a tissue-resident memory phenotype, marked by high expression of PD-1, CD69, and the integrin CD103, suggesting that these cells had previously undergone activation and differentiation following antigen encounter. Notably, within tumors, these cells lacked expression of other TCR-induced markers, including CD39, indicating that these cells were not subject to chronic antigen stimulation in the tumor microenvironment. Moreover, increased frequencies of $CD39^{neg}$ $CD8^+$ TILs were associated with poorer responses to immune checkpoint blockade (ICB) therapy in lung cancer patients. In contrast, other studies have reported decreased overall survival in patients with higher levels of exhausted $CD8^+$ TILs. As bystander $CD8^+$ TILs do not show signs of exhaustion, these cells may be contributing to tumor control by nonspecific cancer cell killing based on innate-like signals. Alternatively, passenger clones within tumors may simply be a byproduct of infiltration by tumor-specific T cells and may have no functional

importance of their own. Further research is required to dissect these possibilities and to conclusively determine whether a similar paradigm exists for $CD4^+$ Tconv cells, as recently suggested by the Newell group[261]. In the context of the present study, a broader comparison of TCRrg $CD4^+$ Tconv cells isolated from non-lymphoid organs may reveal additional phenotypic and/or functional differences between driver and passenger clones.

Peripheral selection for self-reactive clones on the basis of sensitivity to spMHC-II

In assessing the relative contributions of driver and passenger clones, another question arises: to what extent does the pool of T cells participating in an immune response evolve as the response persists? If T cells bearing higher sensitivities to antigen benefit from preferential activation and proliferation at limiting doses of antigen, then such cells may predominate the early stages of an immune response and prevent robust involvement of lower-sensitivity clones. On the other hand, if higher-sensitivity T cells eventually peter out or become terminally exhausted, an ongoing immune response may become dominated by their lower-sensitivity counterparts. Both scenarios imply selection of T cell clones based on their sensitivity to pMHC-II ligands, a phenomenon that remains under active investigation. In early work on this topic, Savage *et al.* immunized mice with pigeon cytochrome c (PCC) in Ribi adjuvant and stained $CD4^+$ T cells with I-E^k tetramers bearing related moth cytochrome c peptide (MCC)[155]. By using a range of MCC:I-E^k tetramer staining concentrations, the authors calculated apparent K_D values for their cytochrome c-reactive $CD4^+$ T cell population after primary immunization. A repeat of this analysis after secondary immunization found a decrease in apparent K_D amongst cytochrome c-reactive $CD4^+$ T cells, corresponding to an increase in TCR:p:MHC-II affinity. Since then, several groups have provided conflicting evidence for peripheral selection, with studies showing that $CD4^+$ and $CD8^+$

T cells with higher sensitivities for antigen dominate[152–154] over or give way to[121,144] clones with lower sensitivities for antigen. Divergent findings by these studies may be explained by differences in the immunization strategies or infection models used, the techniques employed to measure sensitivity to antigen, and the timepoints chosen for analysis. This latter point is especially important: both high- and low-sensitivity clones have been shown to respond during primary immune challenges and differentiate into memory T cells. However, a recall response may trigger selection expansion of higher-sensitivity memory T cells, whereas a persistent immune challenge (or one with higher doses of antigen) may give lower-sensitivity effectors the upper hand[149]. Collectively, these findings suggest that immune challenges of differing intensity and duration direct the evolution of the responding T cell population and its overall sensitivity to antigen in distinct ways.

Of note, as a proxy for $CD4^+$ T cell sensitivity to antigen, many studies use TCR:pMHC-II affinity – as measured by surface plasmon resonance (SPR) or two-dimensional micropipette-based (2D-MP) assays – or T cell avidity, as assessed by binding of pMHC-II multimers. However, as demonstrated by our study and others, binding to pMHC-II ligands *in vitro* does not guarantee functional $CD4^+$ Tconv cell responses following antigen encounter *in vivo*. $CD4^+$ T cell sensitivity and function may instead be more tightly linked to the duration of the TCR:pMHC-II interaction, which is often captured by $t_{1/2}$. To test this, Yousefi *et al.* recently developed a TCR-ligand pair whose interaction half-life could be manipulated optogenetically[262]. In leveraging this system, the authors found that more prolonged interactions between their TCR and its ligand resulted in greater intracellular calcium flux compared to shorter, yet more frequent TCR-ligand pairings. This finding lends support to the kinetic proofreading model of T cell ligand discrimination, which posits that T cells differentiate between self- and foreign-derived ligands by exhibiting longer

interactions with the latter[263]. Differences in $t_{1/2}$ may also explain the distinct behaviors exhibited by our various C4-reactive clones. Ongoing work seeks to characterize the binding kinetics of the MJ23, RET, TGN, and additional TCRs to C4/I-A^b by SPR and 2D-MP. Doing so will allow us to assess whether differences in binding parameters like $t_{1/2}$ track with changes in the propensity of C4-reactive clones to infiltrate the prostate.

Such analyses may reveal either a positive or negative association between $t_{1/2}$ and organ infiltration – or may fail to support the existence of such an association. According to kinetic proofreading, self-reactive $CD4^+$ T cells that exhibit longer interactions with spMHC-II molecules are thought to be more sensitive to antigen. Such cells are expected to exhibit higher extents of T cell signaling, based on increased calcium mobilization, diacylglycerol (DAG) formation, and CD69 upregulation[262,264]. However, this improved T cell signaling does not translate to more potent $CD4^+$ Tconv cell responses, as studies of foreign-reactive T cells have connected higher $t_{1/2}$ values to decreased polarization towards DCs and decreased proliferation[144,265,266].

Moreover, a central tenet of the kinetic proofreading model – that self-reactive T cells exhibit shorter interactions with spMHC-II ligands – holds primarily as a result of central T cell tolerance, by which clones that more durably bind to self-antigens are deleted or diverted into the tTreg cell lineage. A recent study by the Huseby group supports a role for $t_{1/2}$ in fate determination of thymocytes reactive to the self-antigen Padi4, although peripheral deletion of the self-reactive clones they describe may also factor into their observations[137]. In this study, Stadinski *et al.* note that the association between TCR:pMHC-II affinity and clonal deletion (or tTreg cell differentiation) is not influenced by binding on-rates (k_{on}). This finding suggests that TCR off-rates (k_{off}) and the associated metric of $t_{1/2}$ are more relevant determinants of self-reactive thymocyte fate, and that the immune system selects against $CD4^+$ Tconv cells whose TCRs can

engage in long-lasting interactions with self-antigens. However, our work demonstrates that the TCRs present within the endogenous $CD4^+$ Tconv cell repertoire remain inherently capable of binding self-antigen, facilitating T cell signal transduction, and promoting infiltration of non-lymphoid organs. Additionally, our observation that clones reactive to widespread self-antigens predominate within the organ-infiltrating $CD4^+$ Tconv cell population suggests that increased antigen availability promotes the function of self-reactive $CD4^+$ T cells across a range of TCR:spMHC-II affinities and half-lives, in line with similar findings reported for $CD8^+$ T cells[266]. Shorter TCR:spMHC-II half-lives may instead facilitate serial triggering of multiple TCRs on the surface of a self-reactive $CD4^+$ Tconv cell, leading to the latter's activation and resistance to cell-intrinsic mechanisms of peripheral T cell tolerance[267,268].

B eell-independent Tfh cell differentiation, maintenance, and function in settings of persistent antigen encounter

In this vein, many self-reactive $CD4^+$ Tconv cells exist in settings in which chronic antigen stimulation can occur. How do these cells differentiate and maintain functional responsiveness in the presence of readily accessible self-antigens? Insights into this question may be gleaned from studies of chronic viral infection. In this setting, it is well appreciated that both $CD4^+$ and $CD8^+$ T cells undergo progressive dysfunction upon persistent recognition of antigen. For example, $CD4^+$ Tconv cells specific for lymphocytic choriomeningitis virus (LCMV)-derived peptides rapidly upregulate a Th1 cell program and produce IFN-γ in mice infected with the acute LCMV Armstrong strain[269]. In contrast, mice infected with the chronic LCMV Clone 13 strain harbor LCMV-specific $CD4^+$ Tconv cells that lose IFN-γ expression over time and become refractory to rechallenge[270]. Subsequent studies, however, have reported that persistent viral infection induces

the progressive differentiation of $CD4^+$ Tconv cells into Tfh cells; such cells sustain virus-specific antibody production by B cells and are essential for viral clearance[271,272]. Moreover, in acute infection models, such as *L. monocytogenes*, increasing antigen doses correlated with increased Tfh cell differentiation among pathogen-reactive $CD4^+$ Tconv cells. Our work fits well with these previous reports, in finding that $CD4^+$ Tconv cells reactive to widespread self-antigens adopt canonical features of Tfh cells.

Notably, several infection and immunization studies demonstrate that environments with high antigen availability can facilitate Tfh cell induction in a B cell-independent manner. Following infection with chronic LCMV, Fahey *et al.* showed similar extents of CXCR5, ICOS, and OX-40 upregulation by $CD4^+$ Tconv cells in WT and B cell-deficient μMT mice[271]. In addition, Choi *et al.* demonstrated that robust Bcl6 and CXCR5 induction by $CD4^+$ Tconv cells could still occur in μMT mice during the early phases of acute LCMV infection[273]. These findings match our observations of Group 3 TCRrg $CD4^+$ Tconv cells, which express hallmarks of Tfh cells even when transferred into animals treated with anti-CD20 antibody. Of note, B cell depletion following anti-CD20 administration is incomplete, with a minor fraction of $CD20^{lo/neg}$ GC B cells and plasma cells remaining 7 days post-treatment[243]. While it remains formally possible that these fully differentiated B cells could support the differentiation and maintenance of Tfh-like Group 3 clones, a more likely possibility is that DCs can induce and maintain a Tfh-like program in Group 3 clones by virtue of the abundance of cognate self-antigens. Future studies may leverage $Zbtb46^{DTR}$ mice to ablate conventional DCs and address the relative contributions of DCs versus B cells in diverting Group 3 clones towards a Tfh-like phenotype[274].

However, using both anti-CD20-treated WT mice and DT-treated $Mb1^{Cre}$ x $Rosa26^{LSL\text{-}DTR}$ mice, we found that B cell depletion led to a decrease in the frequency of polyclonal Group 3-like

PD-1^{hi} Bcl6^{hi} Eomes^{+} CD4^{+} Tconv cells. This difference in B cell dependence between polyclonal and TCRrg Group 3 cells remains enigmatic. One possibility is that, in our transfer experiments, Group 3 TCRrg thymocytes have already undergo thymic maturation in a B cell-sufficient environment. Early interactions with thymic B cells may contribute to the agonist signals exhibited by Group 3 TCRrg thymocytes. As a result, T:B interactions during thymic development may cause Group 3 TCRrg thymocytes to be transcriptionally and/or epigenetically poised to adopt a Tfh-like state in the periphery. This possibility may be tested by performing RNAseq or ATACseq[275] of Group 3 TCRrg thymocytes isolated from B cell-depleted versus control animals. Additionally, in-depth phenotyping of polyclonal thymocytes from B cell-depleted versus control mice may provide further insights into the ontogeny of self-reactive Tfh-like cells[276].

Whether or not B cells influence the induction and maintenance of self-reactive Tfh-like cells, our IF microscopy findings demonstrate that these two cell types may still interact with one another. The normal frequencies of GC B cells in Group 3 TCRrg mice do not rule out the possibility that Group 3 clones potentiate B cell responses. Moreover, these results also raise the alternative hypothesis that Group 3 clones regulate autoreactive B cells at steady state. Numerous studies have identified autoreactive B cells within the SLOs of mice and humans in the absence of autoimmune disease[69,277,278]. In healthy animals, autoreactive B cells display hallmarks of anergy, including decreased B cell receptor (BCR; IgM) surface expression and blunted antibody production following ligation of antigen. However, in certain settings of autoimmunity, autoreactive B cells receive signals that enable them to form GCs and produce autoantibodies. To assess whether Group 3 clones are capable of imposing B cell anergy, deleting anergic B cells, or restraining autoreactive GCs, one can transfer Group 3 TCRrg CD4^{+} Tconv cells into autoimmune-prone mouse models or into infected mice. The impact of adoptive transfer on endogenous T and

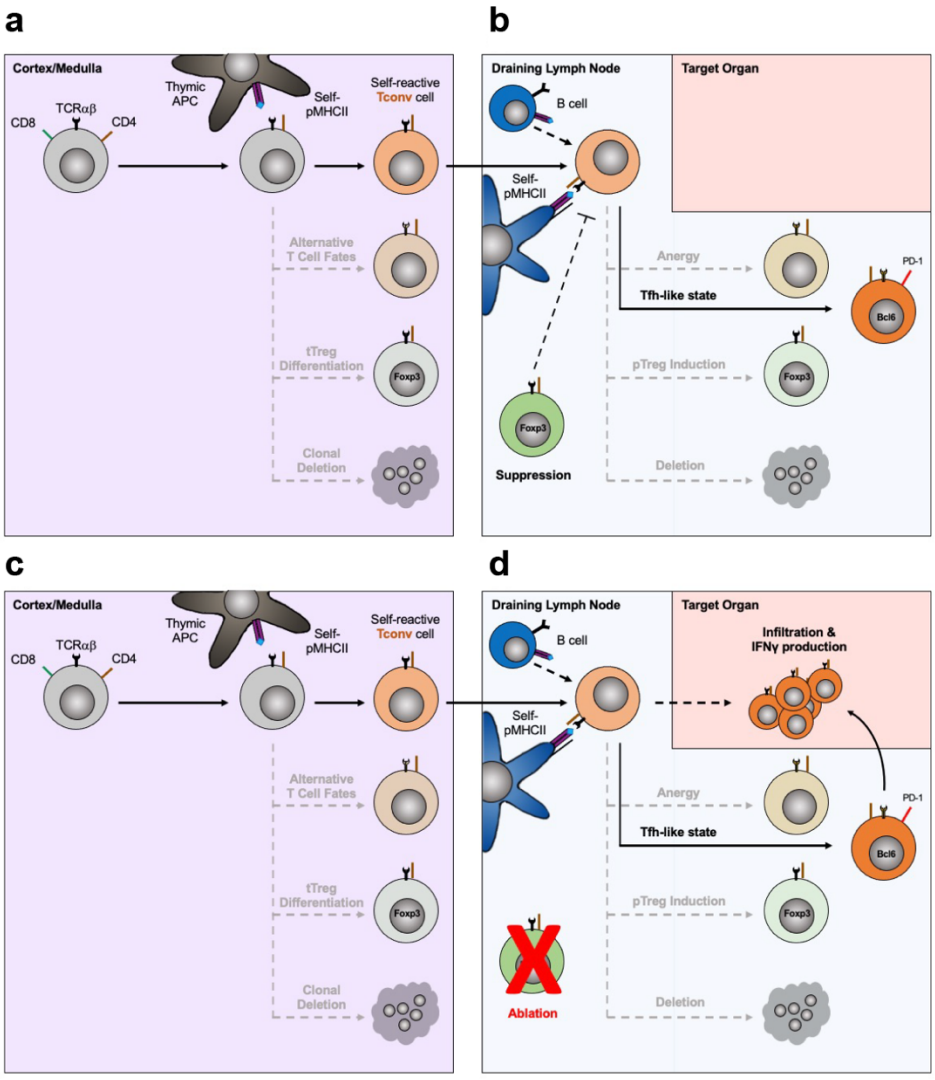

Figure 19 | Working model of immune regulation of CD4⁺ Tconv cells reactive to widely expressed self-antigens.

Thymocytes bearing TCRs that react to endogenous MHC class II-restricted self-antigens expressed by dendritic cells (DCs) egress from the thymus as CD4⁺ Tconv cells (**a**, **c**). At steady state, these broadly self-reactive CD4⁺ Tconv cells display hallmarks of antigen encounter in the periphery and upregulate signature markers associated with the Tfh cell fate (**b**). Upon Treg cell ablation, naturally occurring Tfh-like ("nTfh") cells downregulate Bcl6, infiltrate non-lymphoid organs, and produce interferon-gamma (IFNγ), indicating a switch to a pathogenic Th1 cell program (**d**). A major role for alternate mechanisms of central and peripheral T cell tolerance has not been identified. Moreover, the relative contributions of DCs versus B cells in inducing the nTfh cell program remain unclear.

B cells could be tracked over time. Conversely, to test the ability of Group 3 clones to induce GCs, future studies could perform similar experiments in mice that harbor intact B cells but lack GCs at baseline; these include the *Icos*$^{-/-}$, *Cd40lg*$^{-/-}$, and *CD4*^{Cre} x *Bcl6*$^{fl/fl}$ strains[279–281]. Lastly, it is possible that Group 3 clones upregulate Bcl6 and associated markers simply as a consequence of chronic antigen stimulation, rather than as part of a defined functional or regulatory module of self-reactive CD4$^+$ Tconv cells. Future endeavors comparing the responses of Group 3 clones to CD4$^+$ Tconv cells whose cognate self-antigen is known may address this possibility.

Eomes as a defining feature of self-reactive "nTfh" cells

The identification of Eomes as a defining marker of TCRrg and polyclonal nTfh cells was surprising, as Eomes has more frequently been associated with Th1 cells and CD8$^+$ cytotoxic T lymphocytes (CTLs)[282,283]. Nevertheless, recent reports have shown that, in both CD4$^+$ and CD8$^+$ T cells, Eomes may be upregulated through TCR engagement, co-stimulation, and sensing of various cytokines, including Type I IFNs, IL-2, IL-4, and IL-15[283–286]. These signals may not be required for maintenance of Eomes expression once it is induced[287]. T cell-specific deletion of Eomes led to decreased IFN-γ and granulocyte-macrophage colony-stimulating factor (GM-CSF) secretion by CD4$^+$ T cells following anti-CD3 stimulation. As in CD8$^+$ T cells, Eomes is capable of inducing IFN-γ expression by CD4$^+$ T cells in a T-bet-independent fashion[288]. However, the mechanisms by which Eomes operates and is induced in Tfh cells – including the nTfh cells we define herein – remain incompletely understood.

Eomes expression in nTfh cells may promote the plasticity of these cells, as demonstrated by their loss of Bcl6 and production of IFN-γ following systemic Treg cell ablation. CD4$^+$ T cells have the capacity to express hallmarks of multiple Th cell lineages simultaneously, and often do

so in settings of autoimmunity[289]. As in other Th subsets, plasticity in Tfh cells is driven by the integration of distinct cytokine cues, co-stimulatory signals, and metabolic factors[290]. However, one notable difference lies in Tfh cells' expression of Bcl6, which can repress other lineage-defining transcription factors and the effector T cell-associated transcription factor, Blimp-1[291]. The ability of nTfh cells to express high levels of both Bcl6 and Eomes merits further investigation.

Given the importance of Eomes for memory $CD8^+$ T cell differentiation, Eomes may also impose the central memory-like T (T_{CM}) cell phenotype exhibited by nTfh cells. In our characterization of Group 3 TCRrg $CD4^+$ Tconv cell clones, we noted maintained expression of CD62L by these clones, despite obvious hallmarks of antigen encounter. $CD44^{hi}$ $CD62L^{hi}$ T_{CM} cells share this feature with nTfh cells, as the former have also undergone activation in response to pMHC-II ligands. Notably, in $CD8^+$ T cells, Eomes deficiency leads to a profound loss of cells bearing the T_{CM} phenotype[245]. If Eomes plays a similar role in $CD4^+$ Tconv cells, we predict that loss of Eomes would hinder the induction of nTfh cells. If so, phenotypic characterization of *CD4*^{Cre} x *Eomes*$^{fl/fl}$ mice would show a decrease in Tfh-like cells at steady state. In addition, intrathymic transfer experiments in which *Rag1*$^{-/-}$ *Eomes*$^{-/-}$ thymocytes are retrovirally transduced with a Group 3 TCR may reveal whether Eomes is required for the adoption of a Tfh-like or T_{CM}-like phenotype, or if TCR:spMHC-II interactions are sufficient to drive Group 3 cells into this unique state.

Given its function in promoting CTL responses, Eomes may also confer cytolytic abilities onto nTfh cells, which these cells can leverage to control autoreactive B cell responses. While this possibility remains untested for our Group 3 clones, expression of Eomes by $CD4^+$ Tconv cells has been associated with increased expression of granzyme B in models of autoimmune neuroinflammation[292,293]. As elevated frequencies of Eomes-expressing $CD4^+$ Tconv cells have

been reported in mice with EAE and in patients with progressive forms of MS, these cells may impact the severity and chronicity of autoimmune disease. A recent study also implicates cytotoxic Eomes$^+$ CD4$^+$ Tconv cells in the control of B-cell chronic lymphocytic leukemia[246], an intriguing observation considering our findings showing the potential for Eomes$^+$ CD4$^+$ Tconv cells to engage with B cells at steady state. Despite the tempting hypothesis that Eomes$^+$ nTfh cells may direct their cytotoxic functions towards B cells, DCs or other APCs may also be targeted by cytotoxic CD4$^+$ Tconv cells. A broader profiling of APC subsets in Group 3 TCRrg mice may elucidate the immune cell types influenced by nTfh cells. Lastly, Eomes may be dispensable for the ability of nTfh cells to promote deletion of autoreactive or anergic B cells; this function may be accomplished via other mechanisms, including the provision of FasL or CD40L by T cells to follicular or GC B cells[294,295].

CD73 and FR4: specific markers of anergic CD4$^+$ Tconv cells?

In many of our experiments, a fraction of Group 3 TCRrg CD4$^+$ Tconv cells expressed high levels of CD73 and FR4, two markers recently proposed to distinguish murine CD4$^+$ T cells exhibiting hallmarks of anergy. In work by Mueller and colleagues, clones whose TCRs were reactive to widely expressed self-antigens progressively increased their surface expression of CD44, PD-1, CD73, and FR4[248,296]. Notably, these "anergic-phenotype" cells produced negligible amounts of common Th effector cytokines, such as IL-2, and remained Ki67^{lo}, indicative of limited proliferative potential at steady state. In contrast, the self-reactive nTfh cells described here display elevated expression of Bcl6, CD62L, CD69, and Ki67. The numerous phenotypic differences between these two cell populations suggest that self-reactive nTfh cells represent a distinct subset of CD4$^+$ Tconv cells. Further reinforcing this claim is our observation that the homeostasis of

polyclonal nTfh clones is dependent on B cells, whereas the homeostasis of anergic-phenotype cells is not. Thus, high-density expression of CD73 and FR4 may be shared by Treg and $CD4^+$ Tconv cells recognizing abundant self-antigens in settings of immune homeostasis, rather than being limited to $CD4^+$ Tconv cells experiencing hyporesponsiveness to spMHC-II ligands. Notably, the functional importance of increased CD73 and FR4 expression has yet to be demonstrated; experiments that force overexpression of these markers in $CD4^+$ Tconv cells reactive to a defined antigen may reveal a role for these markers in immune regulation.

Requirement of immune perturbation to unleash self-reactive $CD4^+$ Tconv cells

We found that many of our self-reactive $CD4^+$ Tconv cell clones exhibited greater organ infiltration in the setting of systemic Treg cell depletion, which induces widespread inflammation and releases pathogenic clones from Treg cell-mediated suppression. However, at steady state, organ infiltration by self-reactive $CD4^+$ Tconv cells rarely occurred, indicating that some form of immune perturbation was required to enable self-directed responses against host tissues. Given that the selective removal of Treg cells is achieved via an artificial experimental system, it is important to understand how more physiological mechanisms can shift the immune system away from homeostasis and facilitate the autoimmune functions of self-reactive $CD4^+$ Tconv cells. Our studies of C4-reactive clones in response to microbial infection (using *Lm[C4]*) address this by demonstrating that organ infiltration occurs in settings in which C4/I-Ab and inflammatory cues are more readily available. Notably, infection with the parental *Lm* strain did not trigger expansion or prostatic infiltration by C4-reactive clones, suggesting that inflammation alone cannot unleash self-reactive $CD4^+$ Tconv cells. This finding comports with the requirement of exogenous myelin-derived antigens for EAE induction in WT mice, as immunization with adjuvant and pertussis

toxin alone fails to trigger neuroinflammation[297–299]. Once myelin-reactive CD4$^+$ Tconv cells are primed, however, they are capable of transferring disease to unimmunized animals, suggesting that persistent autoimmune responses can be enabled by a single occurrence of immune perturbation in the presence of sufficient antigen[300].

In contrast, several mouse models of spontaneous organ-specific autoimmunity feature TCRtg mice in which all T cells bear reactivity to an MHC-II restricted self-antigen[301–305]. Self-reactive TCRtg mice do not require immunization or infection for autoimmune organ infiltration to occur. Instead, as Treg cell development in TCRrg mice is limited due to intraclonal competition for Treg-inducing ligands[139], the increased CD4$^+$ Tconv cell to Treg cell (Th/Tr) ratio in these mice likely enables the activation and function of self-reactive CD4$^+$ Tconv cells. Thus, therapies that increase the Th/Tr ratio, such as ICB therapies for cancer patients, may favor the expansion of self-reactive CD4$^+$ Tconv cells that can mediate immune-related adverse events. Indeed, anti-CTLA-4 administration is associated with several autoimmune toxicities, presumably due to its ability to induce antibody-dependent cellular cytotoxicity among Treg cells, which constitutively express high levels of CTLA-4[306,307]. On the other hand, therapies that decrease the Th/Tr ratio, such as through transfer of autologous Treg cells, show remarkable potential for ameliorating active autoimmune disease[308].

Moreover, TCRtg models of spontaneous autoimmunity reveal that, in settings of Treg cell scarcity, self-reactive CD4$^+$ Tconv cells already have access to the antigens, co-stimulatory molecules, and cytokines needed to undergo priming. Given our observation that a subset of self-reactive CD4$^+$ Tconv cells adopts a Tfh-like phenotype, cytokines that promote Tfh cell differentiation – including IL-6[309] and IL-21[310] – must also be readily available to these cells at steady state. Where do these accessory signals come from? It is possible that sensing of commensal

microbes could generate innate signals that then prompt DC maturation, cytokine production, and presentation of self-antigens[311]. This point may be addressed by generating self-reactive TCRrg mice in germ-free conditions. Studying the fate of self-reactive $CD4^+$ Tconv cells in GF mice fed an elemental diet may also rule out inflammatory cues derived from dietary antigen intake[312]. Lastly, recognition of endogenous retroviruses (ERVs) by virus-specific $CD4^+$ Tconv and $CD8^+$ T cells may make cytokines and co-stimulation more readily accessible to self-reactive $CD4^+$ Tconv cells[313]. However, of the limited studies that focus on ERVs, one suggests that peptides derived from ERV gene products may, in some instances, act as self-antigens capable of prompting deletion of ERV-reactive thymocytes[314]. Much more work is required to implicate ERV expression in the subversion of immune tolerance and development of autoimmunity. Altogether, a deeper understanding of the factors causing inflammatory cytokine production in the absence of overt immune challenges should shed light on the resources self-reactive $CD4^+$ Tconv cells can access at steady state.

Unlike mice, humans predominantly live in a state of constant immune challenge, as demonstrated by the frequent opportunistic infections that manifest in immunodeficient patients. Given these observations and the appreciation of a strong environmental component to autoimmune etiology, several studies have sought to draw associations between microbial infections and the incidence of autoimmunity. Of note, Epstein-Barr virus (EBV) infections have been associated with the onset of MS, rheumatoid arthritis (RA), and systemic lupus erythematosus (SLE)[315]. For the latter two diseases, molecular mimicry has been suggested as a possible mechanism linking EBV infection and autoimmunity. Molecular mimicry entails the activation of autoreactive B and/or T cells through the recognition of foreign-derived antigens that exhibit extensive similarity to endogenous self-antigens[316]. However, self-reactive lymphocytes do not

always require contact with foreign antigens that resemble self. Other mechanisms by which microbial infections can promote activation of self-reactive $CD4^+$ Tconv cells include the secretion of superantigens that nonspecifically crosslink TCRs[317]; and epitope spreading, in which self-antigens become available to self-reactive $CD4^+$ Tconv cells due to their release from damaged tissues and/or their physical proximity to foreign antigens[318]. The relative contributions of these processes to autoimmune risk and pathogenesis likely vary based on the disease in question, the frequency and persistence of microbial infection, the expression patterns of targeted self-antigens, and the prevalence and sensitivity of $CD4^+$ Tconv cells reactive to the self-antigens involved. Intriguingly, infections may give rise to inflammatory signals, such as Type I IFNs, that may transiently inhibit Treg cell expansion or function[319]. This phenomenon could enable activation of self-reactive $CD4^+$ Tconv cells and initiation of autoimmune responses.

Conclusion

In summary, our work demonstrates both the existence of naturally occurring $CD4^+$ Tconv cell clones reactive to endogenous self-antigens, and the divergent strategies used by the immune system to regulate these cells. Clones reactive to TSAs are diverted into the tTreg cell lineage based on their sensitivity to antigen. However, lower-sensitivity TSA-reactive $CD4^+$ Tconv cells still display the ability to infiltrate non-lymphoid organs, particularly when antigen density, inflammatory cues, and their prevalence relative to Treg cells are increased. In contrast, clones reactive to more widespread self-antigens are recurrently shunted into a $Bcl6^{hi}$ $PD\text{-}1^{hi}$ $Eomes^+$ state. These “nTfh” cells exhibit minimal evidence of clonal deletion or Treg cell differentiation in either the thymus or the periphery, despite signs of overt self-reactivity. When released from Treg cell-mediated suppression, nTfh cells enter non-lymphoid organs and adopt a Th1 cell

program marked by the expression of IFN-γ. Taken together, these findings argue against a primary role for clonal deletion in maintaining immune homeostasis and stress the importance of dominant tolerance in the form of Treg cells. In future work, a robust characterization of additional autoreactive TCRs, along with the identification of self-antigens recognized by nTfh cells, will further elucidate the ways in which TCR:spMHC-II interactions govern the regulation of self-reactive $CD4^+$ Tconv cells. Moreover, our current and future findings hold implications for the design of cancer immunotherapies that balance antitumor efficacy with autoimmune toxicity.

Future Issues

1. To what extent does prostatic infiltration by C4-reactive $CD4^+$ Tconv cell clones correlate with TCR:C4/I-A^b affinity or $t_{1/2}$ of the TCR:C4/I-Ab interaction?
2. Would clones with varying sensitivities to C4/I-Ab exhibit similar degrees of prostatic infiltration following non-specific activation *in vitro*? Experiments in this vein would test whether sensitivity to antigen affects self-reactive $CD4^+$ Tconv cell function at the level of priming versus at the level of effector function.
3. Which mechanisms of peripheral T cell tolerance restrain higher-sensitivity C4-reactive $CD4^+$ Tconv cell clones in settings of Treg cell ablation? Would decreasing the availability of C4/I-Ab give these clones a competitive advantage over clones with lower sensitivity to C4/I-Ab?
4. Do C4-reactive Treg versus $CD4^+$ Tconv cell TCRs exert different outcomes with regards to differentiation into Th cell lineages and/or memory cells based on their sensitivity to antigen? Are recall responses similar between C4-reactive $CD4^+$ Tconv cells exhibiting differing antigen sensitivities?

5. What is the nature of the self-antigens recognized by the organ-infiltrating Group 1 and Group 3 $CD4^+$ Tconv cell clones?
6. Are Bcl6, PD-1, and Eomes – the markers used to identify nTfh cells – required for nTfh cell induction, maintenance, or function? Does Eomes impart a cytotoxic program in $CD4^+$ Tconv cells?
7. Do Tfh-like Group 3 cells potentiate or regulate B cell responses at steady state? In either case, what are the mechanisms by which Group 3 clones impact B cell homeostasis and/or function?
8. In which ways do B cells contribute to the differentiation, homeostasis, and function of nTfh cells? Are Group 3 TCRrg $CD4^+$ Tconv cells, or their polyclonal equivalent, affected by perturbations in B cell antigen presentation (such as in BCR transgenic mice or in mice lacking MHC-II on B cells)?
9. Can nTfh cells be specifically expanded or depleted in settings of autoimmunity or antitumor immunity? How would modulation of this self-reactive $CD4^+$ Tconv cell compartment impact the potency of self-directed immune responses?

REFERENCES

1. Delves, P. J. & Roitt, I. M. The immune system. First of two parts. *N. Engl. J. Med.* **343**, 37–49 (2000).

2. Zinkernagel, R. M. *et al.* On immunological memory. *Annu. Rev. Immunol.* **14**, 333–367 (1996).

3. O'Sullivan, T. E., Sun, J. C. & Lanier, L. L. Natural Killer Cell Memory. *Immunity* **43**, 634–645 (2015).

4. Netea, M. G. *et al.* Trained immunity: A program of innate immune memory in health and disease. *Science* **352**, aaf1098 (2016).

5. Soares, M. P., Teixeira, L. & Moita, L. F. Disease tolerance and immunity in host protection against infection. *Nat. Rev. Immunol.* **17**, 83–96 (2017).

6. Janeway, C. A., Goodnow, C. C. & Medzhitov, R. Danger - pathogen on the premises! Immunological tolerance. *Curr. Biol. CB* **6**, 519–522 (1996).

7. Boehm, T. Quality control in self/nonself discrimination. *Cell* **125**, 845–858 (2006).

8. Takeuchi, O. & Akira, S. Pattern recognition receptors and inflammation. *Cell* **140**, 805–820 (2010).

9. Mogensen, T. H. Pathogen recognition and inflammatory signaling in innate immune defenses. *Clin. Microbiol. Rev.* **22**, 240–273, Table of Contents (2009).

10. Hilligan, K. L. & Ronchese, F. Antigen presentation by dendritic cells and their instruction of CD4+ T helper cell responses. *Cell. Mol. Immunol.* **17**, 587–599 (2020).

11. Ardouin, L. *et al.* Broad and Largely Concordant Molecular Changes Characterize Tolerogenic and Immunogenic Dendritic Cell Maturation in Thymus and Periphery. *Immunity* **45**, 305–318 (2016).

12. Sasaki, A. Evolution of antigen drift/switching: continuously evading pathogens. *J. Theor. Biol.* **168**, 291–308 (1994).

13. Kärre, K., Ljunggren, H. G., Piontek, G. & Kiessling, R. Selective rejection of H-2-deficient lymphoma variants suggests alternative immune defence strategy. *Nature* **319**, 675–678 (1986).

14. Guevara-Patiño, J. A., Turk, M. J., Wolchok, J. D. & Houghton, A. N. Immunity to cancer through immune recognition of altered self: studies with melanoma. *Adv. Cancer Res.* **90**, 157–177 (2003).

15. Matzinger, P. The danger model: a renewed sense of self. *Science* **296**, 301–305 (2002).

16. Pradeu, T. & Cooper, E. L. The danger theory: 20 years later. *Front. Immunol.* **3**, 287 (2012).

17. Schuetz, C. *et al.* An immunodeficiency disease with RAG mutations and granulomas. *N. Engl. J. Med.* **358**, 2030–2038 (2008).

18. Niehues, T., Perez-Becker, R. & Schuetz, C. More than just SCID--the phenotypic range of combined immunodeficiencies associated with mutations in the recombinase activating genes (RAG) 1 and 2. *Clin. Immunol. Orlando Fla* **135**, 183–192 (2010).

19. Hogquist, K. A. & Jameson, S. C. The self-obsession of T cells: how TCR signaling thresholds affect fate 'decisions' and effector function. *Nat. Immunol.* **15**, 815–823 (2014).

20. McDonald, B. D., Bunker, J. J., Erickson, S. A., Oh-Hora, M. & Bendelac, A. Crossreactive αβ T Cell Receptors Are the Predominant Targets of Thymocyte Negative Selection. *Immunity* **43**, 859–869 (2015).

21. Xing, Y. & Hogquist, K. A. T-cell tolerance: central and peripheral. *Cold Spring Harb. Perspect. Biol.* **4**, a006957 (2012).

22. Nemazee, D. Mechanisms of central tolerance for B cells. *Nat. Rev. Immunol.* **17**, 281–294 (2017).

23. Tan, C., Noviski, M., Huizar, J. & Zikherman, J. Self-reactivity on a spectrum: A sliding scale of peripheral B cell tolerance. *Immunol. Rev.* **292**, 37–60 (2019).

24. Zinkernagel, R. M. & Doherty, P. C. Restriction of in vitro T cell-mediated cytotoxicity in lymphocytic choriomeningitis within a syngeneic or semiallogeneic system. *Nature* **248**, 701–702 (1974).

25. Roche, P. A. & Furuta, K. The ins and outs of MHC class II-mediated antigen processing and presentation. *Nat. Rev. Immunol.* **15**, 203–216 (2015).

26. Luckheeram, R. V., Zhou, R., Verma, A. D. & Xia, B. $CD4^+$T cells: differentiation and functions. *Clin. Dev. Immunol.* **2012**, 925135 (2012).

27. Godfrey, D. I., Uldrich, A. P., McCluskey, J., Rossjohn, J. & Moody, D. B. The burgeoning family of unconventional T cells. *Nat. Immunol.* **16**, 1114–1123 (2015).

28. Pellicci, D. G., Koay, H.-F. & Berzins, S. P. Thymic development of unconventional T cells: how NKT cells, MAIT cells and γδ T cells emerge. *Nat. Rev. Immunol.* **20**, 756–770 (2020).

29. Garcia, K. C. & Adams, E. J. How the T cell receptor sees antigen--a structural view. *Cell* **122**, 333–336 (2005).

30. Sim, B. C., Zerva, L., Greene, M. I. & Gascoigne, N. R. Control of MHC restriction by TCR Valpha CDR1 and CDR2. *Science* **273**, 963–966 (1996).

31. Chlewicki, L. K., Holler, P. D., Monti, B. C., Clutter, M. R. & Kranz, D. M. High-affinity, peptide-specific T cell receptors can be generated by mutations in CDR1, CDR2 or CDR3. *J. Mol. Biol.* **346**, 223–239 (2005).

32. Zareie, P. *et al.* Canonical T cell receptor docking on peptide-MHC is essential for T cell signaling. *Science* **372**, eabe9124 (2021).

33. Lin, J., Miller, M. J. & Shaw, A. S. The c-SMAC: sorting it all out (or in). *J. Cell Biol.* **170**, 177–182 (2005).

34. Artyomov, M. N., Lis, M., Devadas, S., Davis, M. M. & Chakraborty, A. K. CD4 and CD8 binding to MHC molecules primarily acts to enhance Lck delivery. *Proc. Natl. Acad. Sci. U. S. A.* **107**, 16916–16921 (2010).

35. Ehrlich, L. I. R., Ebert, P. J. R., Krummel, M. F., Weiss, A. & Davis, M. M. Dynamics of p56lck translocation to the T cell immunological synapse following agonist and antagonist stimulation. *Immunity* **17**, 809–822 (2002).

36. Wang, H. *et al.* ZAP-70: an essential kinase in T-cell signaling. *Cold Spring Harb. Perspect. Biol.* **2**, a002279 (2010).

37. Macian, F. NFAT proteins: key regulators of T-cell development and function. *Nat. Rev. Immunol.* **5**, 472–484 (2005).

38. Smith-Garvin, J. E., Koretzky, G. A. & Jordan, M. S. T cell activation. *Annu. Rev. Immunol.* **27**, 591–619 (2009).

39. Bretscher, P. A. A two-step, two-signal model for the primary activation of precursor helper T cells. *Proc. Natl. Acad. Sci. U. S. A.* **96**, 185–190 (1999).

40. Moon, J. J. *et al.* Naive CD4(+) T cell frequency varies for different epitopes and predicts repertoire diversity and response magnitude. *Immunity* **27**, 203–213 (2007).

41. Saravia, J., Chapman, N. M. & Chi, H. Helper T cell differentiation. *Cell. Mol. Immunol.* **16**, 634–643 (2019).

42. Hirahara, K. & Nakayama, T. CD4 + T-cell subsets in inflammatory diseases: beyond the T h 1/T h 2 paradigm. *Int. Immunol.* **28**, 163–171 (2016).

43. Pepper, M. & Jenkins, M. K. Origins of CD4(+) effector and central memory T cells. *Nat. Immunol.* **12**, 467–471 (2011).

44. Werlen, G., Hausmann, B., Naeher, D. & Palmer, E. Signaling life and death in the thymus: timing is everything. *Science* **299**, 1859–1863 (2003).

45. Takahama, Y. Journey through the thymus: stromal guides for T-cell development and selection. *Nat. Rev. Immunol.* **6**, 127–135 (2006).

46. Bassing, C. H., Swat, W. & Alt, F. W. The mechanism and regulation of chromosomal V(D)J recombination. *Cell* **109 Suppl**, S45-55 (2002).

47. Shlyakhtenko, L. S. *et al.* Molecular mechanism underlying RAG1/RAG2 synaptic complex formation. *J. Biol. Chem.* **284**, 20956–20965 (2009).

48. Michie, A. M. & Zúñiga-Pflücker, J. C. Regulation of thymocyte differentiation: pre-TCR signals and beta-selection. *Semin. Immunol.* **14**, 311–323 (2002).

49. Klein, L., Kyewski, B., Allen, P. M. & Hogquist, K. A. Positive and negative selection of the T cell repertoire: what thymocytes see (and don't see). *Nat. Rev. Immunol.* **14**, 377–391 (2014).

50. Singer, A., Adoro, S. & Park, J.-H. Lineage fate and intense debate: myths, models and mechanisms of CD4- versus CD8-lineage choice. *Nat. Rev. Immunol.* **8**, 788–801 (2008).

51. Schatz, D. G., Oettinger, M. A. & Schlissel, M. S. V(D)J recombination: molecular biology and regulation. *Annu. Rev. Immunol.* **10**, 359–383 (1992).

52. Honey, K., Nakagawa, T., Peters, C. & Rudensky, A. Cathepsin L regulates CD4+ T cell selection independently of its effect on invariant chain: a role in the generation of positively selecting peptide ligands. *J. Exp. Med.* **195**, 1349–1358 (2002).

53. Gommeaux, J. *et al.* Thymus-specific serine protease regulates positive selection of a subset of CD4+ thymocytes. *Eur. J. Immunol.* **39**, 956–964 (2009).

54. Bouillet, P. *et al.* Proapoptotic Bcl-2 relative Bim required for certain apoptotic responses, leukocyte homeostasis, and to preclude autoimmunity. *Science* **286**, 1735–1738 (1999).

55. Gray, D. H. D. *et al.* The BH3-only proteins Bim and Puma cooperate to impose deletional tolerance of organ-specific antigens. *Immunity* **37**, 451–462 (2012).

56. Vignali, D. A. A., Collison, L. W. & Workman, C. J. How regulatory T cells work. *Nat. Rev. Immunol.* **8**, 523–532 (2008).

57. Li, J., Tan, J., Martino, M. M. & Lui, K. O. Regulatory T-Cells: Potential Regulator of Tissue Repair and Regeneration. *Front. Immunol.* **9**, 585 (2018).

58. Lio, C.-W. J. & Hsieh, C.-S. A two-step process for thymic regulatory T cell development. *Immunity* **28**, 100–111 (2008).

59. Liston, A. *et al.* Differentiation of regulatory Foxp3+ T cells in the thymic cortex. *Proc. Natl. Acad. Sci. U. S. A.* **105**, 11903–11908 (2008).

60. Owen, D. L. *et al.* Thymic regulatory T cells arise via two distinct developmental programs. *Nat. Immunol.* **20**, 195–205 (2019).

61. Anderson, M. S. & Su, M. A. AIRE expands: new roles in immune tolerance and beyond. *Nat. Rev. Immunol.* **16**, 247–258 (2016).

62. Metzger, T. C. & Anderson, M. S. Control of central and peripheral tolerance by Aire. *Immunol. Rev.* **241**, 89–103 (2011).

63. Guerau-de-Arellano, M., Martinic, M., Benoist, C. & Mathis, D. Neonatal tolerance revisited: a perinatal window for Aire control of autoimmunity. *J. Exp. Med.* **206**, 1245–1252 (2009).

64. Taniguchi, R. T. *et al.* Detection of an autoreactive T-cell population within the polyclonal repertoire that undergoes distinct autoimmune regulator (Aire)-mediated selection. *Proc. Natl. Acad. Sci. U. S. A.* **109**, 7847–7852 (2012).

65. Malchow, S. *et al.* Aire Enforces Immune Tolerance by Directing Autoreactive T Cells into the Regulatory T Cell Lineage. *Immunity* **44**, 1102–1113 (2016).

66. Klein, L., Robey, E. A. & Hsieh, C.-S. Central CD4+ T cell tolerance: deletion versus regulatory T cell differentiation. *Nat. Rev. Immunol.* **19**, 7–18 (2019).

67. Koble, C. & Kyewski, B. The thymic medulla: a unique microenvironment for intercellular self-antigen transfer. *J. Exp. Med.* **206**, 1505–1513 (2009).

68. Leventhal, D. S. *et al.* Dendritic Cells Coordinate the Development and Homeostasis of Organ-Specific Regulatory T Cells. *Immunity* **44**, 847–859 (2016).

69. Perera, J., Meng, L., Meng, F. & Huang, H. Autoreactive thymic B cells are efficient antigen-presenting cells of cognate self-antigens for T cell negative selection. *Proc. Natl. Acad. Sci. U. S. A.* **110**, 17011–17016 (2013).

70. Breed, E. R. *et al.* Type 2 cytokines in the thymus activate Sirpα+ dendritic cells to promote clonal deletion. *Nat. Immunol.* **23**, 1042–1051 (2022).

71. Anderson, M. S. *et al.* The cellular mechanism of Aire control of T cell tolerance. *Immunity* **23**, 227–239 (2005).

72. Kieback, E. *et al.* Thymus-Derived Regulatory T Cells Are Positively Selected on Natural Self-Antigen through Cognate Interactions of High Functional Avidity. *Immunity* **44**, 1114–1126 (2016).

73. Cebula, A. *et al.* Dormant pathogenic CD4+ T cells are prevalent in the peripheral repertoire of healthy mice. *Nat. Commun.* **10**, 4882 (2019).

74. Danke, N. A., Koelle, D. M., Yee, C., Beheray, S. & Kwok, W. W. Autoreactive T cells in healthy individuals. *J. Immunol. Baltim. Md 1950* **172**, 5967–5972 (2004).

75. Maeda, Y. *et al.* Detection of self-reactive $CD8^+$ T cells with an anergic phenotype in healthy individuals. *Science* **346**, 1536–1540 (2014).

76. Yu, W. *et al.* Clonal Deletion Prunes but Does Not Eliminate Self-Specific αβ CD8(+) T Lymphocytes. *Immunity* **42**, 929–941 (2015).

77. Bluestone, J. A. Mechanisms of tolerance. *Immunol. Rev.* **241**, 5–19 (2011).

78. Hammer, G. E. & Ma, A. Molecular control of steady-state dendritic cell maturation and immune homeostasis. *Annu. Rev. Immunol.* **31**, 743–791 (2013).

79. Tang, Q. *et al.* CD28/B7 regulation of anti-CD3-mediated immunosuppression in vivo. *J. Immunol. Baltim. Md 1950* **170**, 1510–1516 (2003).

80. Schwartz, R. H. T cell anergy. *Annu. Rev. Immunol.* **21**, 305–334 (2003).

81. Hirsch, R., Eckhaus, M., Auchincloss, H., Sachs, D. H. & Bluestone, J. A. Effects of in vivo administration of anti-T3 monoclonal antibody on T cell function in mice. I. Immunosuppression of transplantation responses. *J. Immunol. Baltim. Md 1950* **140**, 3766–3772 (1988).

82. Hirsch, R., Gress, R. E., Pluznik, D. H., Eckhaus, M. & Bluestone, J. A. Effects of in vivo administration of anti-CD3 monoclonal antibody on T cell function in mice. II. In vivo activation of T cells. *J. Immunol. Baltim. Md 1950* **142**, 737–743 (1989).

83. Pape, K. A., Merica, R., Mondino, A., Khoruts, A. & Jenkins, M. K. Direct evidence that functionally impaired CD4+ T cells persist in vivo following induction of peripheral tolerance. *J. Immunol. Baltim. Md 1950* **160**, 4719–4729 (1998).

84. Fathman, C. G. & Lineberry, N. B. Molecular mechanisms of CD4+ T-cell anergy. *Nat. Rev. Immunol.* **7**, 599–609 (2007).

85. Steinman, R. M., Hawiger, D. & Nussenzweig, M. C. Tolerogenic dendritic cells. *Annu. Rev. Immunol.* **21**, 685–711 (2003).

86. Yadav, M., Stephan, S. & Bluestone, J. A. Peripherally induced tregs - role in immune homeostasis and autoimmunity. *Front. Immunol.* **4**, 232 (2013).

87. Lathrop, S. K. *et al.* Peripheral education of the immune system by colonic commensal microbiota. *Nature* **478**, 250–254 (2011).

88. Kim, K. S. *et al.* Dietary antigens limit mucosal immunity by inducing regulatory T cells in the small intestine. *Science* **351**, 858–863 (2016).

89. Yi, J. *et al.* Unregulated antigen-presenting cell activation by T cells breaks self tolerance. *Proc. Natl. Acad. Sci. U. S. A.* **116**, 1007–1016 (2019).

90. Samstein, R. M., Josefowicz, S. Z., Arvey, A., Treuting, P. M. & Rudensky, A. Y. Extrathymic generation of regulatory T cells in placental mammals mitigates maternal-fetal conflict. *Cell* **150**, 29–38 (2012).

91. van der Veeken, J. *et al.* Genetic tracing reveals transcription factor Foxp3-dependent and Foxp3-independent functionality of peripherally induced Treg cells. *Immunity* **55**, 1173-1184.e7 (2022).

92. Torgerson, T. R. & Ochs, H. D. Immune dysregulation, polyendocrinopathy, enteropathy, X-linked: forkhead box protein 3 mutations and lack of regulatory T cells. *J. Allergy Clin. Immunol.* **120**, 744–750; quiz 751–752 (2007).

93. Kim, J. M., Rasmussen, J. P. & Rudensky, A. Y. Regulatory T cells prevent catastrophic autoimmunity throughout the lifespan of mice. *Nat. Immunol.* **8**, 191–197 (2007).

94. Chinen, T. *et al.* An essential role for the IL-2 receptor in Treg cell function. *Nat. Immunol.* **17**, 1322–1333 (2016).

95. Wing, K. *et al.* CTLA-4 control over Foxp3+ regulatory T cell function. *Science* **322**, 271–275 (2008).

96. Chaudhry, A. *et al.* Interleukin-10 signaling in regulatory T cells is required for suppression of Th17 cell-mediated inflammation. *Immunity* **34**, 566–578 (2011).

97. Sakaguchi, S., Yamaguchi, T., Nomura, T. & Ono, M. Regulatory T cells and immune tolerance. *Cell* **133**, 775–787 (2008).

98. Josefowicz, S. Z., Lu, L.-F. & Rudensky, A. Y. Regulatory T cells: mechanisms of differentiation and function. *Annu. Rev. Immunol.* **30**, 531–564 (2012).

99. Levine, A. G., Arvey, A., Jin, W. & Rudensky, A. Y. Continuous requirement for the TCR in regulatory T cell function. *Nat. Immunol.* **15**, 1070–1078 (2014).

100. Vahl, J. C. *et al.* Continuous T cell receptor signals maintain a functional regulatory T cell pool. *Immunity* **41**, 722–736 (2014).

101. Schmidt, A. M. *et al.* Regulatory T cells require TCR signaling for their suppressive function. *J. Immunol. Baltim. Md 1950* **194**, 4362–4370 (2015).

102. Sullivan, J. M., Höllbacher, B. & Campbell, D. J. Cutting Edge: Dynamic Expression of Id3 Defines the Stepwise Differentiation of Tissue-Resident Regulatory T Cells. *J. Immunol. Baltim. Md 1950* **202**, 31–36 (2019).

103. Perry, J. A. *et al.* PD-L1-PD-1 interactions limit effector regulatory T cell populations at homeostasis and during infection. *Nat. Immunol.* **23**, 743–756 (2022).

104. Moran, A. E. *et al.* T cell receptor signal strength in Treg and iNKT cell development demonstrated by a novel fluorescent reporter mouse. *J. Exp. Med.* **208**, 1279–1289 (2011).

105. Zemmour, D. *et al.* Single-cell gene expression reveals a landscape of regulatory T cell phenotypes shaped by the TCR. *Nat. Immunol.* **19**, 291–301 (2018).

106. Onishi, Y., Fehervari, Z., Yamaguchi, T. & Sakaguchi, S. Foxp3+ natural regulatory T cells preferentially form aggregates on dendritic cells in vitro and actively inhibit their maturation. *Proc. Natl. Acad. Sci. U. S. A.* **105**, 10113–10118 (2008).

107. Tekguc, M., Wing, J. B., Osaki, M., Long, J. & Sakaguchi, S. Treg-expressed CTLA-4 depletes CD80/CD86 by trogocytosis, releasing free PD-L1 on antigen-presenting cells. *Proc. Natl. Acad. Sci. U. S. A.* **118**, e2023739118 (2021).

108. Sojka, D. K., Huang, Y.-H. & Fowell, D. J. Mechanisms of regulatory T-cell suppression - a diverse arsenal for a moving target. *Immunology* **124**, 13–22 (2008).

109. Kedl, R. M. *et al.* T cells compete for access to antigen-bearing antigen-presenting cells. *J. Exp. Med.* **192**, 1105–1113 (2000).

110. Akkaya, B. *et al.* Regulatory T cells mediate specific suppression by depleting peptide-MHC class II from dendritic cells. *Nat. Immunol.* **20**, 218–231 (2019).

111. Campillo-Davo, D., Flumens, D. & Lion, E. The Quest for the Best: How TCR Affinity, Avidity, and Functional Avidity Affect TCR-Engineered T-Cell Antitumor Responses. *Cells* **9**, E1720 (2020).

112. Altman, J. D. *et al.* Phenotypic analysis of antigen-specific T lymphocytes. *Science* **274**, 94–96 (1996).

113. Boniface, J. J. *et al.* Initiation of signal transduction through the T cell receptor requires the multivalent engagement of peptide/MHC ligands [corrected]. *Immunity* **9**, 459–466 (1998).

114. Choi, H.-K. *et al. Catch bond models explain how force amplifies TCR signaling and antigen discrimination*. http://biorxiv.org/lookup/doi/10.1101/2022.01.17.476694 (2022) doi:10.1101/2022.01.17.476694.

115. Stone, J. D., Chervin, A. S. & Kranz, D. M. T-cell receptor binding affinities and kinetics: impact on T-cell activity and specificity. *Immunology* **126**, 165–176 (2009).

116. Huang, J. *et al.* The kinetics of two-dimensional TCR and pMHC interactions determine T-cell responsiveness. *Nature* **464**, 932–936 (2010).

117. Rosette, C. *et al.* The impact of duration versus extent of TCR occupancy on T cell activation: a revision of the kinetic proofreading model. *Immunity* **15**, 59–70 (2001).

118. Wooldridge, L. *et al.* Tricks with tetramers: how to get the most from multimeric peptide-MHC. *Immunology* **126**, 147–164 (2009).

119. Andargachew, R., Martinez, R. J., Kolawole, E. M. & Evavold, B. D. CD4 T Cell Affinity Diversity Is Equally Maintained during Acute and Chronic Infection. *J. Immunol. Baltim. Md 1950* **201**, 19–30 (2018).

120. Sabatino, J. J., Huang, J., Zhu, C. & Evavold, B. D. High prevalence of low affinity peptide-MHC II tetramer-negative effectors during polyclonal CD4+ T cell responses. *J. Exp. Med.* **208**, 81–90 (2011).

121. Martinez, R. J., Andargachew, R., Martinez, H. A. & Evavold, B. D. Low-affinity CD4+ T cells are major responders in the primary immune response. *Nat. Commun.* **7**, 13848 (2016).

122. Cho, Y.-L. *et al.* TCR Signal Quality Modulates Fate Decisions of Single CD4+ T Cells in a Probabilistic Manner. *Cell Rep.* **20**, 806–818 (2017).

123. Herman, S. *et al.* Regulatory T cells form stable and long-lasting cell cluster with myeloid dendritic cells (DC). *Int. Immunol.* **24**, 417–426 (2012).

124. Klann, J. E. *et al.* Integrin Activation Controls Regulatory T Cell-Mediated Peripheral Tolerance. *J. Immunol. Baltim. Md 1950* **200**, 4012–4023 (2018).

125. Chen, J. *et al.* Strong adhesion by regulatory T cells induces dendritic cell cytoskeletal polarization and contact-dependent lethargy. *J. Exp. Med.* **214**, 327–338 (2017).

126. Muthuswamy, R. *et al.* Ability of mature dendritic cells to interact with regulatory T cells is imprinted during maturation. *Cancer Res.* **68**, 5972–5978 (2008).

127. Skokos, D. *et al.* Peptide-MHC potency governs dynamic interactions between T cells and dendritic cells in lymph nodes. *Nat. Immunol.* **8**, 835–844 (2007).

128. Kumar, R. *et al.* Increased sensitivity of antigen-experienced T cells through the enrichment of oligomeric T cell receptor complexes. *Immunity* **35**, 375–387 (2011).

129. Stefanová, I., Dorfman, J. R. & Germain, R. N. Self-recognition promotes the foreign antigen sensitivity of naive T lymphocytes. *Nature* **420**, 429–434 (2002).

130. Hochweller, K. *et al.* Dendritic cells control T cell tonic signaling required for responsiveness to foreign antigen. *Proc. Natl. Acad. Sci. U. S. A.* **107**, 5931–5936 (2010).

131. Persaud, S. P., Parker, C. R., Lo, W.-L., Weber, K. S. & Allen, P. M. Intrinsic CD4+ T cell sensitivity and response to a pathogen are set and sustained by avidity for thymic and peripheral complexes of self peptide and MHC. *Nat. Immunol.* **15**, 266–274 (2014).

132. Hsieh, C.-S. *et al.* Recognition of the peripheral self by naturally arising CD25+ CD4+ T cell receptors. *Immunity* **21**, 267–277 (2004).

133. Hsieh, C.-S., Zheng, Y., Liang, Y., Fontenot, J. D. & Rudensky, A. Y. An intersection between the self-reactive regulatory and nonregulatory T cell receptor repertoires. *Nat. Immunol.* **7**, 401–410 (2006).

134. Jordan, M. S., Riley, M. P., von Boehmer, H. & Caton, A. J. Anergy and suppression regulate CD4(+) T cell responses to a self peptide. *Eur. J. Immunol.* **30**, 136–144 (2000).

135. Jordan, M. S. *et al.* Thymic selection of CD4+CD25+ regulatory T cells induced by an agonist self-peptide. *Nat. Immunol.* **2**, 301–306 (2001).

136. Lee, H.-M., Bautista, J. L., Scott-Browne, J., Mohan, J. F. & Hsieh, C.-S. A broad range of self-reactivity drives thymic regulatory T cell selection to limit responses to self. *Immunity* **37**, 475–486 (2012).

137. Stadinski, B. D. *et al.* A temporal thymic selection switch and ligand binding kinetics constrain neonatal Foxp3+ Treg cell development. *Nat. Immunol.* **20**, 1046–1058 (2019).

138. Stritesky, G. L. *et al.* Murine thymic selection quantified using a unique method to capture deleted T cells. *Proc. Natl. Acad. Sci.* (2013) doi:10.1073/pnas.1217532110.

139. Bautista, J. L. *et al.* Intraclonal competition limits the fate determination of regulatory T cells in the thymus. *Nat. Immunol.* **10**, 610–617 (2009).

140. Leonard, J. D. *et al.* Identification of Natural Regulatory T Cell Epitopes Reveals Convergence on a Dominant Autoantigen. *Immunity* **47**, 107-117.e8 (2017).

141. Klawon, D. E. J. *et al.* Altered selection on a single self-ligand promotes susceptibility to organ-specific T cell infiltration. *J. Exp. Med.* **218**, e20200701 (2021).

142. Sloan-Lancaster, J. & Allen, P. M. Altered peptide ligand-induced partial T cell activation: molecular mechanisms and role in T cell biology. *Annu. Rev. Immunol.* **14**, 1–27 (1996).

143. Rogers, P. R., Grey, H. M. & Croft, M. Modulation of naive CD4 T cell activation with altered peptide ligands: the nature of the peptide and presentation in the context of costimulation are critical for a sustained response. *J. Immunol. Baltim. Md 1950* **160**, 3698–3704 (1998).

144. Corse, E., Gottschalk, R. A., Krogsgaard, M. & Allison, J. P. Attenuated T cell responses to a high-potency ligand in vivo. *PLoS Biol.* **8**, e1000481 (2010).

145. Jones, M. C. *et al. Peptide Avidity for TCR on CD4 Effectors Determines the Extent of Memory Generation*. http://biorxiv.org/lookup/doi/10.1101/2022.05.09.491158 (2022) doi:10.1101/2022.05.09.491158.

146. Zehn, D., Lee, S. Y. & Bevan, M. J. Complete but curtailed T-cell response to very low-affinity antigen. *Nature* **458**, 211–214 (2009).

147. Johanns, T. M. *et al.* Naturally occurring altered peptide ligands control Salmonella-specific CD4+ T cell proliferation, IFN-gamma production, and protective potency. *J. Immunol. Baltim. Md 1950* **184**, 869–876 (2010).

148. Shakiba, M. *et al.* TCR signal strength defines distinct mechanisms of T cell dysfunction and cancer evasion. *J. Exp. Med.* **219**, e20201966 (2022).

149. Gallegos, A. M. *et al.* Control of T cell antigen reactivity via programmed TCR downregulation. *Nat. Immunol.* **17**, 379–386 (2016).

150. Mallone, R. *et al.* Functional avidity directs T-cell fate in autoreactive CD4+ T cells. *Blood* **106**, 2798–2805 (2005).

151. Bettini, M. *et al.* TCR affinity and tolerance mechanisms converge to shape T cell diabetogenic potential. *J. Immunol. Baltim. Md 1950* **193**, 571–579 (2014).

152. Busch, D. H. & Pamer, E. G. T cell affinity maturation by selective expansion during infection. *J. Exp. Med.* **189**, 701–710 (1999).

153. Williams, M. A., Ravkov, E. V. & Bevan, M. J. Rapid culling of the CD4+ T cell repertoire in the transition from effector to memory. *Immunity* **28**, 533–545 (2008).

154. Amrani, A. *et al.* Progression of autoimmune diabetes driven by avidity maturation of a T-cell population. *Nature* **406**, 739–742 (2000).

155. Savage, P. A., Boniface, J. J. & Davis, M. M. A kinetic basis for T cell receptor repertoire selection during an immune response. *Immunity* **10**, 485–492 (1999).

156. Tao, X., Constant, S., Jorritsma, P. & Bottomly, K. Strength of TCR signal determines the costimulatory requirements for Th1 and Th2 CD4+ T cell differentiation. *J. Immunol. Baltim. Md 1950* **159**, 5956–5963 (1997).

157. Rogers, P. R. & Croft, M. Peptide dose, affinity, and time of differentiation can contribute to the Th1/Th2 cytokine balance. *J. Immunol. Baltim. Md 1950* **163**, 1205–1213 (1999).

158. Brogdon, J. L., Leitenberg, D. & Bottomly, K. The potency of TCR signaling differentially regulates NFATc/p activity and early IL-4 transcription in naive CD4+ T cells. *J. Immunol. Baltim. Md 1950* **168**, 3825–3832 (2002).

159. Shiner, E. K., Holbrook, B. C. & Alexander-Miller, M. A. CD4+ T cell subset differentiation and avidity setpoint are dictated by the interplay of cytokine and antigen mediated signals. *PloS One* **9**, e100175 (2014).

160. van Panhuys, N., Klauschen, F. & Germain, R. N. T-cell-receptor-dependent signal intensity dominantly controls CD4(+) T cell polarization In Vivo. *Immunity* **41**, 63–74 (2014).

161. Gomez-Rodriguez, J. *et al.* Itk-mediated integration of T cell receptor and cytokine signaling regulates the balance between Th17 and regulatory T cells. *J. Exp. Med.* **211**, 529–543 (2014).

162. Purvis, H. A. *et al.* Low-strength T-cell activation promotes Th17 responses. *Blood* **116**, 4829–4837 (2010).

163. DiToro, D. *et al.* Differential IL-2 expression defines developmental fates of follicular versus nonfollicular helper T cells. *Science* **361**, eaao2933 (2018).

164. Fazilleau, N., McHeyzer-Williams, L. J., Rosen, H. & McHeyzer-Williams, M. G. The function of follicular helper T cells is regulated by the strength of T cell antigen receptor binding. *Nat. Immunol.* **10**, 375–384 (2009).

165. Kotov, D. I. *et al.* TCR Affinity Biases Th Cell Differentiation by Regulating CD25, Eef1e1, and Gbp2. *J. Immunol. Baltim. Md 1950* **202**, 2535–2545 (2019).

166. Johnston, R. J., Choi, Y. S., Diamond, J. A., Yang, J. A. & Crotty, S. STAT5 is a potent negative regulator of TFH cell differentiation. *J. Exp. Med.* **209**, 243–250 (2012).

167. Nurieva, R. I. *et al.* STAT5 protein negatively regulates T follicular helper (Tfh) cell generation and function. *J. Biol. Chem.* **287**, 11234–11239 (2012).

168. Keck, S. *et al.* Antigen affinity and antigen dose exert distinct influences on CD4 T-cell differentiation. *Proc. Natl. Acad. Sci. U. S. A.* **111**, 14852–14857 (2014).

169. Crotty, S. T Follicular Helper Cell Biology: A Decade of Discovery and Diseases. *Immunity* **50**, 1132–1148 (2019).

170. Schulz, O. *et al.* CD40 triggering of heterodimeric IL-12 p70 production by dendritic cells in vivo requires a microbial priming signal. *Immunity* **13**, 453–462 (2000).

171. Roco, J. A. *et al.* Class-Switch Recombination Occurs Infrequently in Germinal Centers. *Immunity* **51**, 337-350.e7 (2019).

172. Stebegg, M. *et al.* Regulation of the Germinal Center Response. *Front. Immunol.* **9**, 2469 (2018).

173. Jaiswal, A. I., Dubey, C., Swain, S. L. & Croft, M. Regulation of CD40 ligand expression on naive CD4 T cells: a role for TCR but not co-stimulatory signals. *Int. Immunol.* **8**, 275–285 (1996).

174. Ruedl, C., Bachmann, M. F. & Kopf, M. The antigen dose determines T helper subset development by regulation of CD40 ligand. *Eur. J. Immunol.* **30**, 2056–2064 (2000).

175. Ren, H. M. *et al.* IL-21 from high-affinity CD4 T cells drives differentiation of brain-resident CD8 T cells during persistent viral infection. *Sci. Immunol.* **5**, eabb5590 (2020).

176. Victora, G. D. & Nussenzweig, M. C. Germinal centers. *Annu. Rev. Immunol.* **30**, 429–457 (2012).

177. Chan, T. D. *et al.* Antigen affinity controls rapid T-dependent antibody production by driving the expansion rather than the differentiation or extrafollicular migration of early plasmablasts. *J. Immunol. Baltim. Md 1950* **183**, 3139–3149 (2009).

178. De Silva, N. S. & Klein, U. Dynamics of B cells in germinal centres. *Nat. Rev. Immunol.* **15**, 137–148 (2015).

179. Merkenschlager, J. *et al.* Dynamic regulation of TFH selection during the germinal centre reaction. *Nature* **591**, 458–463 (2021).

180. Wang, P., Shih, C.-M., Qi, H. & Lan, Y.-H. A Stochastic Model of the Germinal Center Integrating Local Antigen Competition, Individualistic T-B Interactions, and B Cell Receptor Signaling. *J. Immunol. Baltim. Md 1950* **197**, 1169–1182 (2016).

181. Rahman, A. & Isenberg, D. A. Systemic Lupus Erythematosus. *N. Engl. J. Med.* **358**, 929–939 (2008).

182. Linterman, M. A. *et al.* Follicular helper T cells are required for systemic autoimmunity. *J. Exp. Med.* **206**, 561–576 (2009).

183. Lee, S. K. *et al.* Interferon-γ excess leads to pathogenic accumulation of follicular helper T cells and germinal centers. *Immunity* **37**, 880–892 (2012).

184. Calvani, N., Richards, H. B., Tucci, M., Pannarale, G. & Silvestris, F. Up-regulation of IL-18 and predominance of a Th1 immune response is a hallmark of lupus nephritis. *Clin. Exp. Immunol.* **138**, 171–178 (2004).

185. Tucci, M., Lombardi, L., Richards, H. B., Dammacco, F. & Silvestris, F. Overexpression of interleukin-12 and T helper 1 predominance in lupus nephritis. *Clin. Exp. Immunol.* **154**, 247–254 (2008).

186. Fossati-Jimack, L. *et al.* Markedly different pathogenicity of four immunoglobulin G isotype-switch variants of an antierythrocyte autoantibody is based on their capacity to interact in vivo with the low-affinity Fcgamma receptor III. *J. Exp. Med.* **191**, 1293–1302 (2000).

187. Peng, S. L., Szabo, S. J. & Glimcher, L. H. T-bet regulates IgG class switching and pathogenic autoantibody production. *Proc. Natl. Acad. Sci. U. S. A.* **99**, 5545–5550 (2002).

188. Xia, Y. *et al.* The constant region contributes to the antigenic specificity and renal pathogenicity of murine anti-DNA antibodies. *J. Autoimmun.* **39**, 398–411 (2012).

189. Kenefeck, R. *et al.* Follicular helper T cell signature in type 1 diabetes. *J. Clin. Invest.* **125**, 292–303 (2015).

190. Walker, L. S. K. & von Herrath, M. CD4 T cell differentiation in type 1 diabetes. *Clin. Exp. Immunol.* **183**, 16–29 (2016).

191. Quinn, J. L. & Axtell, R. C. Emerging Role of Follicular T Helper Cells in Multiple Sclerosis and Experimental Autoimmune Encephalomyelitis. *Int. J. Mol. Sci.* **19**, E3233 (2018).

192. Walker, L. S. K. The link between circulating follicular helper T cells and autoimmunity. *Nat. Rev. Immunol.* (2022) doi:10.1038/s41577-022-00693-5.

193. Li, T., Wu, B., Yang, T., Zhang, L. & Jin, K. The outstanding antitumor capacity of CD4+ T helper lymphocytes. *Biochim. Biophys. Acta Rev. Cancer* **1874**, 188439 (2020).

194. Tran, E. *et al.* Cancer immunotherapy based on mutation-specific CD4+ T cells in a patient with epithelial cancer. *Science* **344**, 641–645 (2014).

195. Wei, S. C. *et al.* Distinct Cellular Mechanisms Underlie Anti-CTLA-4 and Anti-PD-1 Checkpoint Blockade. *Cell* **170**, 1120-1133.e17 (2017).

196. Wei, S. C. *et al.* Combination anti-CTLA-4 plus anti-PD-1 checkpoint blockade utilizes cellular mechanisms partially distinct from monotherapies. *Proc. Natl. Acad. Sci. U. S. A.* **116**, 22699–22709 (2019).

197. Schumacher, T. N. & Thommen, D. S. Tertiary lymphoid structures in cancer. *Science* **375**, eabf9419 (2022).

198. Sautès-Fridman, C., Petitprez, F., Calderaro, J. & Fridman, W. H. Tertiary lymphoid structures in the era of cancer immunotherapy. *Nat. Rev. Cancer* **19**, 307–325 (2019).

199. Cicalese, M. P., Salek-Ardakani, S. & Fousteri, G. Editorial: Follicular Helper T Cells in Immunity and Autoimmunity. *Front. Immunol.* **11**, 1042 (2020).

200. Cui, C. *et al.* Neoantigen-driven B cell and CD4 T follicular helper cell collaboration promotes anti-tumor CD8 T cell responses. *Cell* **184**, 6101-6118.e13 (2021).

201. Moroz, A. *et al.* IL-21 enhances and sustains CD8+ T cell responses to achieve durable tumor immunity: comparative evaluation of IL-2, IL-15, and IL-21. *J. Immunol. Baltim. Md 1950* **173**, 900–909 (2004).

202. Zander, R. *et al.* CD4+ T Cell Help Is Required for the Formation of a Cytolytic CD8+ T Cell Subset that Protects against Chronic Infection and Cancer. *Immunity* **51**, 1028-1042.e4 (2019).

203. Li, Y. *et al.* Targeting IL-21 to tumor-reactive T cells enhances memory T cell responses and anti-PD-1 antibody therapy. *Nat. Commun.* **12**, 951 (2021).

204. Overacre-Delgoffe, A. E. *et al.* Microbiota-specific T follicular helper cells drive tertiary lymphoid structures and anti-tumor immunity against colorectal cancer. *Immunity* **54**, 2812-2824.e4 (2021).

205. Chaurio, R. A. *et al.* TGF-β-mediated silencing of genomic organizer SATB1 promotes Tfh cell differentiation and formation of intra-tumoral tertiary lymphoid structures. *Immunity* **55**, 115-128.e9 (2022).

206. Gubin, M. M. *et al.* Checkpoint blockade cancer immunotherapy targets tumour-specific mutant antigens. *Nature* **515**, 577–581 (2014).

207. Sahin, U. *et al.* Personalized RNA mutanome vaccines mobilize poly-specific therapeutic immunity against cancer. *Nature* **547**, 222–226 (2017).

208. Yarchoan, M., Johnson, B. A., Lutz, E. R., Laheru, D. A. & Jaffee, E. M. Targeting neoantigens to augment antitumour immunity. *Nat. Rev. Cancer* **17**, 209–222 (2017).

209. Li, S. *et al.* Characterization of neoantigen-specific T cells in cancer resistant to immune checkpoint therapies. *Proc. Natl. Acad. Sci. U. S. A.* **118**, e2025570118 (2021).

210. Tay, R. E., Richardson, E. K. & Toh, H. C. Revisiting the role of CD4+ T cells in cancer immunotherapy-new insights into old paradigms. *Cancer Gene Ther.* **28**, 5–17 (2021).

211. Schreiber, R. D., Old, L. J. & Smyth, M. J. Cancer immunoediting: integrating immunity's roles in cancer suppression and promotion. *Science* **331**, 1565–1570 (2011).

212. O'Donnell, J. S., Teng, M. W. L. & Smyth, M. J. Cancer immunoediting and resistance to T cell-based immunotherapy. *Nat. Rev. Clin. Oncol.* **16**, 151–167 (2019).

213. Chao, J. L. *et al.* Effector T cell responses unleashed by regulatory T cell ablation exacerbate oral squamous cell carcinoma. *Cell Rep. Med.* **2**, 100399 (2021).

214. Dash, P. *et al.* Paired analysis of TCRα and TCRβ chains at the single-cell level in mice. *J. Clin. Invest.* **121**, 288–295 (2011).

215. Koike, N., Pilon-Thomas, S. & Mulé, J. J. Nonmyeloablative chemotherapy followed by T-cell adoptive transfer and dendritic cell-based vaccination results in rejection of established melanoma. *J. Immunother. Hagerstown Md 1997* **31**, 402–412 (2008).

216. Yan, L. *et al.* Selected prfA* mutations in recombinant attenuated Listeria monocytogenes strains augment expression of foreign immunogens and enhance vaccine-elicited humoral and cellular immune responses. *Infect. Immun.* **76**, 3439–3450 (2008).

217. Dobin, A. *et al.* STAR: ultrafast universal RNA-seq aligner. *Bioinformatics* **29**, 15–21 (2013).

218. Liao, Y., Smyth, G. K. & Shi, W. featureCounts: an efficient general purpose program for assigning sequence reads to genomic features. *Bioinformatics* **30**, 923–930 (2014).

219. Robinson, M. D., McCarthy, D. J. & Smyth, G. K. edgeR: a Bioconductor package for differential expression analysis of digital gene expression data. *Bioinformatics* **26**, 139–140 (2010).

220. McCarthy, D. J., Chen, Y. & Smyth, G. K. Differential expression analysis of multifactor RNA-Seq experiments with respect to biological variation. *Nucleic Acids Res.* **40**, 4288–4297 (2012).

221. Benjamini, Y. & Hochberg, Y. Controlling the False Discovery Rate: A Practical and Powerful Approach to Multiple Testing. *J. R. Stat. Soc. Ser. B Methodol.* **57**, 289–300 (1995).

222. Crotty, S. T Follicular Helper Cell Differentiation, Function, and Roles in Disease. *Immunity* **41**, 529–542 (2014).

223. Vinuesa, C. G., Linterman, M. A., Yu, D. & MacLennan, I. C. M. Follicular Helper T Cells. *Annu. Rev. Immunol.* **34**, 335–368 (2016).

224. Schindelin, J. *et al.* Fiji: an open-source platform for biological-image analysis. *Nat. Methods* **9**, 676–682 (2012).

225. Moser, B. K. & Stevens, G. R. Homogeneity of Variance in the Two-Sample Means Test. *Am. Stat.* **46**, 19 (1992).

226. DeVoss, J. *et al.* Spontaneous autoimmunity prevented by thymic expression of a single self-antigen. *J. Exp. Med.* **203**, 2727–2735 (2006).

227. Fan, Y. *et al.* Thymus-specific deletion of insulin induces autoimmune diabetes. *EMBO J.* **28**, 2812–2824 (2009).

228. Wucherpfennig, K. W. *et al.* Clonal expansion and persistence of human T cells specific for an immunodominant myelin basic protein peptide. *J. Immunol. Baltim. Md 1950* **152**, 5581–5592 (1994).

229. Reijonen, H. *et al.* Detection of GAD65-specific T-cells by major histocompatibility complex class II tetramers in type 1 diabetic patients and at-risk subjects. *Diabetes* **51**, 1375–1382 (2002).

230. The Wellcome Trust Case Control Consortium. Genome-wide association study of 14,000 cases of seven common diseases and 3,000 shared controls. *Nature* **447**, 661–678 (2007).

231. Risk Alleles for Multiple Sclerosis Identified by a Genomewide Study. *N. Engl. J. Med.* **357**, 851–862 (2007).

232. Sakaguchi, S., Sakaguchi, N., Asano, M., Itoh, M. & Toda, M. Immunologic self-tolerance maintained by activated T cells expressing IL-2 receptor alpha-chains (CD25). Breakdown of a single mechanism of self-tolerance causes various autoimmune diseases. *J. Immunol. Baltim. Md 1950* **155**, 1151–1164 (1995).

233. Kim, H.-J., Verbinnen, B., Tang, X., Lu, L. & Cantor, H. Inhibition of follicular T-helper cells by CD8(+) regulatory T cells is essential for self tolerance. *Nature* **467**, 328–332 (2010).

234. Chinen, T., Volchkov, P. Y., Chervonsky, A. V. & Rudensky, A. Y. A critical role for regulatory T cell-mediated control of inflammation in the absence of commensal microbiota. *J. Exp. Med.* **207**, 2323–2330 (2010).

235. Miyazaki, T. *et al.* Mice lacking H2-M complexes, enigmatic elements of the MHC class II peptide-loading pathway. *Cell* **84**, 531–541 (1996).

236. Subramanian, A. *et al.* Gene set enrichment analysis: A knowledge-based approach for interpreting genome-wide expression profiles. *Proc. Natl. Acad. Sci.* **102**, 15545–15550 (2005).

237. Marshall, H. D. *et al.* Differential expression of Ly6C and T-bet distinguish effector and memory Th1 CD4(+) cell properties during viral infection. *Immunity* **35**, 633–646 (2011).

238. Xu, W. *et al.* The Transcription Factor Tox2 Drives T Follicular Helper Cell Development via Regulating Chromatin Accessibility. *Immunity* **51**, 826-839.e5 (2019).

239. Hogquist, K. A. Assays of thymic selection. Fetal thymus organ culture and in vitro thymocyte dulling assay. *Methods Mol. Biol. Clifton NJ* **156**, 219–232 (2001).

240. Haynes, N. M. *et al.* Role of CXCR5 and CCR7 in follicular Th cell positioning and appearance of a programmed cell death gene-1high germinal center-associated subpopulation. *J. Immunol. Baltim. Md 1950* **179**, 5099–5108 (2007).

241. Glatman Zaretsky, A. *et al.* T follicular helper cells differentiate from Th2 cells in response to helminth antigens. *J. Exp. Med.* **206**, 991–999 (2009).

242. Johnston, R. J. *et al.* Bcl6 and Blimp-1 are reciprocal and antagonistic regulators of T follicular helper cell differentiation. *Science* **325**, 1006–1010 (2009).

243. Hamaguchi, Y. *et al.* The Peritoneal Cavity Provides a Protective Niche for B1 and Conventional B Lymphocytes during Anti-CD20 Immunotherapy in Mice. *J. Immunol.* **174**, 4389–4399 (2005).

244. Pearce, E. L. *et al.* Control of effector CD8+ T cell function by the transcription factor Eomesodermin. *Science* **302**, 1041–1043 (2003).

245. Banerjee, A. *et al.* Cutting edge: The transcription factor eomesodermin enables CD8+ T cells to compete for the memory cell niche. *J. Immunol. Baltim. Md 1950* **185**, 4988–4992 (2010).

246. Roessner, P. M. *et al.* EOMES and IL-10 regulate antitumor activity of T regulatory type 1 CD4+ T cells in chronic lymphocytic leukemia. *Leukemia* **35**, 2311–2324 (2021).

247. Kawabe, T. *et al.* Requirements for the differentiation of innate T-bethigh memory-phenotype CD4+ T lymphocytes under steady state. *Nat. Commun.* **11**, 3366 (2020).

248. Kalekar, L. A. *et al.* CD4+ T cell anergy prevents autoimmunity and generates regulatory T cell precursors. *Nat. Immunol.* **17**, 304–314 (2016).

249. Alonso, R. *et al.* Induction of anergic or regulatory tumor-specific CD4+ T cells in the tumor-draining lymph node. *Nat. Commun.* **9**, 2113 (2018).

250. Buch, T. *et al.* A Cre-inducible diphtheria toxin receptor mediates cell lineage ablation after toxin administration. *Nat. Methods* **2**, 419–426 (2005).

251. Hobeika, E. *et al.* Testing gene function early in the B cell lineage in mb1-cre mice. *Proc. Natl. Acad. Sci. U. S. A.* **103**, 13789–13794 (2006).

252. Olivares-Villagómez, D., Wensky, A. K., Wang, Y. & Lafaille, J. J. Repertoire requirements of CD4+ T cells that prevent spontaneous autoimmune encephalomyelitis. *J. Immunol. Baltim. Md 1950* **164**, 5499–5507 (2000).

253. Li, M. O. & Rudensky, A. Y. T cell receptor signalling in the control of regulatory T cell differentiation and function. *Nat. Rev. Immunol.* **16**, 220–233 (2016).

254. Moran, A. E. & Hogquist, K. A. T-cell receptor affinity in thymic development: TCR affinity in thymic development. *Immunology* **135**, 261–267 (2012).

255. Tai, X., Cowan, M., Feigenbaum, L. & Singer, A. CD28 costimulation of developing thymocytes induces Foxp3 expression and regulatory T cell differentiation independently of interleukin 2. *Nat. Immunol.* **6**, 152–162 (2005).

256. Sprouse, M. L. *et al.* Cutting Edge: Low-Affinity TCRs Support Regulatory T Cell Function in Autoimmunity. *J. Immunol. Baltim. Md 1950* **200**, 909–914 (2018).

257. Goldrath, A. W., Luckey, C. J., Park, R., Benoist, C. & Mathis, D. The molecular program induced in T cells undergoing homeostatic proliferation. *Proc. Natl. Acad. Sci. U. S. A.* **101**, 16885–16890 (2004).

258. Gingrich, J. R., Barrios, R. J., Foster, B. A. & Greenberg, N. M. Pathologic progression of autochthonous prostate cancer in the TRAMP model. *Prostate Cancer Prostatic Dis.* **2**, 70–75 (1999).

259. Alexander-Miller, M. A., Leggatt, G. R., Sarin, A. & Berzofsky, J. A. Role of antigen, CD8, and cytotoxic T lymphocyte (CTL) avidity in high dose antigen induction of apoptosis of effector CTL. *J. Exp. Med.* **184**, 485–492 (1996).

260. Simoni, Y. *et al.* Bystander CD8+ T cells are abundant and phenotypically distinct in human tumour infiltrates. *Nature* **557**, 575–579 (2018).

261. Li, S. *et al.* Bystander $CD4^+$ T cells infiltrate human tumors and are phenotypically distinct. *OncoImmunology* **11**, 2012961 (2022).

262. Yousefi, O. S. *et al.* Optogenetic control shows that kinetic proofreading regulates the activity of the T cell receptor. *eLife* **8**, e42475 (2019).

263. McKeithan, T. W. Kinetic proofreading in T-cell receptor signal transduction. *Proc. Natl. Acad. Sci. U. S. A.* **92**, 5042–5046 (1995).

264. Tischer, D. K. & Weiner, O. D. Light-based tuning of ligand half-life supports kinetic proofreading model of T cell signaling. *eLife* **8**, e42498 (2019).

265. Carreño, L. J. *et al.* T-cell antagonism by short half-life pMHC ligands can be mediated by an efficient trapping of T-cell polarization toward the APC. *Proc. Natl. Acad. Sci. U. S. A.* **107**, 210–215 (2010).

266. Irving, M. *et al.* Interplay between T cell receptor binding kinetics and the level of cognate peptide presented by major histocompatibility complexes governs CD8+ T cell responsiveness. *J. Biol. Chem.* **287**, 23068–23078 (2012).

267. Valitutti, S., Müller, S., Cella, M., Padovan, E. & Lanzavecchia, A. Serial triggering of many T-cell receptors by a few peptide–MHC complexes. *Nature* **375**, 148–151 (1995).

268. Valitutti, S. The Serial Engagement Model 17 Years After: From TCR Triggering to Immunotherapy. *Front. Immunol.* **3**, (2012).

269. Künzli, M., Reuther, P., Pinschewer, D. D. & King, C. G. Opposing effects of T cell receptor signal strength on CD4 T cells responding to acute versus chronic viral infection. *eLife* **10**, e61869 (2021).

270. Brooks, D. G., Teyton, L., Oldstone, M. B. A. & McGavern, D. B. Intrinsic functional dysregulation of CD4 T cells occurs rapidly following persistent viral infection. *J. Virol.* **79**, 10514–10527 (2005).

271. Fahey, L. M. *et al.* Viral persistence redirects CD4 T cell differentiation toward T follicular helper cells. *J. Exp. Med.* **208**, 987–999 (2011).

272. Greczmiel, U. *et al.* Sustained T follicular helper cell response is essential for control of chronic viral infection. *Sci. Immunol.* **2**, eaam8686 (2017).

273. Choi, Y. S. *et al.* ICOS receptor instructs T follicular helper cell versus effector cell differentiation via induction of the transcriptional repressor Bcl6. *Immunity* **34**, 932–946 (2011).

274. Satpathy, A. T. *et al.* Zbtb46 expression distinguishes classical dendritic cells and their committed progenitors from other immune lineages. *J. Exp. Med.* **209**, 1135–1152 (2012).

275. Buenrostro, J. D., Giresi, P. G., Zaba, L. C., Chang, H. Y. & Greenleaf, W. J. Transposition of native chromatin for fast and sensitive epigenomic profiling of open chromatin, DNA-binding proteins and nucleosome position. *Nat. Methods* **10**, 1213–1218 (2013).

276. Perera, J. *et al.* Self-Antigen-Driven Thymic B Cell Class Switching Promotes T Cell Central Tolerance. *Cell Rep.* **17**, 387–398 (2016).

277. Quách, T. D. *et al.* Anergic responses characterize a large fraction of human autoreactive naive B cells expressing low levels of surface IgM. *J. Immunol. Baltim. Md 1950* **186**, 4640–4648 (2011).

278. Cambier, J. C., Gauld, S. B., Merrell, K. T. & Vilen, B. J. B-cell anergy: from transgenic models to naturally occurring anergic B cells? *Nat. Rev. Immunol.* **7**, 633–643 (2007).

279. Dong, C., Temann, U. A. & Flavell, R. A. Cutting edge: critical role of inducible costimulator in germinal center reactions. *J. Immunol. Baltim. Md 1950* **166**, 3659–3662 (2001).

280. Renshaw, B. R. *et al.* Humoral immune responses in CD40 ligand-deficient mice. *J. Exp. Med.* **180**, 1889–1900 (1994).

281. Koh, B. *et al.* Bcl6 and Blimp1 reciprocally regulate ST2+ Treg–cell development in the context of allergic airway inflammation. *J. Allergy Clin. Immunol.* **146**, 1121-1136.e9 (2020).

282. Qui, H. Z. *et al.* CD134 Plus CD137 Dual Costimulation Induces Eomesodermin in CD4 T Cells To Program Cytotoxic Th1 Differentiation. *J. Immunol.* **187**, 3555–3564 (2011).

283. Stienne, C. *et al.* Foxo3 Transcription Factor Drives Pathogenic T Helper 1 Differentiation by Inducing the Expression of Eomes. *Immunity* **45**, 774–787 (2016).

284. Sosinowski, T. *et al.* CD8α+ dendritic cell trans presentation of IL-15 to naive CD8+ T cells produces antigen-inexperienced T cells in the periphery with memory phenotype and function. *J. Immunol. Baltim. Md 1950* **190**, 1936–1947 (2013).

285. Miller, C. H. *et al.* Eomes identifies thymic precursors of self-specific memory-phenotype CD8+ T cells. *Nat. Immunol.* **21**, 567–577 (2020).

286. Oh, D. Y. & Fong, L. Cytotoxic CD4+ T cells in cancer: Expanding the immune effector toolbox. *Immunity* **54**, 2701–2711 (2021).

287. Knudson, K. M. *et al.* NFκB–Pim-1–Eomesodermin axis is critical for maintaining CD8 T-cell memory quality. *Proc. Natl. Acad. Sci.* **114**, (2017).

288. Yang, Y., Xu, J., Niu, Y., Bromberg, J. S. & Ding, Y. T-bet and eomesodermin play critical roles in directing T cell differentiation to Th1 versus Th17. *J. Immunol. Baltim. Md 1950* **181**, 8700–8710 (2008).

289. DuPage, M. & Bluestone, J. A. Harnessing the plasticity of CD4+ T cells to treat immune-mediated disease. *Nat. Rev. Immunol.* **16**, 149–163 (2016).

290. Lu, K. T. *et al.* Functional and epigenetic studies reveal multistep differentiation and plasticity of in vitro-generated and in vivo-derived follicular T helper cells. *Immunity* **35**, 622–632 (2011).

291. Choi, J. & Crotty, S. Bcl6-Mediated Transcriptional Regulation of Follicular Helper T cells (TFH). *Trends Immunol.* **42**, 336–349 (2021).

292. Raveney, B. J. E. *et al.* Eomesodermin-expressing T-helper cells are essential for chronic neuroinflammation. *Nat. Commun.* **6**, 8437 (2015).

293. Raveney, B. J. E. *et al.* Involvement of cytotoxic Eomes-expressing CD4+ T cells in secondary progressive multiple sclerosis. *Proc. Natl. Acad. Sci. U. S. A.* **118**, e2021818118 (2021).

294. Rathmell, J. C. *et al.* CD95 (Fas)-dependent elimination of self-reactive B cells upon interaction with CD4+T cells. *Nature* **376**, 181–184 (1995).

295. Rathmell, J. C., Townsend, S. E., Xu, J. C., Flavell, R. A. & Goodnow, C. C. Expansion or Elimination of B Cells In Vivo: Dual Roles for CD40- and Fas (CD95)-Ligands Modulated by the B Cell Antigen Receptor. *Cell* **87**, 319–329 (1996).

296. Martinez, R. J. *et al.* Arthritogenic Self-Reactive $CD4^{+}$ T Cells Acquire an $FR4^{hi}$ $CD73^{hi}$ Anergic State in the Presence of $Foxp3^{+}$ Regulatory T Cells. *J. Immunol.* **188**, 170–181 (2012).

297. Lyman, W. D., Abrams, G. A. & Raine, C. S. Experimental autoimmune encephalomyelitis: isolation and characterization of inflammatory cells from the central nervous system. *J. Neuroimmunol.* **25**, 195–201 (1989).

298. Bittner, S., Afzali, A. M., Wiendl, H. & Meuth, S. G. Myelin Oligodendrocyte Glycoprotein (MOG_{35-55}) Induced Experimental Autoimmune Encephalomyelitis (EAE) in C57BL/6 Mice. *J. Vis. Exp.* 51275 (2014) doi:10.3791/51275.

299. Johanson, D. M. *et al.* Experimental autoimmune encephalomyelitis is associated with changes of the microbiota composition in the gastrointestinal tract. *Sci. Rep.* **10**, 15183 (2020).

300. Miller, S. D. & Karpus, W. J. Experimental autoimmune encephalomyelitis in the mouse. *Curr. Protoc. Immunol.* **Chapter 15**, Unit 15.1 (2007).

301. Kouskoff, V. *et al.* Organ-specific disease provoked by systemic autoimmunity. *Cell* **87**, 811–822 (1996).

302. Goverman, J. Tolerance and autoimmunity in TCR transgenic mice specific for myelin basic protein. *Immunol. Rev.* **169**, 147–159 (1999).

303. Waldner, H., Whitters, M. J., Sobel, R. A., Collins, M. & Kuchroo, V. K. Fulminant spontaneous autoimmunity of the central nervous system in mice transgenic for the myelin proteolipid protein-specific T cell receptor. *Proc. Natl. Acad. Sci.* **97**, 3412–3417 (2000).

304. McHugh, R. S., Shevach, E. M., Margulies, D. H. & Natarajan, K. A T cell receptor transgenic model of severe, spontaneous organ-specific autoimmunity. *Eur. J. Immunol.* **31**, 2094–2103 (2001).

305. Malchow, S. *et al.* Aire-dependent thymic development of tumor-associated regulatory T cells. *Science* **339**, 1219–1224 (2013).

306. Di Giacomo, A. M., Biagioli, M. & Maio, M. The emerging toxicity profiles of anti-CTLA-4 antibodies across clinical indications. *Semin. Oncol.* **37**, 499–507 (2010).

307. Pai, C.-C. S. *et al.* Tumor-conditional anti-CTLA4 uncouples antitumor efficacy from immunotherapy-related toxicity. *J. Clin. Invest.* **129**, 349–363 (2019).

308. Bluestone, J. A. *et al.* Type 1 diabetes immunotherapy using polyclonal regulatory T cells. *Sci. Transl. Med.* **7**, 315ra189 (2015).

309. Choi, Y. S., Eto, D., Yang, J. A., Lao, C. & Crotty, S. Cutting Edge: STAT1 Is Required for IL-6–Mediated Bcl6 Induction for Early Follicular Helper Cell Differentiation. *J. Immunol.* **190**, 3049–3053 (2013).

310. Vogelzang, A. *et al.* A fundamental role for interleukin-21 in the generation of T follicular helper cells. *Immunity* **29**, 127–137 (2008).

311. Stagg, A. J., Hart, A. L., Knight, S. C. & Kamm, M. A. The dendritic cell: its role in intestinal inflammation and relationship with gut bacteria. *Gut* **52**, 1522 (2003).

312. Hara, S. *et al.* Dietary Antigens Induce Germinal Center Responses in Peyer's Patches and Antigen-Specific IgA Production. *Front. Immunol.* **10**, 2432 (2019).

313. Smith, C. C. *et al.* Endogenous retroviral signatures predict immunotherapy response in clear cell renal cell carcinoma. *J. Clin. Invest.* **128**, 4804–4820 (2018).

314. Woodland, D. L., Happ, M. P., Gollob, K. J. & Palmer, E. An endogenous retrovirus mediating deletion of αβ T cells? *Nature* **349**, 529–530 (1991).

315. Harley, J. B. *et al.* Transcription factors operate across disease loci, with EBNA2 implicated in autoimmunity. *Nat. Genet.* **50**, 699–707 (2018).

316. Rojas, M. *et al.* Molecular mimicry and autoimmunity. *J. Autoimmun.* **95**, 100–123 (2018).

317. Proft, T. & Fraser, J. D. Bacterial superantigens. *Clin. Exp. Immunol.* **133**, 299–306 (2003).

318. Powell, A. M. & Black, M. M. Epitope spreading: protection from pathogens, but propagation of autoimmunity? *Clin. Exp. Dermatol.* **26**, 427–433 (2001).

319. Schorer, M. *et al.* Rapid expansion of Treg cells protects from collateral colitis following a viral trigger. *Nat. Commun.* **11**, 1522 (2020).